ADAPTIVE ANGLE TRACKING

Lawrence E. Brennan, et al

Technology Service Corporation

Prepared for:

Office of Naval Research

7 February 1975

Technology Service Corporation

2811 Wilshire Boulevard
Santa Monica, California 90403
(213) 829-7411

ADAPTIVE ANGLE TRACKING

TSC-PD-119-4

7 February 1975

Lawrence E. Brennan
Irving S. Reed

FINAL REPORT

Submitted to:

The Naval Air Systems Command

On

Contract N00019-74-C-0227

APPROVED FOR PUBLIC RELEASE;
DISTRIBUTION UNLIMITED

TABLE OF CONTENTS

1. INTRODUCTION

This is the final report on a one year study of angle tracking with phased array antennas in an external noise environment. While the results of this study are applicable generally to arrays of sensors for measuring the angle of arrival of incident radiation, the emphasis in the simulation portion of the study was placed on radar arrays operating in a jamming environment. This problem is important in a variety of radar ECCM applications, including AI radars and missile seekers.

Two different approaches to the adaptive angle tracking problem were included in the study. The first approach is based on maximization of the likelihood function. Three different angle estimators, each a maximum likelihood estimator under certain assumptions, are discussed in Section 2 of this report. The interesting property of these estimators is that each requires formation of adaptive sum (Σ) and difference (Δ) beams. These are the Σ and Δ beams which would be expected from the earlier theory of adaptive receiving array antennas. The two receiving beams automatically place pattern nulls at the angles of jamming. This adaptive beam control distorts the patterns as a function of the external noise field. The three maximum likelihood angle estimators employ different methods of "compensating" for these distortions in arriving at an estimate of angle.

The second basic approach to angle tracking in a jamming environment is based on the use of symmetrical pairs of array elements. As discussed in Section 3, the sums of symmetrical pair outputs provide the basic inputs to the Σ beam network and corresponding pair differences are used in forming the Δ beam. This symmetry constraint assures that the Σ and Δ beams are

symmetrical around a chosen boresight angle, and hence, will provide unbiased angle estimates for targets near boresight.

The performance of these angle estimators was compared by simulation, employing Monte Carlo techniques to obtain estimates of bias and rms error for each. Results for the difficult case of jammers near the target (within the main beam) are discussed in Section 4. Multiple jammer results are discussed in Section 5. Electronic scanning of the Σ and Δ beams was included in the simulation program. Results for electronic scan off the normal to a linear array are discussed in Section 6. Conclusions of the study are contained in the final section of this report.

2. MAXIMUM LIKELIHOOD ESTIMATORS

The derivation of the equations for the three angle estimators based on maximizing the likelihood function is outlined in this section. Also, the equations for these estimators, which were compared by simulation, are described. The reader is referred to the previous quarterly progress report [1] for details of the derivation.

The outputs of elements of an array antenna are denoted by $X_1, X_2, \ldots, X_N$. Each X_n is a complex number retaining both phase and amplitude information. The noise field is described by its covariance matrix, M, with elements

$$M_{mn} = E\{X_m X_n^*\}$$

where E denotes the expectation or average obtained when only noise is present. Under the usual assumption of Gaussian statistics, which characterizes most noise components of interest, the probability density function or likelihood function for X is

$$P(X|S+N) = \frac{1}{\pi^N |M|} \exp\{-(X-bV(\varepsilon))^* M^{-1} (X-bV(\varepsilon))\} \qquad (1)$$

where: X = column vector of the X_n

b = complex signal amplitude

$\varepsilon = \sin\theta$

θ = angle of incidence of plane wave signal on linear array

$V(\varepsilon)$ = column vector of $V_n(\varepsilon) = \exp\left\{i \frac{2\pi y_n \varepsilon}{\lambda}\right\}$

y_n = coordinate of n^{th} element

λ = wavelength

$|M|$ = determinant of M

While the particular form of $V_n(\varepsilon)$ in Eq. 1 assumes a linear array antenna, the analysis is general and can easily be extended to an arbitrary array of elements.

Both signal and noise are assumed present in one sample of the array output, X. The objective is to estimate the angle of arrival of the signal, or equivalently $\sin\theta = \varepsilon$. The unknown signal amplitude and phase are nuisance parameters, both contained in the complex quantity b. The likelihood function, P, is maximum when Q is minimum, where

$$Q = (X-bV(\varepsilon))^{*}M^{-1}(X-bV(\varepsilon)) \tag{2}$$

We wish to find values of the parameters b and ε which minimize Q.

Expanding this function around a boresight angle $\varepsilon_1 = \sin\theta_1$ gives

$$Q(\varepsilon) = Q(\varepsilon_1) + \left.\frac{dQ}{d\varepsilon}\right|_{\varepsilon_1}(\varepsilon-\varepsilon_1) + \frac{1}{2}\left.\frac{d^2Q}{d\varepsilon^2}\right|_{\varepsilon_1}(\varepsilon-\varepsilon_1)^2 \tag{3}$$

This function has an extremum where its derivative is zero, i.e.,

$$(\hat{\varepsilon}-\varepsilon_1) = -\frac{Q'}{Q''} \tag{4}$$

where primes denote differentation with respect to ε, and $\hat{\varepsilon}$ is the estimated value of ε. This is the basic equation used in deriving the three maximum likelihood estimators.

As shown in [1], the ratio $-Q'/Q''$ reduces to

$$(\hat{\epsilon}-\epsilon_1) = \frac{-b_{11}(\Sigma\bar{\Delta}+\Delta\bar{\Sigma}) + \Sigma\bar{\Sigma}(b_{12}+b_{21})}{b_{11}(\Sigma\bar{\Delta}_\epsilon+\bar{\Sigma}\Delta_\epsilon+2\Delta\bar{\Delta}) - \Sigma\bar{\Sigma}(2b_{22}+b_{13}+b_{31}) - 2(b_{12}+b_{21})\left[\Sigma\bar{\Delta}+\Delta\bar{\Sigma}-\frac{\Sigma\bar{\Sigma}(b_{12}+b_{21})}{b_{11}}\right]}$$

where:

$\Sigma = V^*M^{-1}X$

$\Delta = -V^*DM^{-1}X$

D = diagonal matrix with elements $2\pi i y_n/\lambda$

$V = V(\epsilon)$; see Eq. 1

$\Delta_\epsilon = V^*D^2M^{-1}X$

X = column vector of array element outputs

$b_{11} = V^*M^{-1}V$

$b_{12} = V^*M^{-1}DV$

$b_{21} = \overline{b_{12}}$

$b_{22} = -V^*DM^{-1}DV$

$b_{13} = V^*M^{-1}D^2V$

$b_{31} = \overline{b_{13}}$

The quantities Σ and Δ are the sum and difference beam outputs respectively. In these equations, * denotes conjugate transpose and the bar denotes complex conjugate. This estimator, Eq. 5, is one of the tracking algorithms which were compared by simulation. As discussed in Section 3 of this report, the rms angle error was large using Eq. 5. This is probably due to the fact that differentiation leads to noisier quantities, and Q" is a second derivative. It should also be noted that three receiving beams are required to implement this angle estimator, Σ, Δ, and Δ_ϵ.

The other two maximum likelihood estimators require only two beam outputs, Σ and Δ. They are based on an average of the denominator of Eq. 5.

$$(\hat{\epsilon}-\epsilon_1) = -\frac{Q'}{E(Q'')} \tag{6}$$

where E, as before, denotes the expectation. The two estimators based on Eq. 6 were found to provide better angular accuracy.

The second maximum likelihood estimator tested by simulation is due to R. C. Davis.

$$(\hat{\epsilon}-\epsilon_1) = \frac{b_{11}(\bar{\Sigma}\Delta+\bar{\Delta}\Sigma) - \Sigma\bar{\Sigma}(b_{12}+b_{21})}{2[b_{22}\Sigma\bar{\Sigma} - b_{21}\bar{\Sigma}\Delta - b_{12}\Sigma\bar{\Delta} + b_{11}\Delta\bar{\Delta} - 2(b_{11}b_{22}-b_{12}b_{21})]} \tag{7}$$

The quantities appearing in this expression are defined after Eq. 5.

The third estimator, which was derived during this study and provides the best angle accuracy at low S/N ratios, is again based on Eq. 6.

$$(\hat{\epsilon}-\epsilon_1) = \frac{b_{11}^2(\Sigma\bar{\Delta}+\Delta\bar{\Sigma}) - \Sigma\bar{\Sigma}(b_{12}+b_{21})b_{11}}{2\Sigma\bar{\Sigma}(b_{11}b_{22}-b_{21}b_{12})} \tag{8}$$

This expression is the simplest of the three maximum likelihood estimators and would be the easiest to implement.

One interesting property of these three estimators is the natural occurrence of Σ and Δ beams. Weights for the sum beam are $W_\Sigma' = V^* M^{-1}$, a row vector of array element weights, where prime denotes transpose. Similarly the difference beam weights are $W_\Delta' = -V^* D M^{-1}$. These are the weights which would be expected from maximum S/N adaptive array theory. The weights W_Σ maximize the S/N ratio for a signal at the angle defined by $V(\varepsilon)$. The steering signals for the Δ beam, $-V^* D$, are matched to the derivative of $V(\varepsilon)$. The Σ and Δ beam outputs can be obtained using adaptive control loops, as described by Applebaum[2], with steering signals V^* and $-V^* D$, respectively. Other methods of generating the two array outputs, Σ and Δ, can be used, e.g., weights computed from a sample covariance matrix[3] of the noise field. In each implementation, the array outputs are obtained as illustrated in Figure 1.

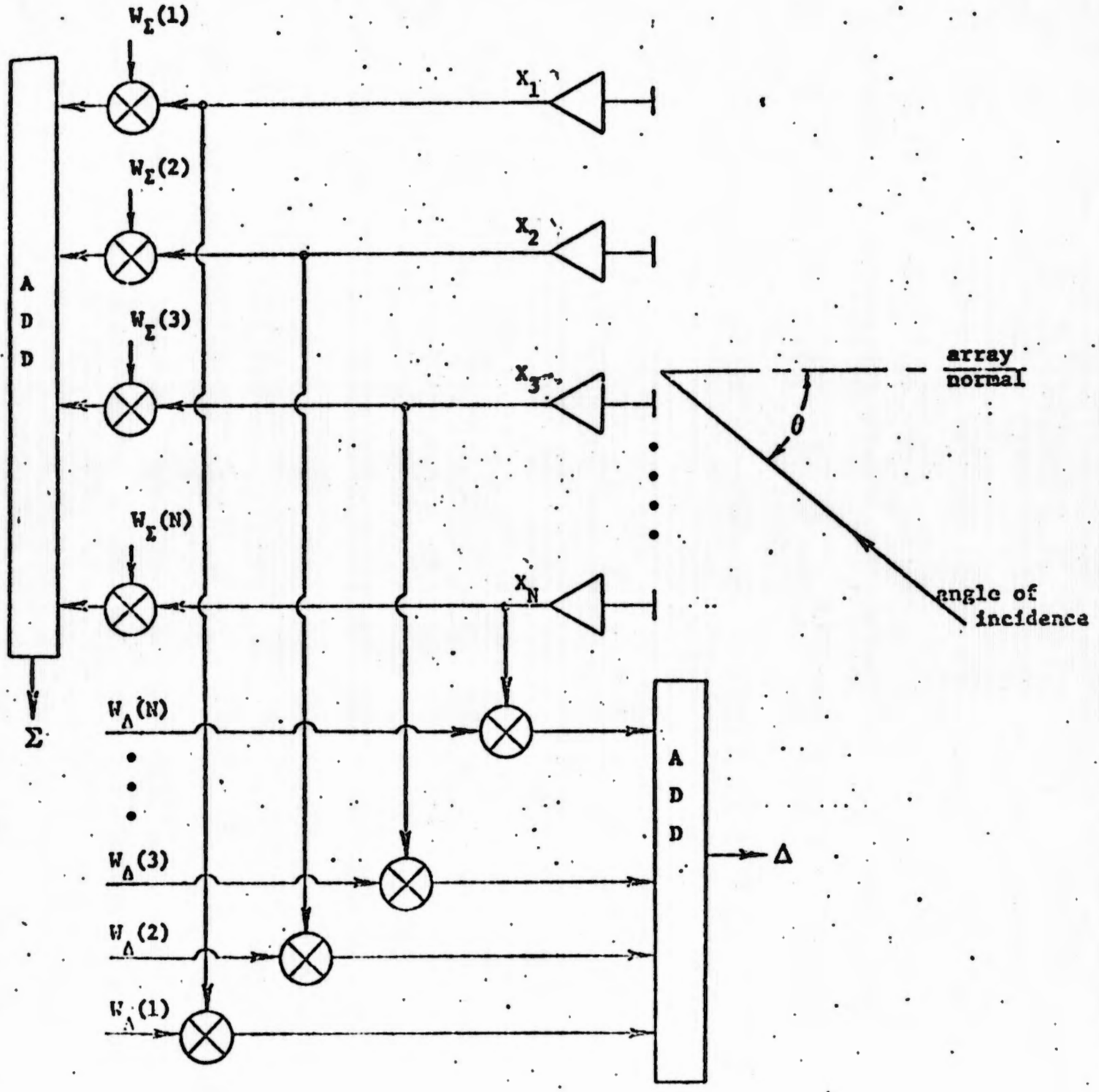

Figure 1. FORMATION OF SUM (Σ) AND DIFFERENCE (Δ) BEAMS

3. SYMMETRICAL PAIRS

The adaptively formed beams, Σ and Δ, described in the preceding section are not constrained to assure symmetry around the boresight angle corresponding to ε_1. In fact, the simulation results of the next section show that these fully adaptive (separately controlled weight for each array element) patterns may bear no resemblance to typical Σ and Δ monopulse patterns. The symmetrical pairs technique was devised to assure symmetry around the boresight angle, while providing some adaptive degrees of freedom for nulling interference.

The theory of adaptive arrays with the symmetrical pairs constraint was presented in [4]. The basic technique is illustrated for a 6 element linear array in Fig. 2. Sums of symmetrically located element outputs, e.g., (V_1+V_6) in Fig. 2, are the inputs to an adaptive network which forms the sum beam. Similarly, differences such as (V_1-V_6) constitute the inputs to the difference beam network. This symmetrical pairs constraint leads to Σ and Δ patterns which are symmetrical around the boresight angle for small values of $(\varepsilon-\varepsilon_1)$. The weights applied in the beam forming networks are again adaptively controlled to null external interference. For an N element linear array there are only N/2 adaptive degrees of freedom in each beam forming network. This reduces the complexity of the adaptive processors, but also reduces the number of separate noise sources which can be nulled.

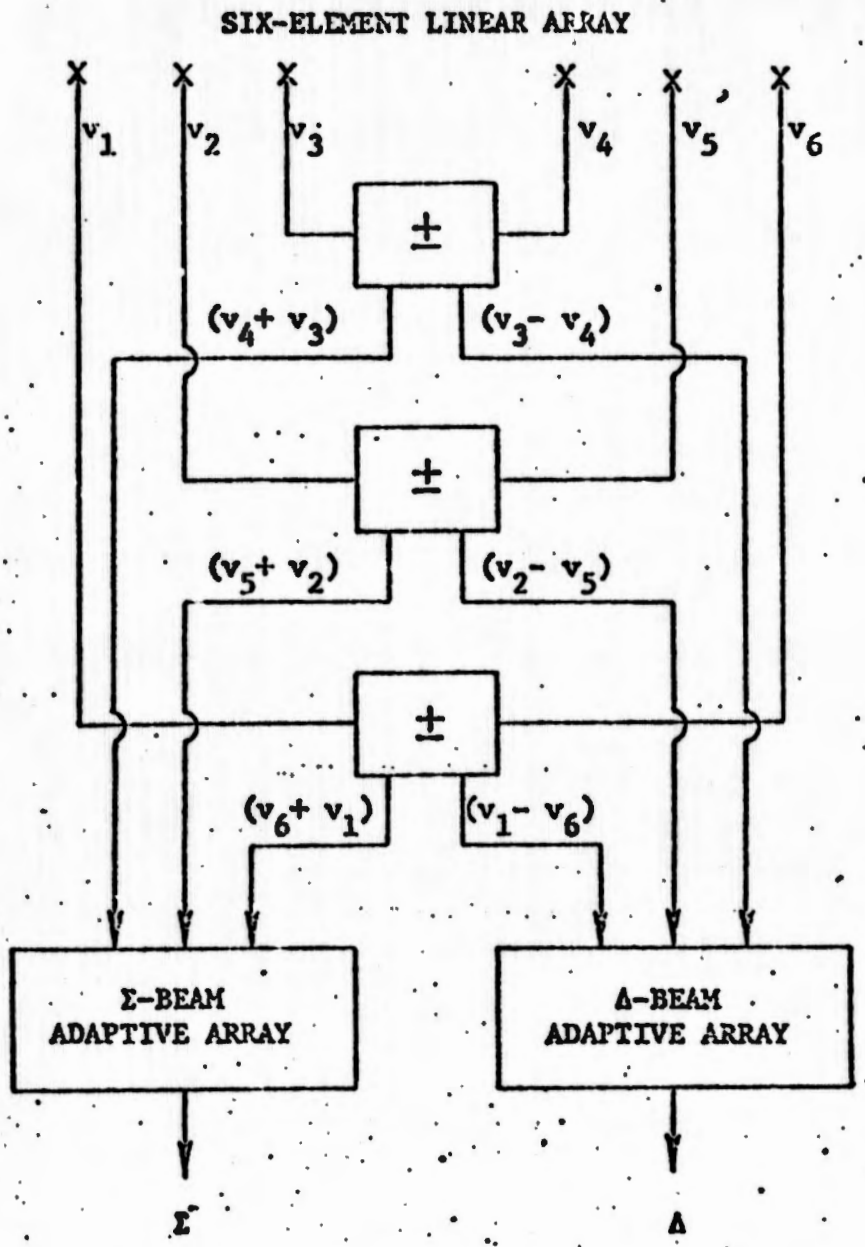

Figure 2.

ADAPTIVE ANGLE TRACKING USING SYMMETRICAL PAIRS

To electronically scan the boresight angle ε_1, a phase shift is introduced in adding the outputs from the two symmetrically located elements. For example, a typical sum beam input has the form $V_1 e^{-i\psi} + V_N e^{i\psi}$. The maximum of the pattern formed by the pair of elements is electronically scanned to the selected boresight angle. Similar phase shifts are introduced in forming the Δ beam inputs.

This symmetrical pairs technique was simulated to compare its performance with the fully adaptive arrays of Section 2. Results presented in the next section show that the symmetry constraint significantly reduces angular accuracy in some cases.

4. MAIN BEAM JAMMING

When one or more jammers are located in the sidelobes of the antenna patterns, minor modifications of the array weights and Σ and Δ patterns suffice to move nulls on to the jammers. An example of sidelobe jamming is included in the next section to illustrate this point. A much more difficult task for the array is to null main beam jammers while estimating target angle. The presence of interference in the main beam, separated by less than a beamwidth from the target, seriously distorts the Σ and Δ patterns. The examples presented in this section show that the adaptive angle trackers can cope very effectively with main beam jamming.

The results presented here were obtained by simulation, using the program listed in Appendix I. In this program, the noise field is defined (jammer angles and J/N, jammer-to-receiver noise ratio per element), and the covariance matrix, M, is computed. The boresight angle, ϵ_1, is selected and adaptive array weights are computed for the Σ and Δ beams. In each case, simulation runs are made for targets at the boresight angle θ_1, at $\theta_1 \pm .5°$, and $\theta_1 \pm 1°$. The signal-to-receiver noise ratio is specified. The jammer inputs, receiver noise, and signals sensed by the array are simulated for each of 100 independent runs. Estimates of the bias and rms errors are obtained from the 100 run sample.

Six different tracking algorithms are compared during each simulation run:

Case 1 - Non-adaptive array, with conventional sum and difference beams optimized for receiver noise only. The angle estimator has the form $(\hat{\epsilon}-\epsilon_1) = K\,\Delta/\Sigma$.

Case 2 - Adaptive Σ and Δ beams with separate weights for each element (fully adaptive). No compensation for beam distortion and $(\hat{\epsilon}-\epsilon_1) = K\,\Delta/\Sigma$.

Case 3 - The adaptive tracking algorithm of Eq. 7 due to R. Davis.

Case 4 - The symmetrical pairs technique described in Section 3.

Case 5 - The fully adaptive array case with $(\hat{\epsilon}-\epsilon_1) = -Q'/Q''$ of Eq. 5.

Case 6 - The new fully adaptive array algorithm employing Eq. 8 to compensate for beam distortion.

A set of simulation results with main beam jamming is outlined in Table 1. Five different locations of a single jammer, 2°, 4°, 6°, 8°, and 10° were investigated. In each of the results shown, the boresight angle and target location were both at 0°, i.e., normal to the 10 element linear array. Isotopic element patterns and $\lambda/2$ spacing between elements were simulated. Note that the array is roughly 5λ long, so the nominal beamwidth is 12°. All jammer locations are within the first null of the normal pattern for this array. Antenna patterns for these 5 examples are shown in Figures 3 through 7. Both the Σ and Δ patterns are shown in each figure, with the Δ pattern identified by the + symbols.

Referring to Table 1, it is clear that the non-adaptive tracker employing conventional Σ and Δ beams, Case 1, does not provide useful angle information in any of the simulation examples. At small jammer

Table 1. Comparison of Tracking Algorithms with Jammer in Main Beam

Tracking Alborithm (Case)		1		2		3		4		5		6	
Angular Error (Degrees)		Bias	RMS	Bias	RMS	Bias	RMS	Bias	RMS	Bias	RMS	Bias	RMS
θ_J = 2°	S/N(dB) = 0	2.0	2.0	-19.2	20.6	-5.0	84.8	-1.1	26.2	21.6	(>100)	.82	35.9
	10	1.5	1.5	-20.0	20.2	.17	6.8	1.1	37.5	55.5	(>100)	-1.3	12.6
	20	1.9	2.0	-19.4	19.4	-.01	1.1	-.7	17.2	-.05	1.2	-.01	1.1
	30	1.6	2.0	-19.4	19.4	.02	.35	.19	2.9	.01	.35	.02	.35
θ_J = 4°	S/N(dB) = 0	4.4	4.4	-8.4	8.5	-.62	19.8	-2.2	29.7	1.85	37.9	.65	8.5
	10	4.4	4.4	-8.5	8.5	-.04	1.45	-.07	8.4	-.15	1.6	-.03	1.43
	20	4.3	4.3	-8.5	8.5	.07	.52	.40	2.7	.05	.51	.07	.52
	30	4.3	4.3	-8.5	8.5	-.02	.151	-.08	.81	-.02	.152	-.02	.151
θ_J = 6°	S/N(dB) = 0	7.5	7.5	-4.4	4.5	.20	4.5	-.6	18	-3.5	37.7	.23	4.5
	10	7.4	7.4	-4.4	4.4	-.02	.95	-.08	3.2	-.08	.09	-.02	.95
	20	7.4	7.5	-4.4	4.4	.04	.34	.15	1.2	.04	.34	.04	.34
	30	7.1	7.3	-4.4	4.4	-.01	.10	-.03	.34	-.01	.10	-.01	.10
θ_J = 8°	S/N(dB) = 0	12.8	12.8	-2.1	2.3	-.48	6.5	.40	7.7	-2.9	12.3	.10	2.8
	10	12.7	12.7	-2.1	2.1	-.01	.70	-.03	1.7	-.05	.72	-.01	.70
	20	12.7	12.9	-2.1	2.1	.03	.25	.08	.60	.03	.25	.03	.25
	30	11.4	12.2	-2.1	2.1	-.01	.07	-.02	.17	-.01	.07	-.01	.07
θ_J = 10°	S/N(dB) = 0	29.2	29.2	-.63	1.3	.49	4.1	.11	3.7	.54	9.8	.06	2.2
	10	28.7	28.8	-.67	.73	-.01	.56	-.02	.95	-.04	.57	-.01	.56
	20	29.8	31.8	-.65	.66	.03	.20	.04	.34	.02	.20	.03	.20
	30	17.5	24.2	-.67	.67	-.01	.06	-.01	.10	-.01	.06	-.01	.06

Scan Angle = 0°; 10 Elements; $\lambda/2$ Spacing ; Target Angle = 0° ; Jammer Power = 10^5

angles, 2° and 4°, it appears that the system is tracking the jammer rather than the target. This is apparent from the bias errors. This would be expected since J/N is 50 dB and S/N is 30 dB or less in all examples. The results for Case 1 serve primarily to illustrate the fact that some form of adaptive tracking is required in this severe jamming environment.

The results for Case 2, adapted Σ and Δ beams without compensation for distortion, also show large bias errors. These bias errors do not improve with increasing S/N ratio. While the adapted patterns used in Case 2, shown in Figures 3a, 4a, 5a, 6a, and 7a have nulls at the jammer angle, the conventional estimator ($K\Delta/\Sigma$) does not provide useful angular data.

The symmetrical pairs technique, Case 4 of Table 1, has small bias errors. These biases would be expected in a small sample of 100 simulation runs. The rms bias should be rougly 0.1 times the rms error and is a random variable of roughly this magnitude. The accuracy of the Case 4 angle estimates improves with S/N as would be expected. The rms error varies roughly as $(S/N)^{-1/2}$ as predicted by theory. The errors obtained with symmetrical pairs are larger in most cases than the errors with fully adaptive arrays and maximum likelihood estimators (Cases 3 and 6). This is not surprising considering the antenna patterns of Figures 3b, 4b, 5b, 6b, and 7b obtained with symmetric pairs. The symmetry constraint requires nulls on both sides of the 0° boresight angle at the jammer angle. These nulls, both in the Σ and Δ patterns severely reduce the antenna gain at boresight. As a result, the effective S/N ratio is reduced and the angular errors are larger.

Figure 3a.

SUM AND DIFFERENCE PATTERNS - FULLY ADAPTIVE ARRAY

10 elements λ/2 spacing 0° scan angle
1 jammer $\theta_j = 2°$ $P_j = 10^6$

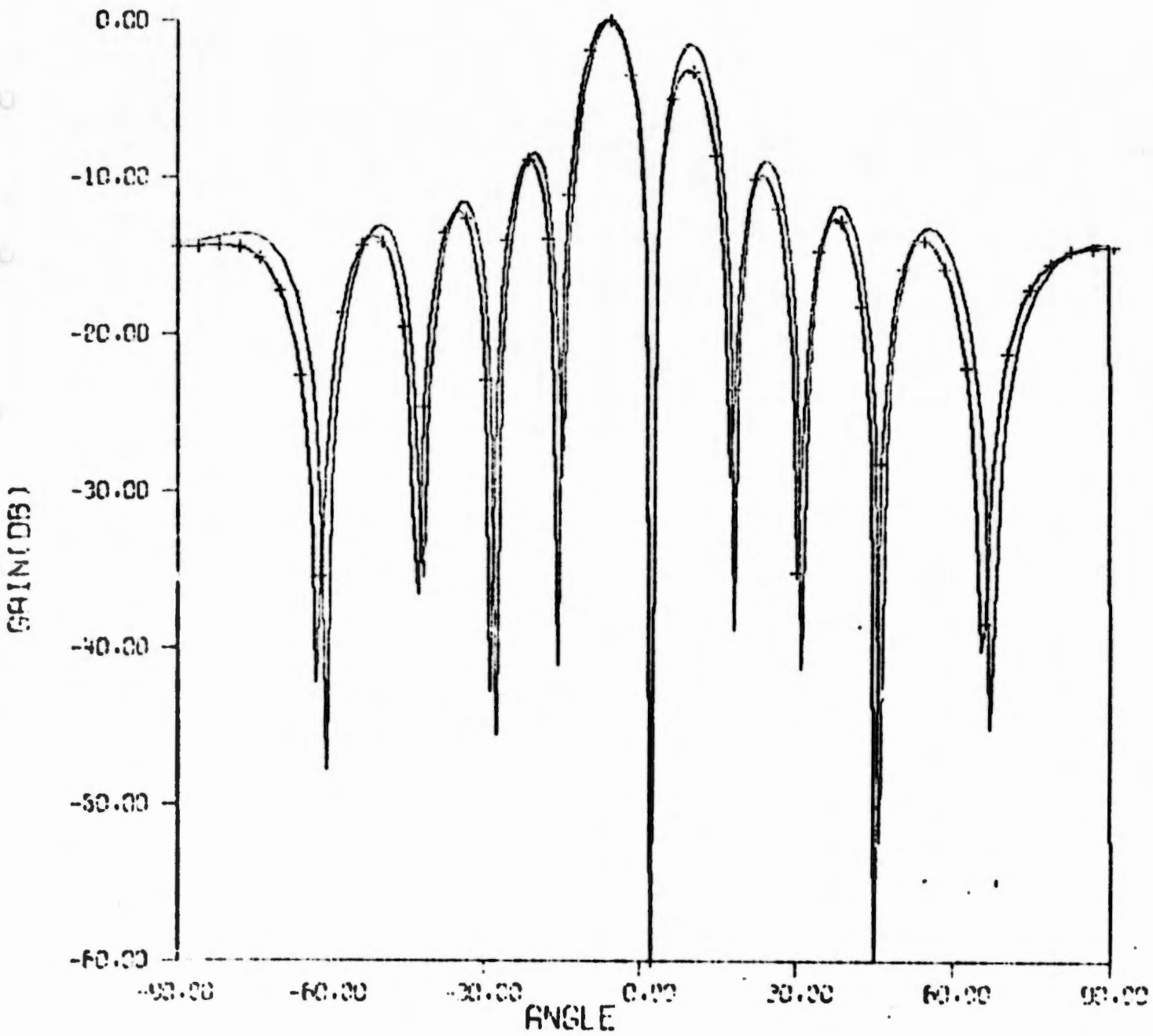

Figure 3b.

SUM AND DIFFERENCE PATTERNS - SYMMETRICAL PAIRS

10 elements λ/2 spacing 0° scan angle
1 jammer $\theta_j = 2°$ $P_j = 10^6$

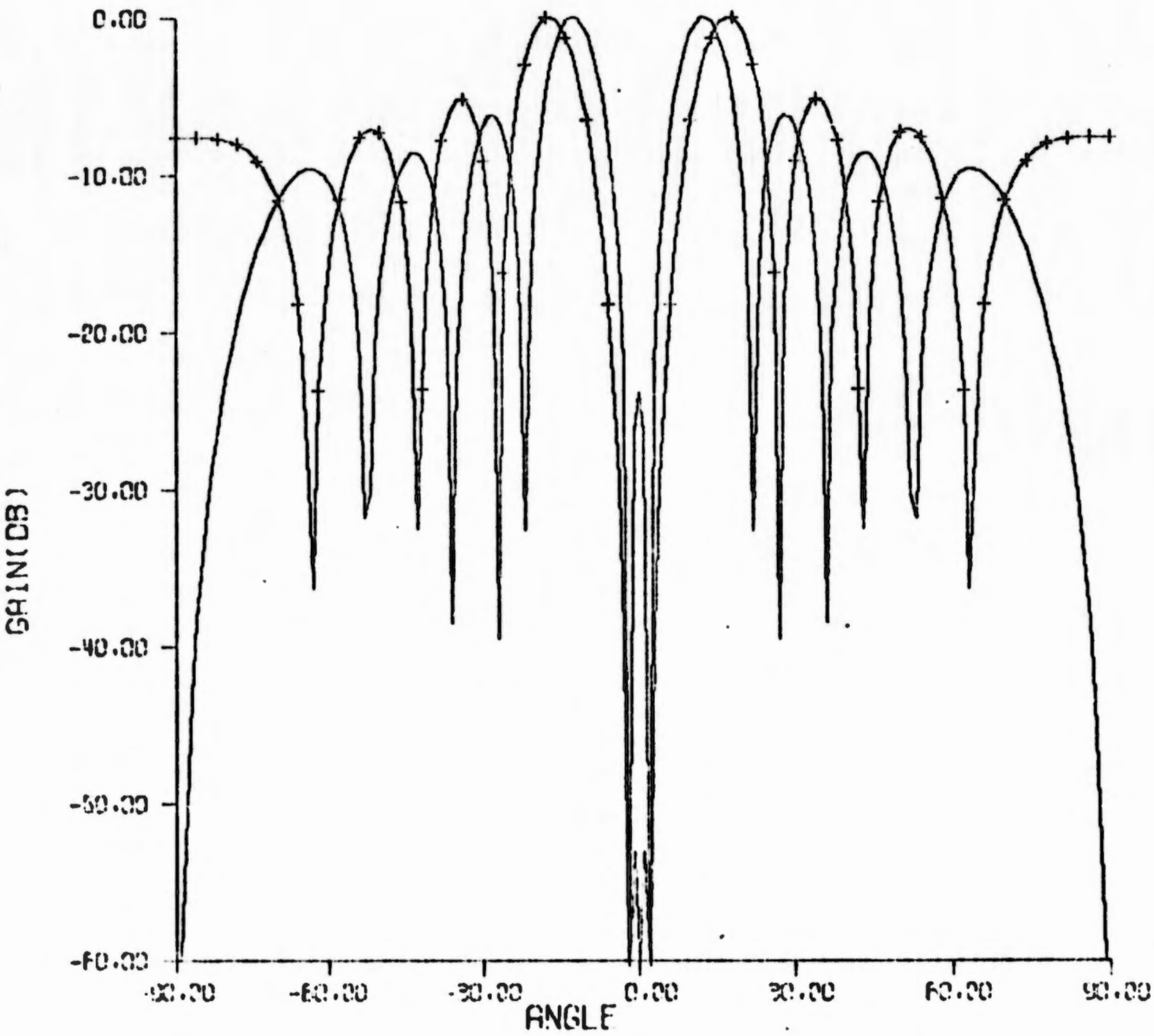

Figure 4a.

SUM AND DIFFERENCE PATTERNS - FULLY ADAPTIVE ARRAY

10 elements λ/2 spacing 0° scan angle
1 jammer $\theta_j = 4°$ $P_j = 10^5$

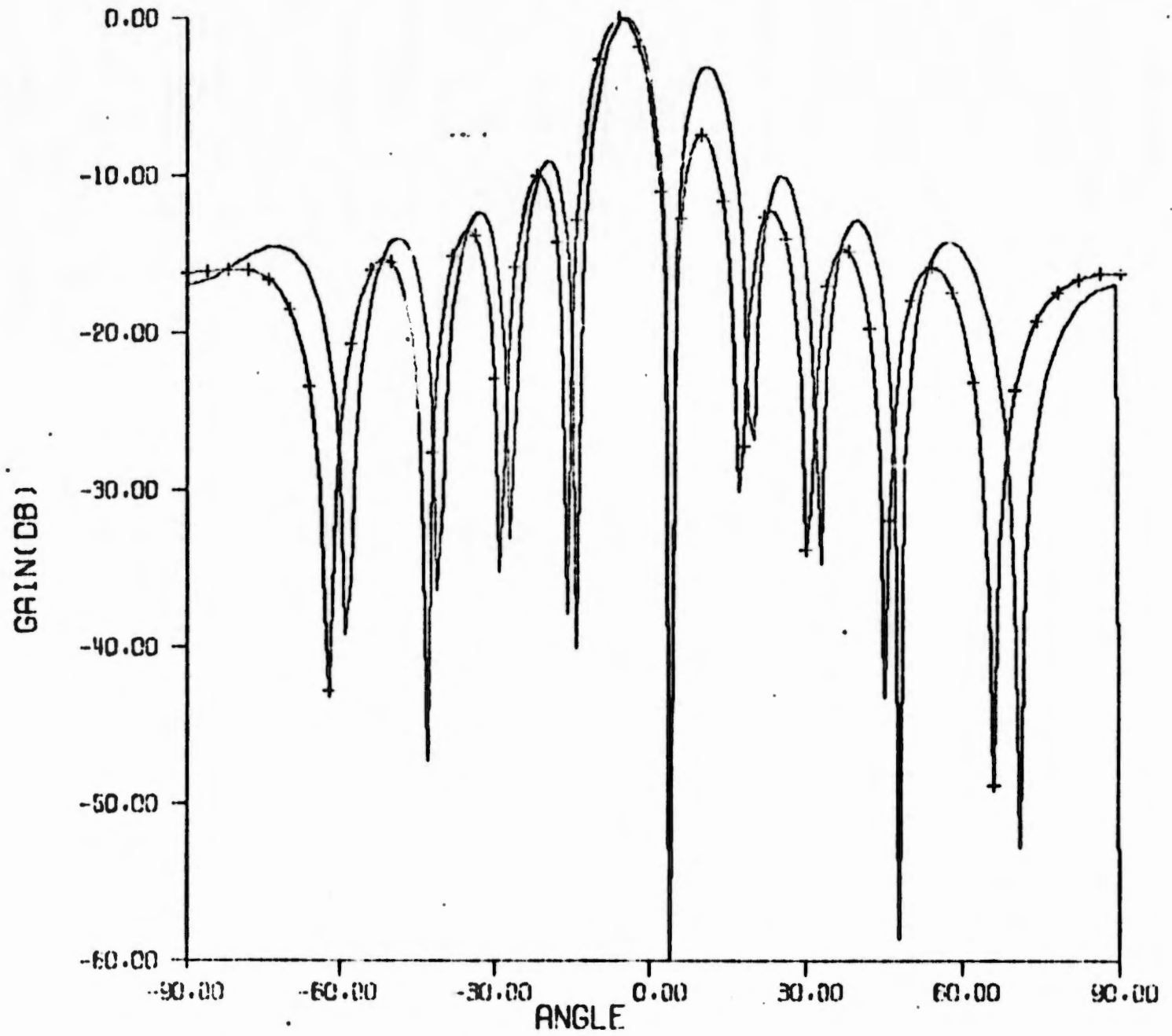

Figure 4b.

SUM AND DIFFERENCE PATTERNS - SYMMETRICAL PAIRS

10 elements λ/2 spacing 0° scan angle
1 jammer $\theta_j = 4°$ $P_j = 10^5$

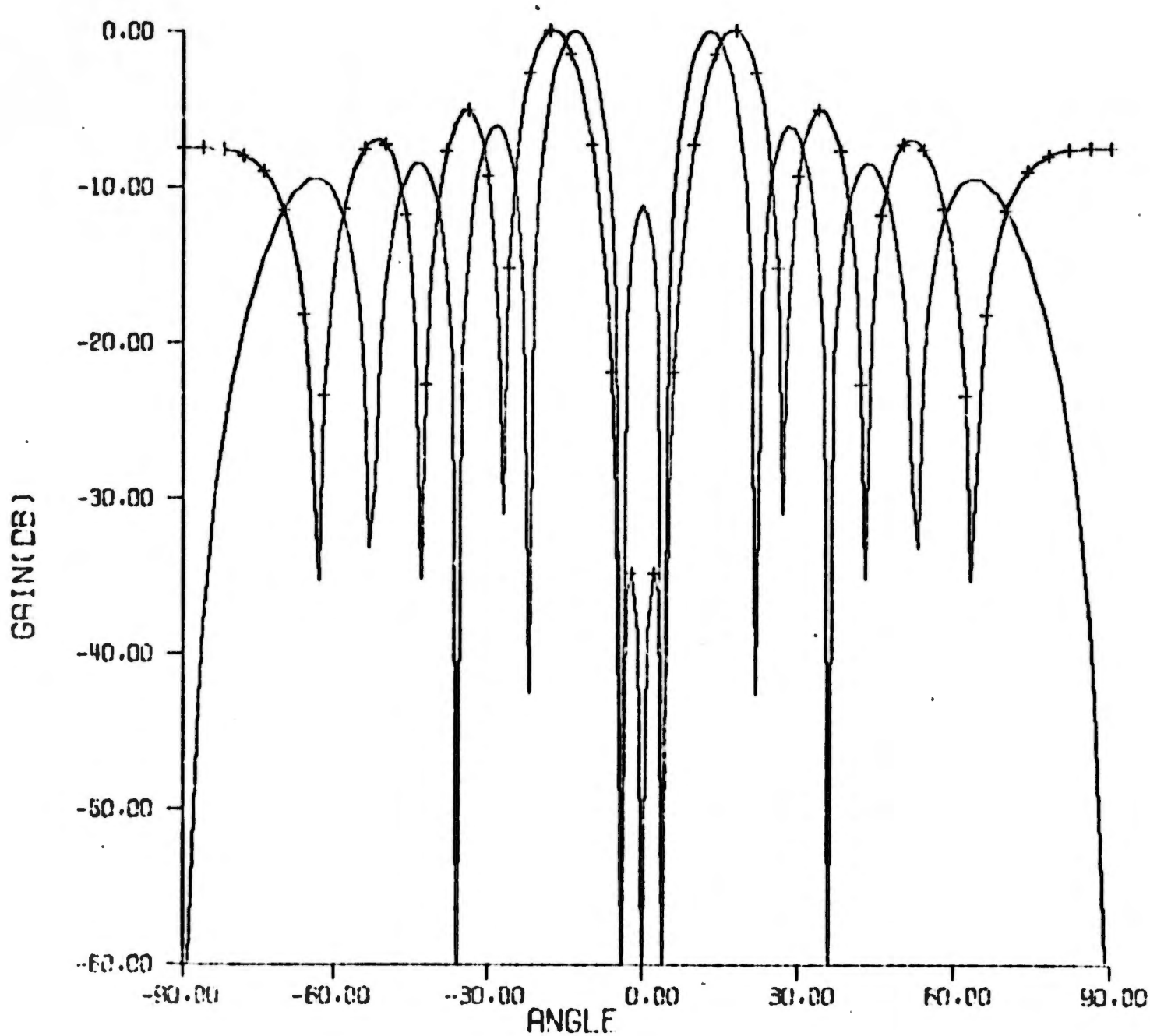

Figure 5a.

SUM AND DIFFERENCE PATTERNS - FULLY ADAPTIVE ARRAY

10 elements λ/2 spacing 0° scan angle
1 jammer $\theta_j = 6°$ $P_j = 10^5$

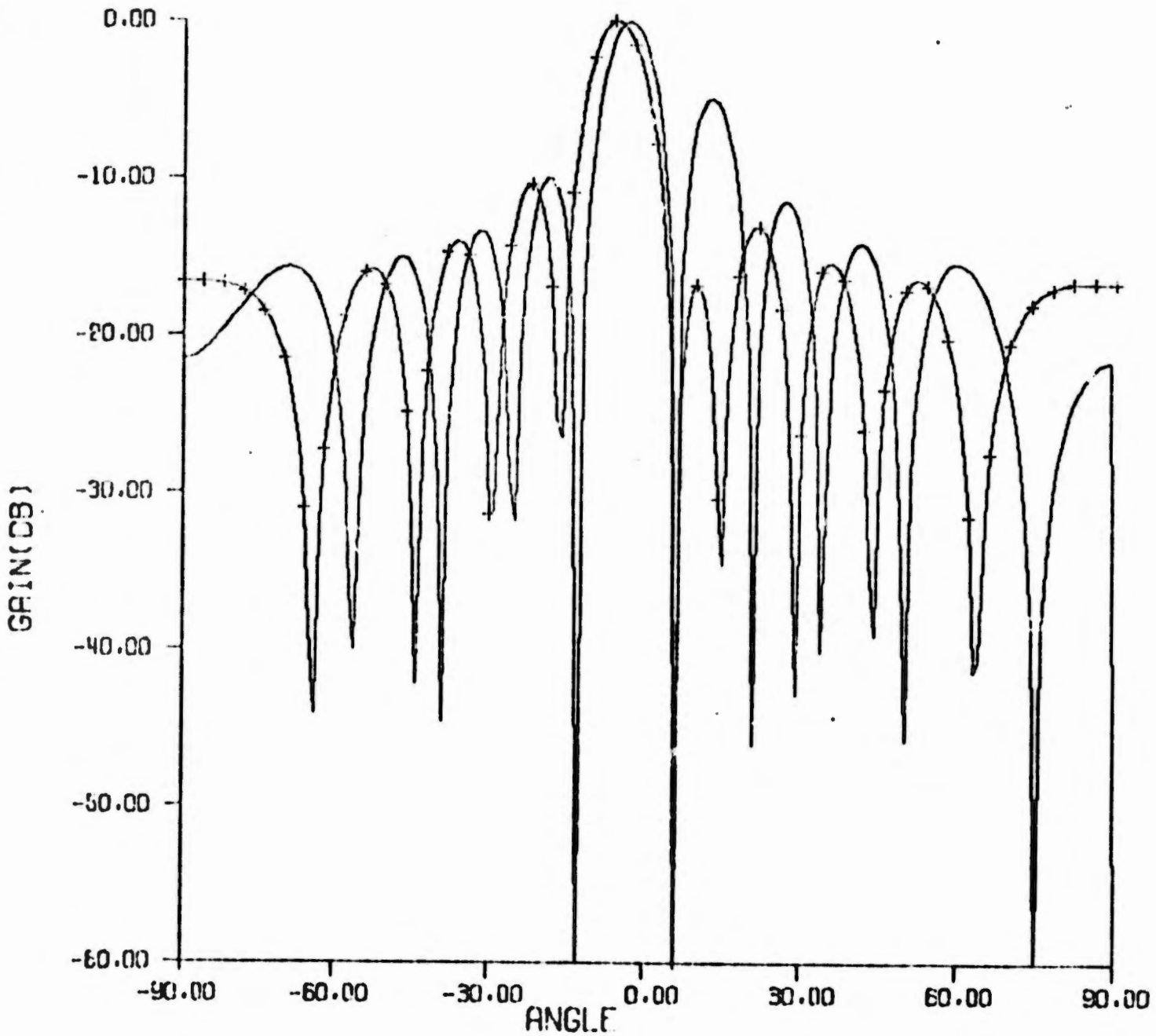

Figure 5b.

SUM AND DIFFERENCE PATTERNS - SYMMETRICAL PAIRS

10 elements λ/2 spacing 0° scan angle
1 jammer $\theta_j = 6°$ $P_j = 10^5$

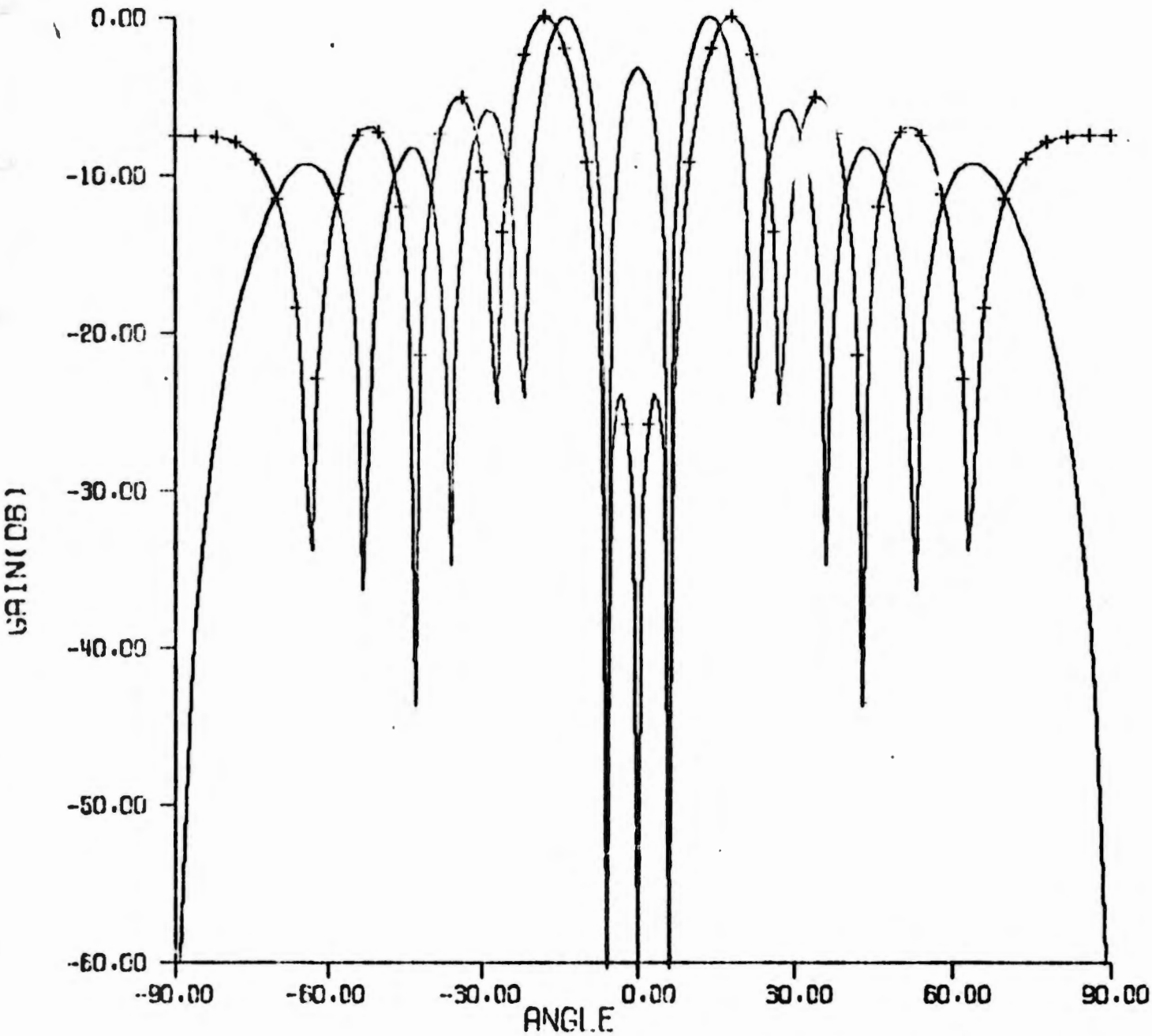

Figure 6a.

SUM AND DIFFERENCE PATTERNS - FULLY ADAPTIVE ARRAY

10 elements λ/2 spacing 0° scan angle
1 jammer $\theta_j = 8°$ $P_j = 10^5$

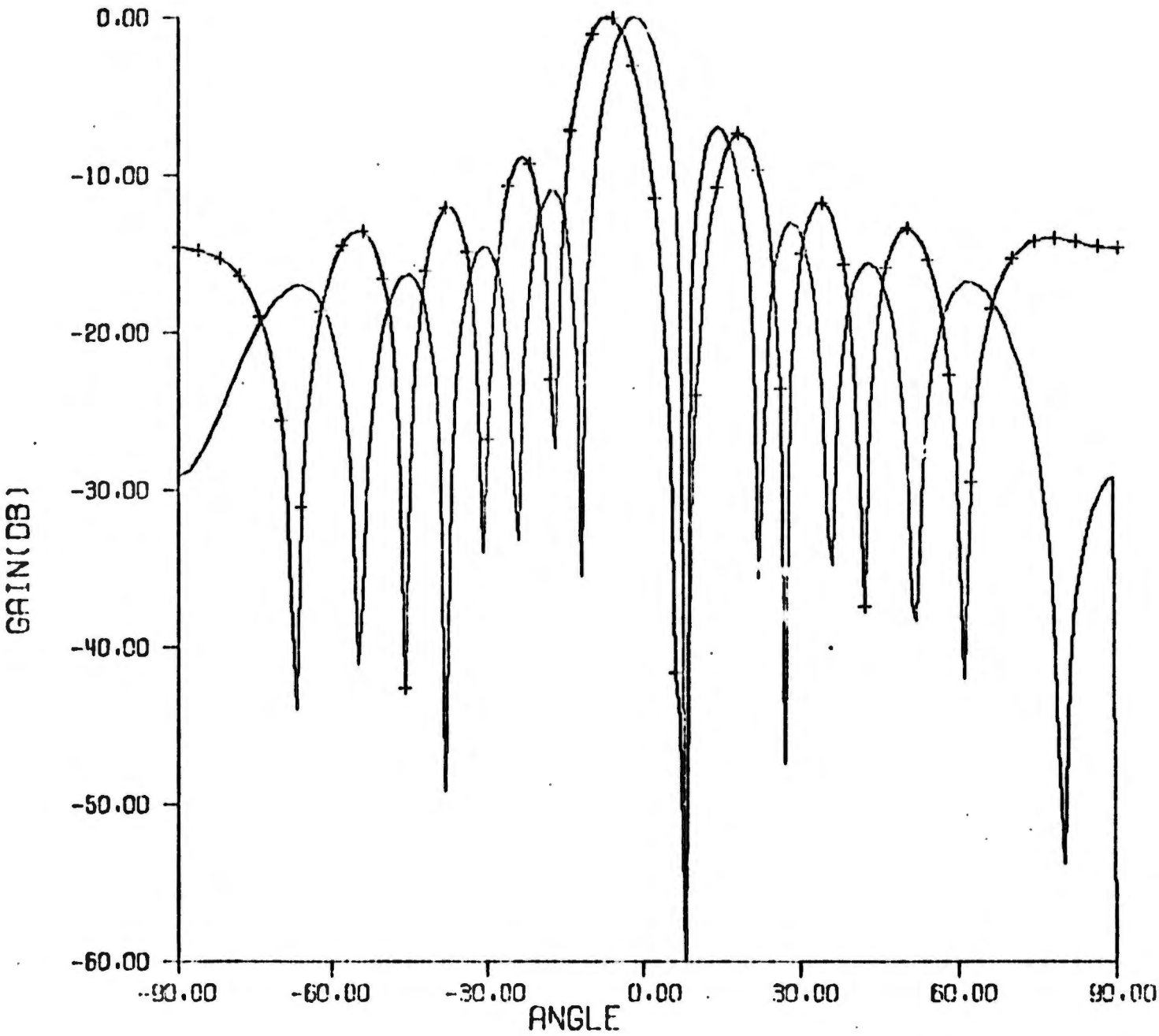

Figure 6b.

SUM AND DIFFERENCE PATTERNS - SYMMETRICAL PAIRS

10 elements λ/2 spacing 0° scan angle
1 jammer $\theta_j = 8°$ $P_j = 10^5$

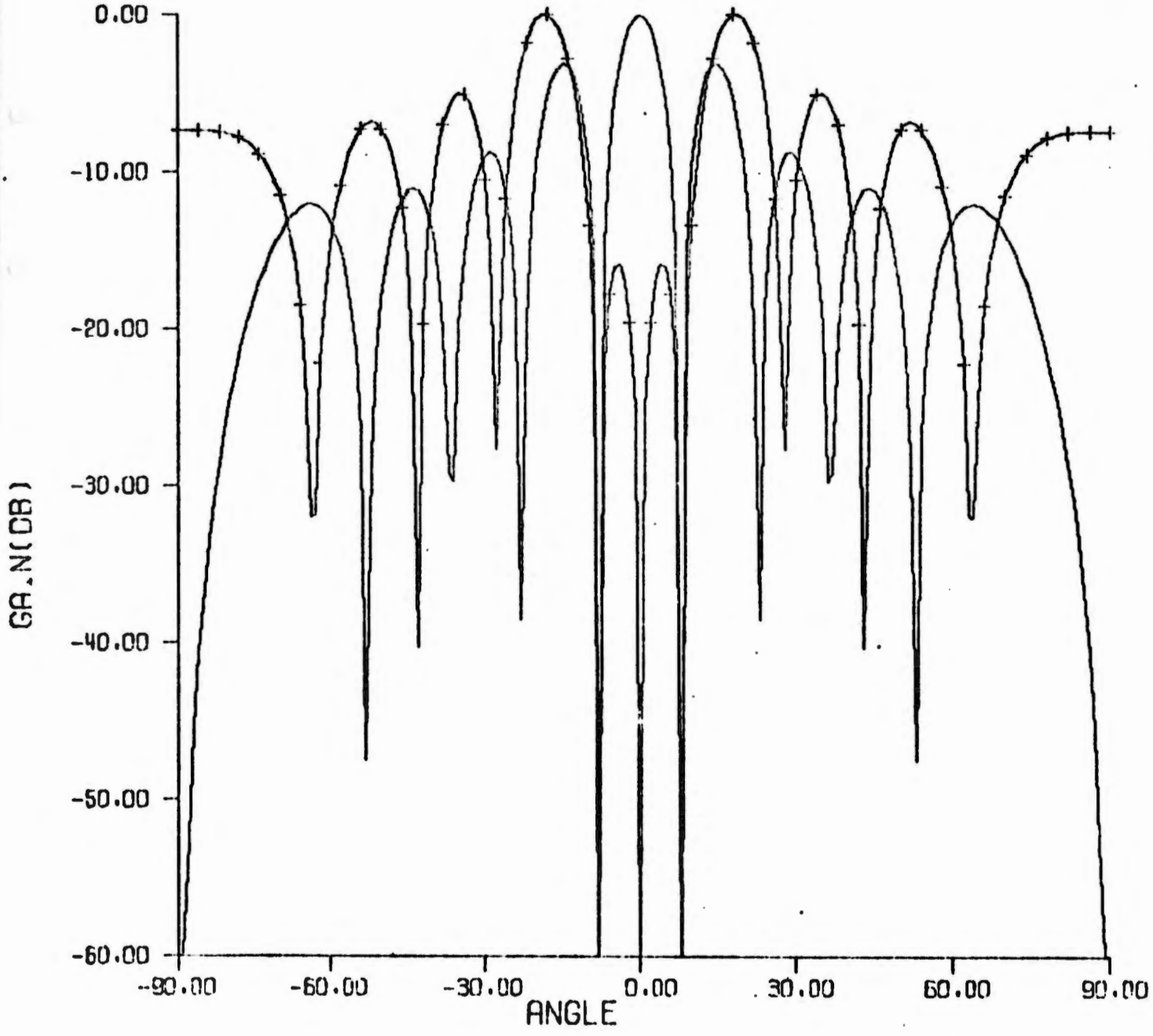

Figure 7a.

SUM AND DIFFERENCE PATTERNS - FULLY ADAPTIVE ARRAY

10 elements λ/2 spacing 0° scan angle
1 jammer $\theta_j = 10°$ $P_j = 10^5$

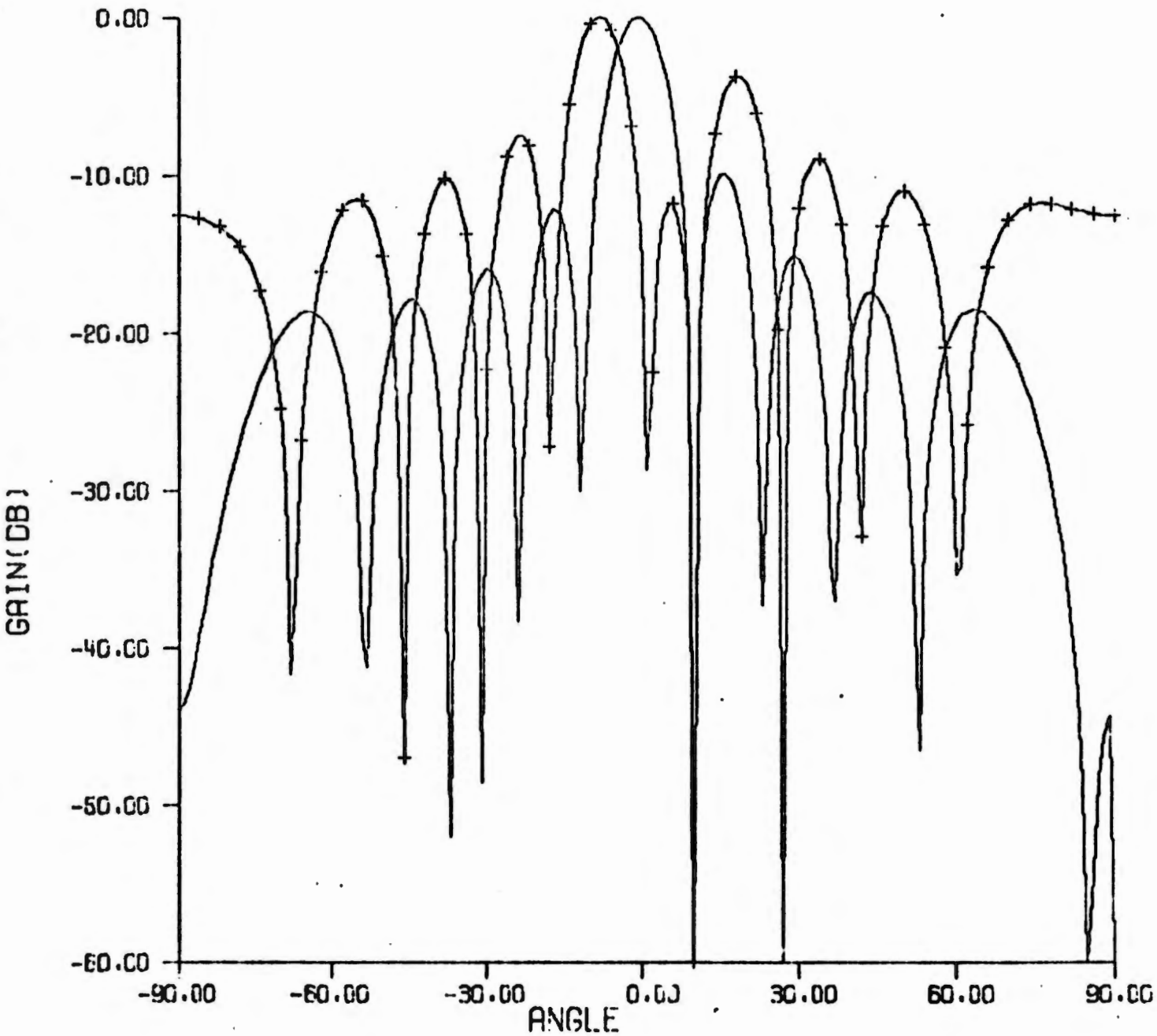

Figure 7b.

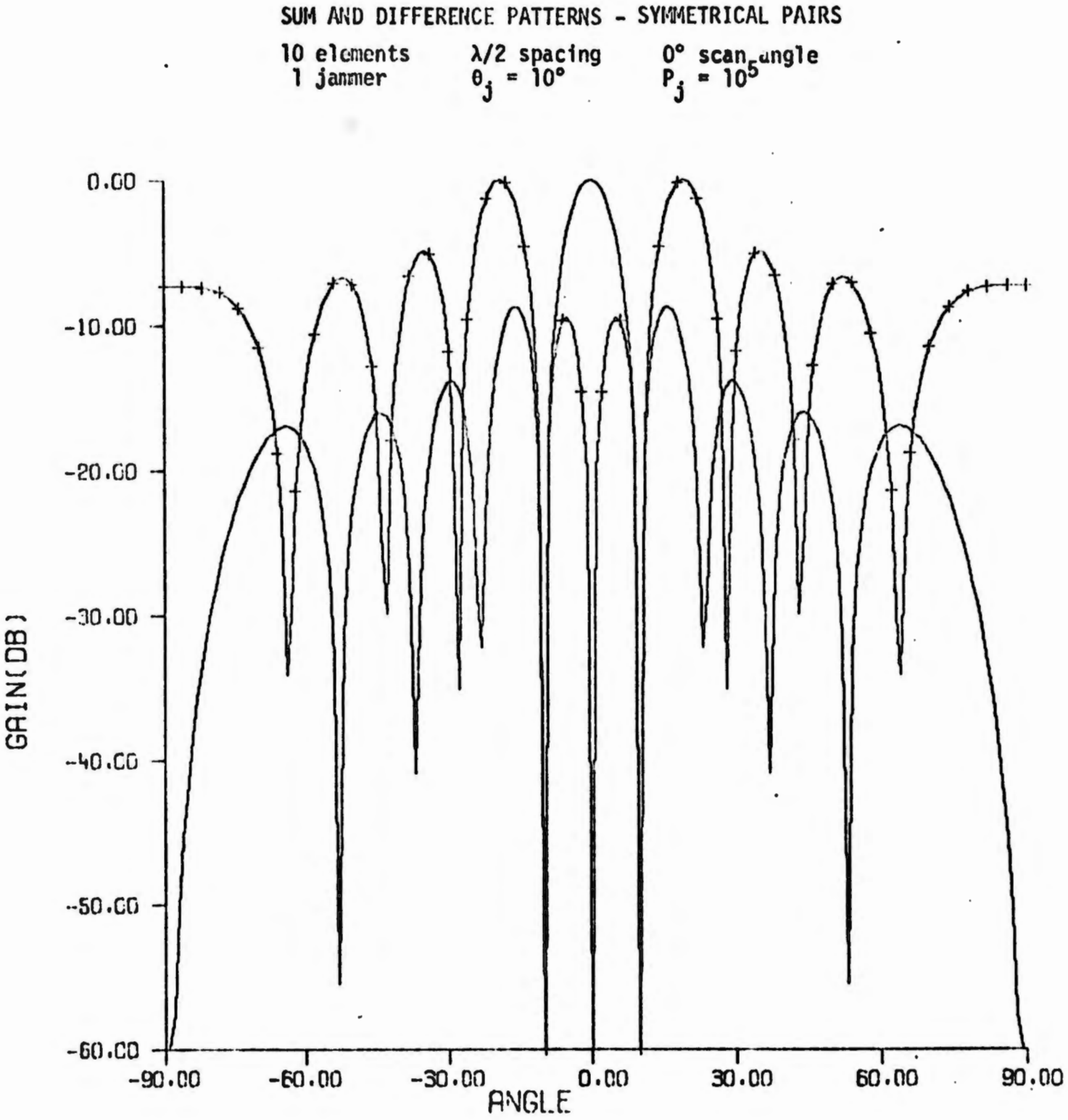
SUM AND DIFFERENCE PATTERNS - SYMMETRICAL PAIRS
10 elements
1 jammer
λ/2 spacing
θj = 10°
0° scan angle
Pj = 10^5
0.00
-10.00
-20.00
-30.00
-40.00
-50.00
-60.00
GAIN(DB)
-90.00
-60.00
-30.00
0.00
30.00
60.00
90.00
ANGLE

The angle estimator $-Q'/Q''$, Case 5, performs well at large S/N ratios. At small S/N ratios, the two estimators based on $-Q'/E(Q'')$ (i.e., Cases 3 and 6) provide better accuracy. The estimator of Case 5 performs poorly at low S/N ratios and is more complicated to implement, so it is not considered a useful algorithm for angle tracking.

The best results are obtained with the new maximum likelihood estimator of Eq. 8. As the results in Table I show, this estimator is considerably better at low S/N ratios than the Eq. 7 estimator developed earlier by R. Davis. At least for the difficult case of main beam jamming, the new algorithm of Case 6 provides the best accuracy.

The accuracy as a function of target location relative to boresight was investigated in each simulation run. One sample is shown in Table 2. The conclusions concerning the relative accuracy of the six tracking techniques are applicable for targets off the boresight angle, as well as the on-boresight configuration of Table 1.

Note in Table 1 that accuracy of the maximum likelihood estimators, Cases 3 and 6, improves as the jammer moves away from the 0° boresight angle. This would be expected, since the Σ and Δ beams each have more gain at the target angle when the null is further from boresight. This effect is more noticeable with symmetrical pairs, Case 4. For purposes of comparison, the rms error for this array in the absence of jamming is 1.43° at 0 dB S/N, .43° at 10 dB, .14 at 20 dB, and .044 at 30 dB. The degradation in accuracy due to a strong jammer at 10° is very small, as can be seen from Table 1. Considering the beam distortions which are evident in Figure 7a, it is apparent that the Case 3 and 6 estimators are very effective in compensating for beam distortion effects.

Table 2. Simulation of Tracking with Target Off-Boresight

TARGET ANGLE(DEG)=-1.00				
CASE 1	BIAS 5.34	ST DEV .099	RMS= 5.344	
CASE 2	BIAS -7.75	ST DEV .361	RMS= 7.758	
CASE 3	BIAS -.01	ST DEV 1.275	RMS= 1.275	
CASE 4	BIAS .35	ST DEV 10.443	RMS=10.449	
CASE 5	BIAS -.25	ST DEV 1.657	RMS= 1.656	
CASE 6	BIAS -.02	ST DEV 1.297	RMS= 1.297	
TARGET ANGLE(DEG)= -.50				
CASE 1	BIAS 4.85	ST DEV .108	RMS= 4.856	
CASE 2	BIAS -8.10	ST DEV .385	RMS= 8.109	
CASE 3	BIAS .13	ST DEV 1.645	RMS= 1.650	
CASE 4	BIAS 1.29	ST DEV 11.644	RMS=11.715	
CASE 5	BIAS -.05	ST DEV 1.920	RMS= 1.920	
CASE 6	BIAS .14	ST DEV 1.655	RMS= 1.661	
TARGET ANGLE(DEG)= 0.00				
CASE 1	BIAS 4.35	ST DEV .063	RMS= 4.351	
CASE 2	BIAS -8.52	ST DEV .333	RMS= 8.530	
CASE 3	BIAS -.04	ST DEV 1.447	RMS= 1.448	
CASE 4	BIAS -.07	ST DEV 8.391	RMS= 8.391	
CASE 5	BIAS -.15	ST DEV 1.600	RMS= 1.607	
CASE 6	BIAS -.03	ST DEV 1.432	RMS= 1.433	
TARGET ANGLE(DEG)= .50				
CASE 1	BIAS 3.8n	ST DEV .078	RMS= 3.861	
CASE 2	BIAS -8.9o	ST DEV .413	RMS= 8.972	
CASE 3	BIAS -.26	ST DEV 1.805	RMS= 1.824	
CASE 4	BIAS -.86	ST DEV 11.110	RMS=11.144	
CASE 5	BIAS -.05	ST DEV 3.149	RMS= 3.216	
CASE 6	BIAS -.27	ST DEV 1.778	RMS= 1.798	
TARGET ANGLE(DEG)= 1.00				
CASE 1	BIAS 3.36	ST DEV .078	RMS= 3.365	
CASE 2	BIAS -9.28	ST DEV .478	RMS= 9.291	
CASE 3	BIAS .71	ST DEV 2.[illegible]	RMS= 2.064	
CASE 4	BIAS .54	ST DEV 10.928	RMS=10.934	
CASE 5	BIAS -.07	ST DEV 2.254	RMS= 2.255	
CASE 6	BIAS .02	ST DEV 2.05[illegible]	RMS= 2.059	

S/N = 10 dB $\theta_J = 4°$ $J/N = 10^5$ 10 elements

The preceding results have considered only the single jammer problem. Multiple jammer results are discussed in the next section.

5. MULTIPLE JAMMERS

The first example of a simulation run with multiple jammers includes only sidelobe jamming. None of the jammers is near the main beam region. The patterns obtained with adaptive arrays and 3 jammers at -45°, 30°, and 60° respectively, are shown in Fig. 8. Note that deep nulls occur at the angles of jamming, due to the large J/N ratio of 50 dB. With symmetrical pairs, the three nulls occur on each side of boresight at jammer angles. Simulation results for 0 dB and 20 dB signal-to-noise ratio are shown in Tables 3a and 3b. Results of simulating the same 10 element array with no jamming are shown in Tables 3c and 3d for purposes of comparison. Note that the maximum likelihood tracker (Case 6) provides essentially the same accuracy in the presence of strong sidelobe jamming as a conventional tracker in the absence of jamming. The symmetrical pairs technique (Case 4) also performs well in the sidelobe jamming environment. Small differences in rms error between the sidelobe jamming and no jamming examples should be disregarded and are due to the small sample size in the simulation (100 samples).

The second example, with adapted antenna patterns illustrated in Fig. 9, includes two main beam jammers. These jammers are located at 4° and 6° and each has a J/N ratio of 50 dB. As expected, the patterns contain nulls at both jammer angles. Results for this two jammer example are contained in Table 4. The symmetrical pairs technique (Case 4) is much less effective than maximum likelihood estimators (Cases 3 and 6) in this example. Referring to Table 1 and the single jammer cases, it is clear that 2 jammers in the main beam (4° and 6°) degrade the accuracy much more than a single jammer at either of these angles. For example,

Figure 8a.

SUM AND DIFFERENCE PATTERNS - FULLY ADAPTIVE ARRAY

10 elements	λ/2 spacing	0° scan angle
3 jammers	θ_J = -45°	$P_J = 10^5$
	30°	10^5
	60°	10^5

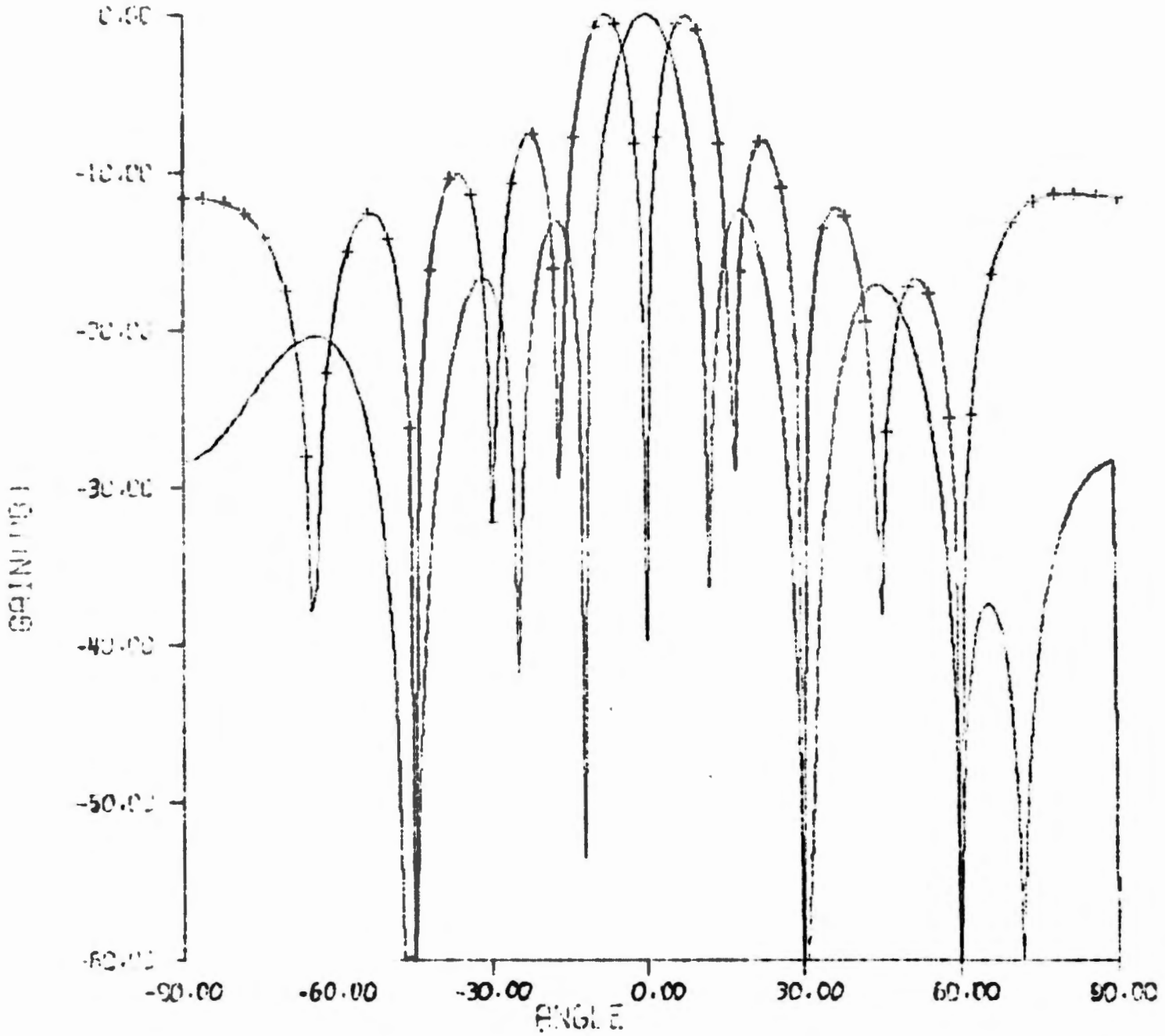

Figure 8b.

SUM AND DIFFERENCE PATTERNS - SYMMETRICAL PAIRS

10 elements	$\lambda/2$ spacing	0° scan angle
3 jammers	θ_J = -45°	$P_J = 10^5$
	30°	10^5
	60°	10^5

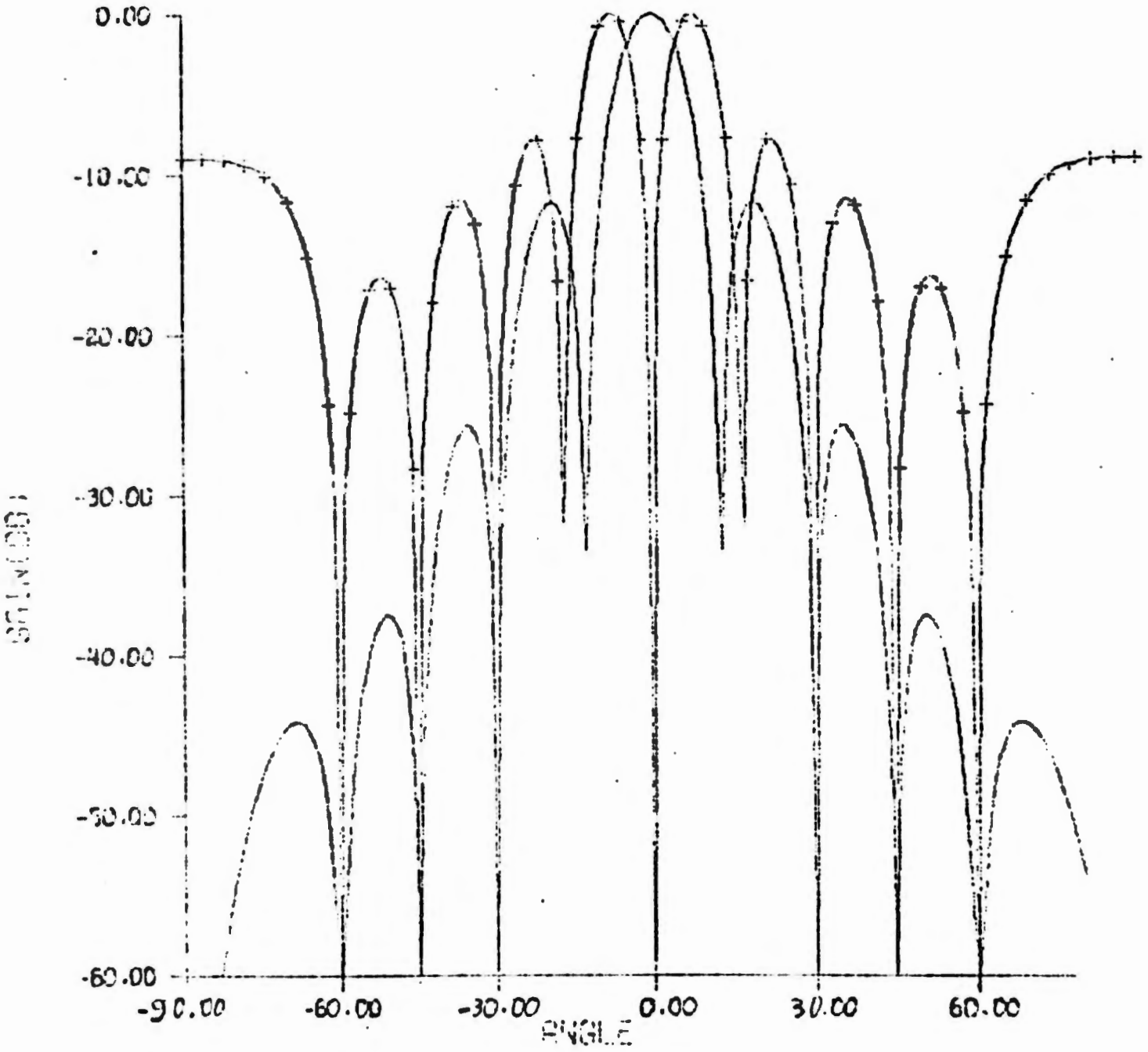

Figure 3a.

Simulation Results with 3 Sidelobe Jammers (S/N = 0 dB)

SIGNAL-TO-NOISE RATIO(DB) 0.000

TARGET ANGLE(DEG)=-1.00

CASE 1 BIAS	.02	ST DEV	3.836	RMS= 3.836
CASE 2 BIAS	-.01	ST DEV	1.711	RMS= 1.711
CASE 3 BIAS	-.04	ST DEV	1.629	RMS= 1.629
CASE 4 BIAS	-.02	ST DEV	1.664	RMS= 1.665
CASE 5 BIAS	.24	ST DEV	4.595	RMS= 4.601
CASE 6 BIAS	-.03	ST DEV	1.654	RMS= 1.654

TARGET ANGLE(DEG)= -.50

CASE 1 BIAS	-.40	ST DEV	6.546	RMS= 6.559
CASE 2 BIAS	-.05	ST DEV	1.770	RMS= 1.771
CASE 3 BIAS	-.05	ST DEV	1.867	RMS= 1.868
CASE 4 BIAS	-.08	ST DEV	1.734	RMS= 1.735
CASE 5 BIAS	-1.32	ST DEV	9.463	RMS= 9.555
CASE 6 BIAS	-.08	ST DEV	1.711	RMS= 1.713

TARGET ANGLE(DEG)= 0.00

CASE 1 BIAS	-1.21	ST DEV	3.279	RMS= 3.494
CASE 2 BIAS	-.16	ST DEV	1.476	RMS= 1.485
CASE 3 BIAS	-.21	ST DEV	1.496	RMS= 1.510
CASE 4 BIAS	-.21	ST DEV	1.442	RMS= 1.457
CASE 5 BIAS	-.11	ST DEV	2.082	RMS= 2.085
CASE 6 BIAS	-.21	ST DEV	1.427	RMS= 1.442

TARGET ANGLE(DEG)= .50

CASE 1 BIAS	-1.48	ST DEV	5.292	RMS= 5.496
CASE 2 BIAS	.05	ST DEV	1.549	RMS= 1.549
CASE 3 BIAS	-.00	ST DEV	1.550	RMS= 1.550
CASE 4 BIAS	-.01	ST DEV	1.507	RMS= 1.507
CASE 5 BIAS	.05	ST DEV	2.956	RMS= 2.957
CASE 6 BIAS	-.01	ST DEV	1.497	RMS= 1.497

TARGET ANGLE(DEG)= 1.00

CASE 1 BIAS	-2.45	ST DEV	4.820	RMS= 5.406
CASE 2 BIAS	.23	ST DEV	1.544	RMS= 1.551
CASE 3 BIAS	.12	ST DEV	1.668	RMS= 1.669
CASE 4 BIAS	.14	ST DEV	1.432	RMS= 1.436
CASE 5 BIAS	-7.11	ST DEV	54.957	RMS=57.409
CASE 6 BIAS	.14	ST DEV	1.483	RMS= 1.489

Scan angle = 0° 10 elements $\lambda/2$ spacing Results in degrees
3 jammers -45°,30°,60° all J/N = 10^5

Table 3b.

Simulation Results with 3 Sidelobe Jammers (S/N = 20 dB)

SIGNAL-TO-NOISE RATIO(DB) 20.000

TARGET ANGLE(DEG)=-1.00

CASE 1 BIAS	-.44	ST DEV	7.660	RMS= 7.673
CASE 2 BIAS	.03	ST DEV	.157	RMS= .160
CASE 3 BIAS	.03	ST DEV	.141	RMS= .145
CASE 4 BIAS	.01	ST DEV	.152	RMS= .153
CASE 5 BIAS	-.03	ST DEV	.168	RMS= .171
CASE 6 BIAS	.01	ST DEV	.152	RMS= .152

TARGET ANGLE(DEG)= -.50

CASE 1 BIAS	-.53	ST DEV	4.998	RMS= 4.927
CASE 2 BIAS	.04	ST DEV	.140	RMS= .145
CASE 3 BIAS	.01	ST DEV	.133	RMS= .133
CASE 4 BIAS	.01	ST DEV	.136	RMS= .136
CASE 5 BIAS	-.00	ST DEV	.139	RMS= .139
CASE 6 BIAS	.00	ST DEV	.135	RMS= .135

TARGET ANGLE(DEG)= 0.00

CASE 1 BIAS	-2.09	ST DEV	5.572	RMS= 5.950
CASE 2 BIAS	.03	ST DEV	.155	RMS= .159
CASE 3 BIAS	-.02	ST DEV	.150	RMS= .152
CASE 4 BIAS	-.02	ST DEV	.151	RMS= .153
CASE 5 BIAS	-.02	ST DEV	.151	RMS= .152
CASE 6 BIAS	-.02	ST DEV	.150	RMS= .152

TARGET ANGLE(DEG)= .50

CASE 1 BIAS	-.95	ST DEV	5.881	RMS= 5.957
CASE 2 BIAS	.08	ST DEV	.140	RMS= .160
CASE 3 BIAS	.00	ST DEV	.133	RMS= .133
CASE 4 BIAS	.01	ST DEV	.136	RMS= .137
CASE 5 BIAS	.01	ST DEV	.137	RMS= .137
CASE 6 BIAS	.01	ST DEV	.136	RMS= .136

TARGET ANGLE(DEG)= 1.00

CASE 1 BIAS	-3.09	ST DEV	6.393	RMS= 7.291
CASE 2 BIAS	.10	ST DEV	.140	RMS= .177
CASE 3 BIAS	-.01	ST DEV	.130	RMS= .131
CASE 4 BIAS	.01	ST DEV	.142	RMS= .142
CASE 5 BIAS	.08	ST DEV	.153	RMS= .160
CASE 6 BIAS	.01	ST DEV	.141	RMS= .141

Scan angle = 0° 10 elements λ/2 spacing Results in degrees
3 jammers -45°,30°,60° All J/N = 10^5

Table 3c

Simulation Results without Jamming (S/N = 0 dB)

SIGNAL-TO-NOISE RATIO(DB) 0.000

TARGET ANGLE(DEG)=-1.00

CASE 1 BIAS	-.15	ST DEV	1.371	RMS= 1.379
CASE 2 BIAS	-.15	ST DEV	1.371	RMS= 1.379
CASE 3 BIAS	-.15	ST DEV	1.309	RMS= 1.318
CASE 4 BIAS	-.15	ST DEV	1.371	RMS= 1.379
CASE 5 BIAS	-.45	ST DEV	2.410	RMS= 2.451
CASE 6 BIAS	-.15	ST DEV	1.371	RMS= 1.379

TARGET ANGLE(DEG)= -.50

CASE 1 BIAS	-.02	ST DEV	1.391	RMS= 1.391
CASE 2 BIAS	-.02	ST DEV	1.391	RMS= 1.391
CASE 3 BIAS	-.01	ST DEV	1.620	RMS= 1.620
CASE 4 BIAS	-.02	ST DEV	1.391	RMS= 1.391
CASE 5 BIAS	-.31	ST DEV	2.467	RMS= 2.486
CASE 6 BIAS	-.02	ST DEV	1.391	RMS= 1.391

TARGET ANGLE(DEG)= 0.00

CASE 1 BIAS	.24	ST DEV	1.355	RMS= 1.376
CASE 2 BIAS	.24	ST DEV	1.355	RMS= 1.376
CASE 3 BIAS	.34	ST DEV	1.729	RMS= 1.763
CASE 4 BIAS	.24	ST DEV	1.355	RMS= 1.376
CASE 5 BIAS	1.47	ST DEV	11.176	RMS=11.272
CASE 6 BIAS	.24	ST DEV	1.355	RMS= 1.376

TARGET ANGLE(DEG)= .50

CASE 1 BIAS	.07	ST DEV	1.746	RMS= 1.748
CASE 2 BIAS	.07	ST DEV	1.746	RMS= 1.748
CASE 3 BIAS	.09	ST DEV	1.677	RMS= 1.680
CASE 4 BIAS	.07	ST DEV	1.746	RMS= 1.748
CASE 5 BIAS	-.10	ST DEV	8.577	RMS= 8.578
CASE 6 BIAS	.07	ST DEV	1.746	RMS= 1.748

TARGET ANGLE(DEG)= 1.00

CASE 1 BIAS	.01	ST DEV	1.730	RMS= 1.730
CASE 2 BIAS	.01	ST DEV	1.730	RMS= 1.730
CASE 3 BIAS	-.01	ST DEV	1.655	RMS= 1.655
CASE 4 BIAS	.01	ST DEV	1.730	RMS= 1.730
CASE 5 BIAS	1.55	ST DEV	16.564	RMS=16.641
CASE 6 BIAS	.01	ST DEV	1.730	RMS= 1.730

Scan angle = 0° 10 elements λ/2 spacing No jamming
Results in degrees

Table 3d.

Simulation Results without Jamming (S/N = 20 dB)

SIGNAL-TO-NOISE RATIO(DB) 20.000

TARGET ANGLE(DEG)=-1.00

CASE 1 BIAS	.00	ST DEV	.153	RMS= .153
CASE 2 BIAS	.00	ST DEV	.153	RMS= .153
CASE 3 BIAS	.03	ST DEV	.142	RMS= .145
CASE 4 BIAS	.00	ST DEV	.153	RMS= .153
CASE 5 BIAS	.03	ST DEV	.170	RMS= .173
CASE 6 BIAS	.00	ST DEV	.153	RMS= .153

TARGET ANGLE(DEG)= -.50

CASE 1 BIAS	.02	ST DEV	.122	RMS= .123
CASE 2 BIAS	.02	ST DEV	.122	RMS= .123
CASE 3 BIAS	.02	ST DEV	.120	RMS= .122
CASE 4 BIAS	.02	ST DEV	.122	RMS= .123
CASE 5 BIAS	.01	ST DEV	.126	RMS= .127
CASE 6 BIAS	.02	ST DEV	.122	RMS= .123

TARGET ANGLE(DEG)= 0.00

CASE 1 BIAS	-.02	ST DEV	.151	RMS= .152
CASE 2 BIAS	-.02	ST DEV	.151	RMS= .152
CASE 3 BIAS	-.02	ST DEV	.151	RMS= .152
CASE 4 BIAS	-.02	ST DEV	.151	RMS= .152
CASE 5 BIAS	-.02	ST DEV	.151	RMS= .152
CASE 6 BIAS	-.02	ST DEV	.151	RMS= .152

TARGET ANGLE(DEG)= .50

CASE 1 BIAS	.00	ST DEV	.144	RMS= .144
CASE 2 BIAS	.00	ST DEV	.144	RMS= .144
CASE 3 BIAS	-.00	ST DEV	.142	RMS= .142
CASE 4 BIAS	.00	ST DEV	.144	RMS= .144
CASE 5 BIAS	.01	ST DEV	.148	RMS= .148
CASE 6 BIAS	.00	ST DEV	.144	RMS= .144

TARGET ANGLE(DEG)= 1.00

CASE 1 BIAS	.02	ST DEV	.139	RMS= .140
CASE 2 BIAS	.02	ST DEV	.139	RMS= .140
CASE 3 BIAS	-.01	ST DEV	.128	RMS= .128
CASE 4 BIAS	.02	ST DEV	.139	RMS= .140
CASE 5 BIAS	.06	ST DEV	.153	RMS= .165
CASE 6 BIAS	.02	ST DEV	.139	RMS= .140

Scan angle = 0° 10 elements λ/2 spacing No jamming
Results in degrees

Figure 9a.

SUM AND DIFFERENCE PATTERNS - FULLY ADAPTIVE ARRAY

10 elements λ/2 spacing 0° scan angle
2 jammers θ_J = 4° $P_J = 10^5$
6° 10^5

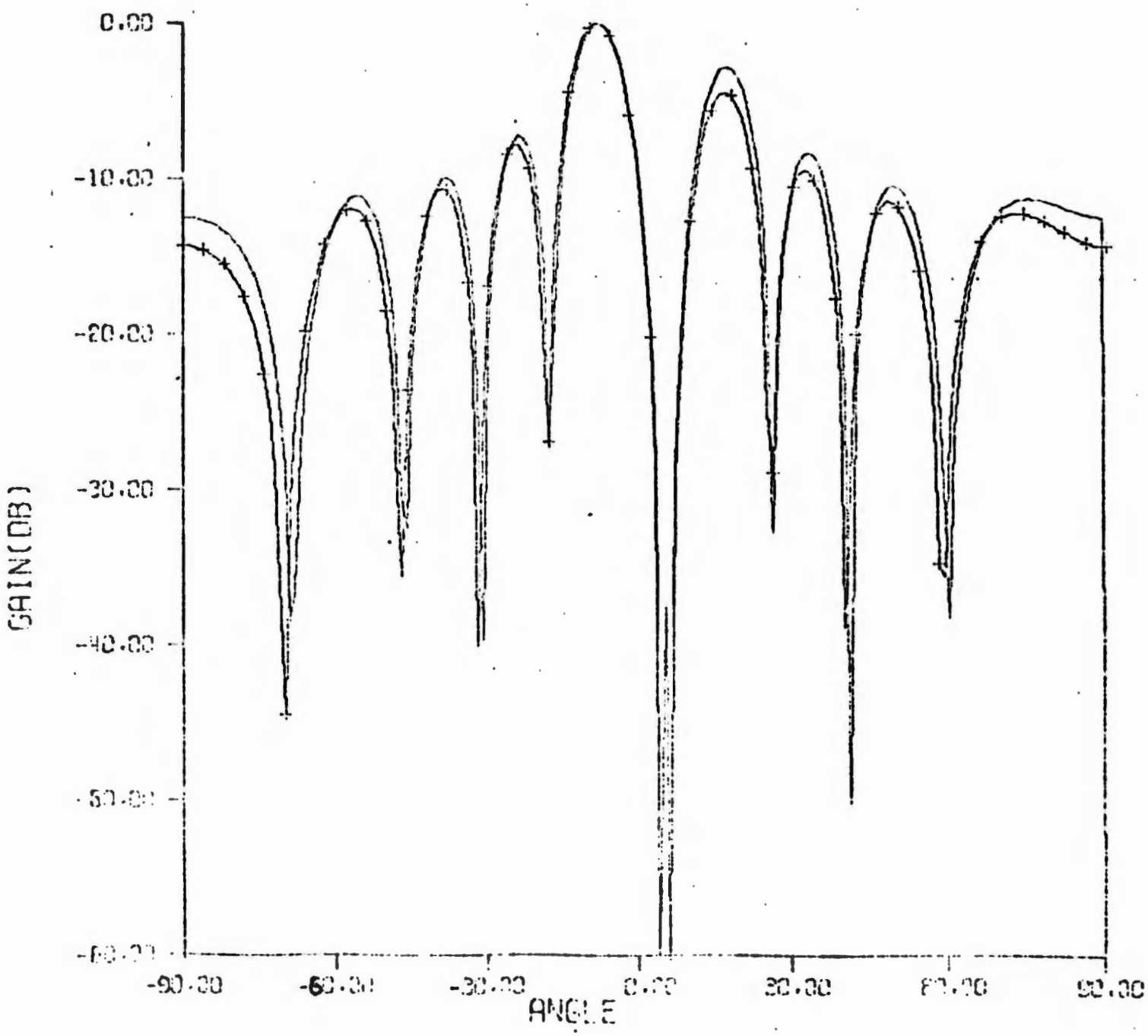

Figure 9b.

SUM AND DIFFERENCE PATTERNS - SYMMETRICAL PAIRS

10 elements λ/2 spacing 0° scan angle
2 jammers θ_J = 4° $P_J = 10^5$
6° 10^5

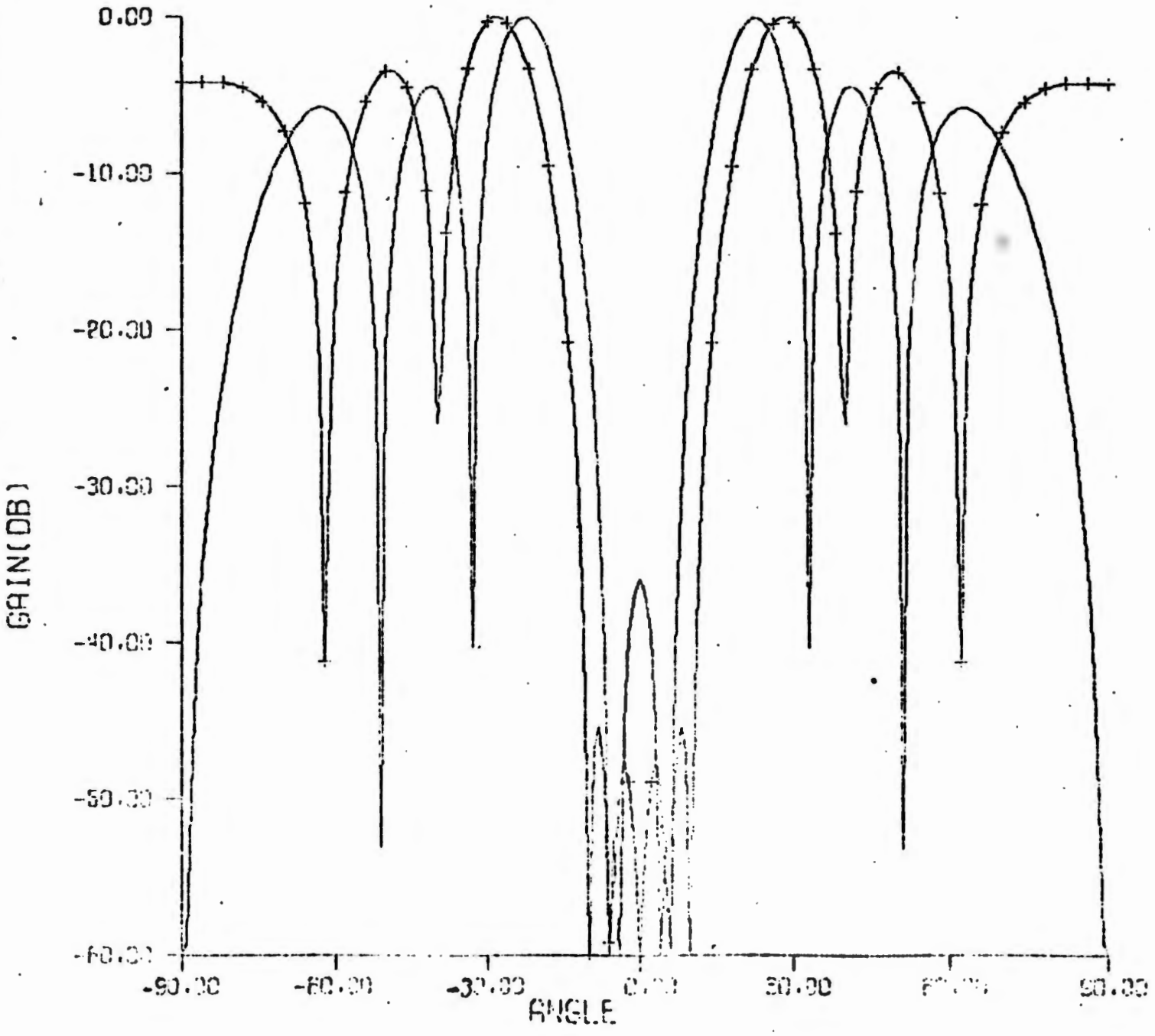

Table 4

Simulation Results with 2 Main Beam Jammers

SIGNAL-TO-NOISE RATIO(DB) 20,000

TARGET ANGLE(DEG)=-1,00

CASE 1	BIAS 6,28	ST DEV 4,292	RMS= 7,604
CASE 2	BIAS -14,24	ST DEV ,139	RMS=14,237
CASE 3	BIAS -,11	ST DEV 1,447	RMS= 1,451
CASE 4	BIAS -5,38	ST DEV 80,534	RMS=80,714
CASE 5	BIAS -,30	ST DEV 1,658	RMS= 1,685
CASE 6	BIAS -,11	ST DEV 1,461	RMS= 1,465

TARGET ANGLE(DEG)= -,50

CASE 1	BIAS 5,84	ST DEV 2,575	RMS= 6,380
CASE 2	BIAS -14,66	ST DEV ,164	RMS=14,657
CASE 3	BIAS ,24	ST DEV 1,717	RMS= 1,733
CASE 4	BIAS 7,32	ST DEV 18,643	RMS=20,028
CASE 5	BIAS ,16	ST DEV 1,906	RMS= 1,913
CASE 6	BIAS ,24	ST DEV 1,724	RMS= 1,741

TARGET ANGLE(DEG)= 0,00

CASE 1	BIAS 5,43	ST DEV 3,218	RMS= 6,314
CASE 2	BIAS -15,13	ST DEV ,193	RMS=15,126
CASE 3	BIAS ,06	ST DEV 2,036	RMS= 2,036
CASE 4	BIAS -,16	ST DEV 28,442	RMS=28,443
CASE 5	BIAS -,09	ST DEV 2,116	RMS= 2,118
CASE 6	BIAS ,06	ST DEV 2,025	RMS= 2,026

TARGET ANGLE(DEG)= ,50

CASE 1	BIAS 4,60	ST DEV 2,482	RMS= 5,230
CASE 2	BIAS -15,60	ST DEV ,207	RMS=15,604
CASE 3	BIAS -,20	ST DEV 2,203	RMS= 2,212
CASE 4	BIAS 5,04	ST DEV 22,292	RMS=22,854
CASE 5	BIAS -,39	ST DEV 2,446	RMS= 2,476
CASE 6	BIAS -,20	ST DEV 2,175	RMS= 2,185

TARGET ANGLE(DEG)= 1,00

CASE 1	BIAS 5,08	ST DEV 3,359	RMS= 6,090
CASE 2	BIAS -16,07	ST DEV ,302	RMS=16,073
CASE 3	BIAS -,59	ST DEV 3,101	RMS= 3,125
CASE 4	BIAS 6,03	ST DEV 23,322	RMS=24,089
CASE 5	BIAS -1,12	ST DEV 5,508	RMS= 5,621
CASE 6	BIAS -,36	ST DEV 3,173	RMS= 3,193

Scan Angle = 0° 10 elements $\lambda/2$ spacing Results in degrees

2 Jammers 4°, 6° each $J/N = 10^5$ (Figure 9)

with a single jammer at 4° and S/N = 20 dB, the rms error for Case 6 is .52°. With two main beam jammers (4° and 6°), the corresponding rms error is 2°. It is also interesting to note in Table 4 that angular error increases as the target approaches the jammers. The rms error for a target at -1° is 1.4° and increases monotonically to 3.2° as the target traverses the interval from -1° to +1°.

The next example of multiple jammers illustrates the effect of continuously distributed interference near the main beam. In this example there are 5 strong interference sources (J/N = 50 dB) at angles of 12°, 14°, 16°, 18°, and 20° respectively. Figure 10 shows the adapted antenna patterns for this environment and a 0° scan angle. With symmetrical pairs, the low gain region occurs on both sides of boresight (see Fig. 10b) resulting in low Σ and Δ beam gains. As shown in Table 5, the accuracy achieved using symmetrical pairs (Case 4) is poor relative to the maximum likelihood estimators (Cases 3, 5, and 6). Because of the large S/N ratio of 20 dB, the three likelihood estimators are roughly equal in performance. Note that the Σ and Δ fully adaptive patterns in Fig. 10a are nearly identical in amplitude in the region around boresight (0°).

The same jamming environment is assumed in the next example of Fig. 11, except that the scan angle is -6°. The boresight angle has been scanned away from the region of interference. As a result the Σ and Δ patterns of Fig. 11a differ more than the corresponding patterns in Fig. 10a. Also, the gain of the symmetrical pairs patterns of Fig. 11b is larger than the corresponding gain of Fig. 10b for 0° boresight angle. Results of simulating the distributed interference (12°-20°) with a -6° boresight

Figure 10a

SUM AND DIFFERENCE PATTERNS - FULLY ADAPTIVE ARRAY

10 elements λ/2 spacing 0° scan angle
5 jammers θ_j = 12° $P_j = 10^5$
14° 10^5
16° 10^5
18° 10^5
20° 10^5

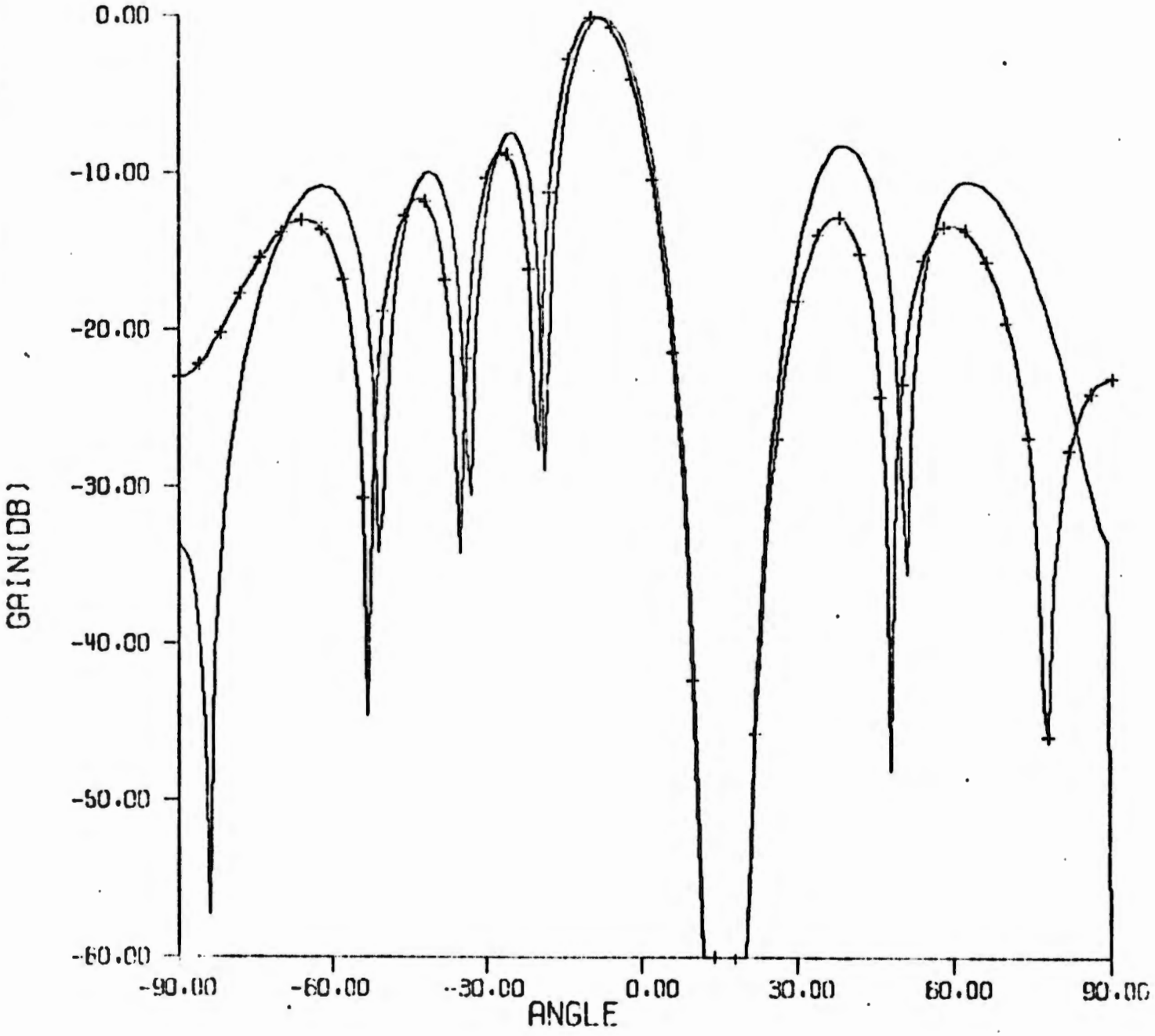

Figure 10b

SUM AND DIFFERENCE PATTERNS - SYMMETRICAL PAIRS

10 elements λ/2 spacing 0° scan angle
5 jammers θ_j = 12°, 14°, 16°, 18°, 20° P_j = 10^5, 10^5, 10^5, 10^5, 10^5

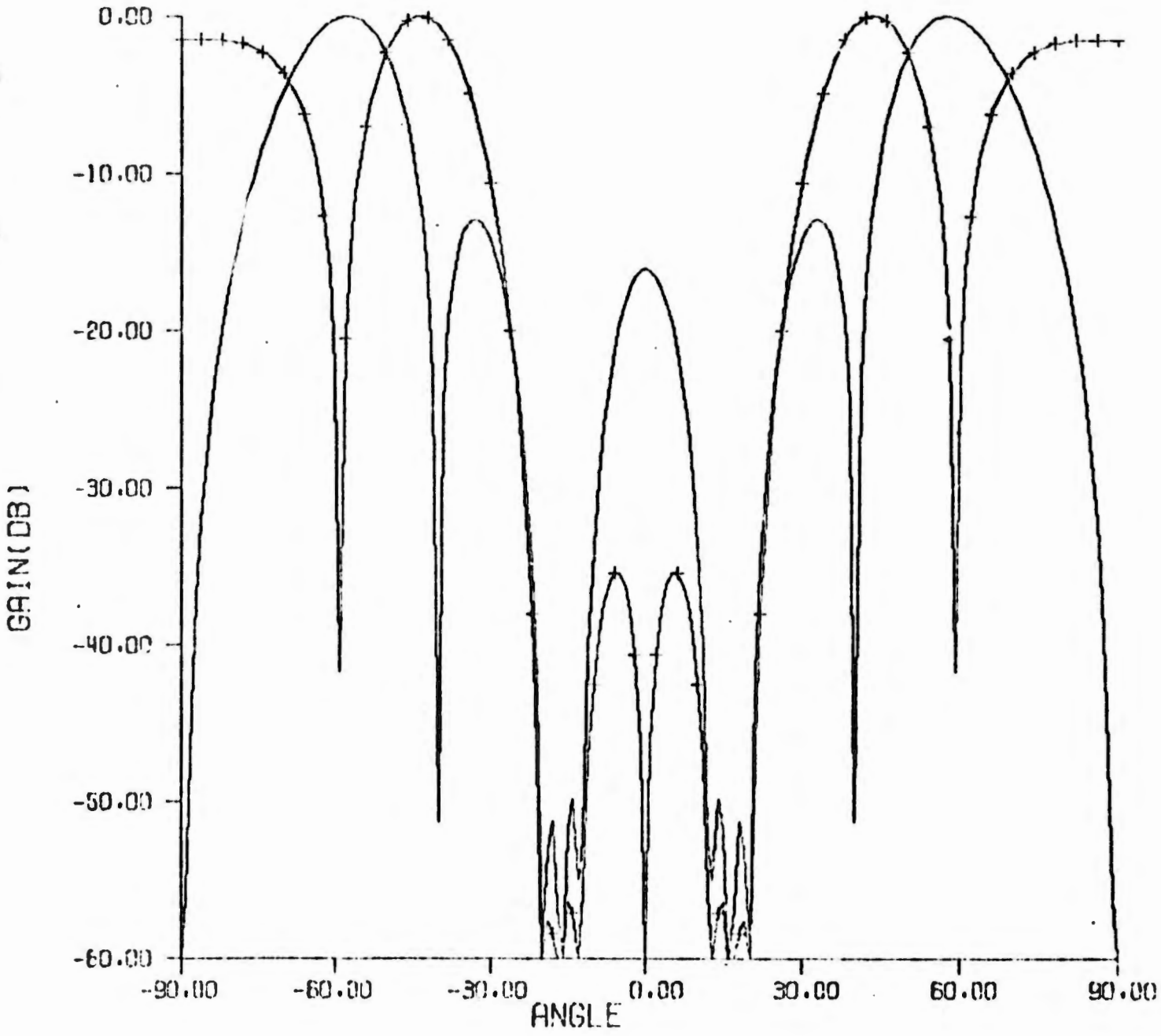

Table 5d.

Simulation Results with 5 Jammers near Main Beam; 0° Scan Angle

TARGET ANGLE(DEG)=-1,00				
CASE 1 BIAS	1,32	ST DEV	16,557	RMS=16,610
CASE 2 BIAS	-6,01	ST DEV	,085	RMS= 6,008
CASE 3 BIAS	-,08	ST DEV	,989	RMS= ,992
CASE 4 BIAS	4,65	ST DEV	19,077	RMS=19,636
CASE 5 BIAS	-,22	ST DEV	1,170	RMS= 1,190
CASE 6 BIAS	-,08	ST DEV	,996	RMS= ,999
TARGET ANGLE(DEG)= -,50				
CASE 1 BIAS	1,43	ST DEV	14,089	RMS=14,162
CASE 2 BIAS	-6,46	ST DEV	,089	RMS= 6,457
CASE 3 BIAS	,02	ST DEV	1,044	RMS= 1,044
CASE 4 BIAS	5,52	ST DEV	12,083	RMS=13,283
CASE 5 BIAS	-,04	ST DEV	1,141	RMS= 1,142
CASE 6 BIAS	,02	ST DEV	1,045	RMS= 1,045
TARGET ANGLE(DEG)= 0,00				
CASE 1 BIAS	-3,68	ST DEV	14,779	RMS=15,231
CASE 2 BIAS	-6,90	ST DEV	,109	RMS= 6,901
CASE 3 BIAS	,18	ST DEV	1,288	RMS= 1,300
CASE 4 BIAS	5,11	ST DEV	15,814	RMS=16,618
CASE 5 BIAS	,13	ST DEV	1,335	RMS= 1,341
CASE 6 BIAS	,18	ST DEV	1,287	RMS= 1,299
TARGET ANGLE(DEG)= ,50				
CASE 1 BIAS	-,21	ST DEV	14,386	RMS=14,388
CASE 2 BIAS	-7,38	ST DEV	,132	RMS= 7,386
CASE 3 BIAS	-,14	ST DEV	1,552	RMS= 1,559
CASE 4 BIAS	7,72	ST DEV	17,558	RMS=19,181
CASE 5 BIAS	-,23	ST DEV	1,563	RMS= 1,579
CASE 6 BIAS	-,14	ST DEV	1,554	RMS= 1,560
TARGET ANGLE(DEG)= 1,00				
CASE 1 BIAS	-2,88	ST DEV	10,250	RMS=10,646
CASE 2 BIAS	-7,32	ST DEV	,127	RMS= 7,324
CASE 3 BIAS	,09	ST DEV	1,485	RMS= 1,488
CASE 4 BIAS	5,89	ST DEV	13,459	RMS=14,690
CASE 5 BIAS	-,04	ST DEV	1,486	RMS= 1,487
CASE 6 BIAS	,09	ST DEV	1,493	RMS= 1,496

S/N = 20 dB 10 elements $\lambda/2$ spacing (Figure 10)

5 jammers θ_J = 12°, 14°, 16°, 18°, 20° all J/N = 10^5

angle are shown in Table 6. Comparing the rms error for these two cases of different scan angle, but identical interference field, shows that the accuracy improves noticeably as the boresight moves away from the interference. For example, the accuracy of the Case 6 maximum likelihood estimator with the target at 0° is improved from 1.3° to .44° rms error.

Table 6

Simulation Results with 5 Jammers near Main Beam; -6° Scan Angle

SIGNAL-TO-NOISE RATIO(DB) 20,000

TARGET ANGLE(DEG)=-1,00

CASE 1 BIAS	6,84	ST DEV 11,702	RMS=13,556
CASE 2 BIAS	-1,67	ST DEV ,072	RMS= 1,674
CASE 3 BIAS	-,05	ST DEV ,367	RMS= ,391
CASE 4 BIAS	,09	ST DEV 4,157	RMS= 4,158
CASE 5 BIAS	-,19	ST DEV ,493	RMS= ,529
CASE 6 BIAS	-,06	ST DEV ,394	RMS= ,398

TARGET ANGLE(DEG)= -,50

CASE 1 BIAS	4,90	ST DEV 16,648	RMS=17,356
CASE 2 BIAS	-2,07	ST DEV ,070	RMS= 2,073
CASE 3 BIAS	-,01	ST DEV ,378	RMS= ,378
CASE 4 BIAS	,38	ST DEV 4,184	RMS= 4,201
CASE 5 BIAS	-,05	ST DEV ,420	RMS= ,423
CASE 6 BIAS	-,01	ST DEV ,379	RMS= ,379

TARGET ANGLE(DEG)= 0,00

CASE 1 BIAS	3,04	ST DEV 14,733	RMS=15,044
CASE 2 BIAS	-2,47	ST DEV ,079	RMS= 2,469
CASE 3 BIAS	,06	ST DEV ,432	RMS= ,436
CASE 4 BIAS	,56	ST DEV 4,769	RMS= 4,802
CASE 5 BIAS	,04	ST DEV ,434	RMS= ,436
CASE 6 BIAS	,06	ST DEV ,431	RMS= ,435

TARGET ANGLE(DEG)= ,50

CASE 1 BIAS	4,06	ST DEV 16,617	RMS=17,105
CASE 2 BIAS	-2,69	ST DEV ,094	RMS= 2,696
CASE 3 BIAS	-,05	ST DEV ,511	RMS= ,513
CASE 4 BIAS	-,39	ST DEV 4,096	RMS= 4,115
CASE 5 BIAS	-,08	ST DEV ,482	RMS= ,483
CASE 6 BIAS	-,05	ST DEV ,512	RMS= ,514

TARGET ANGLE(DEG)= 1,00

CASE 1 BIAS	5,77	ST DEV 18,192	RMS=19,086
CASE 2 BIAS	-3,29	ST DEV ,084	RMS= 3,296
CASE 3 BIAS	-,01	ST DEV ,472	RMS= ,472
CASE 4 BIAS	,02	ST DEV 4,432	RMS= 4,432
CASE 5 BIAS	-,08	ST DEV ,419	RMS= ,421
CASE 6 BIAS	-,00	ST DEV ,477	RMS= ,477

10 elements λ/2 spacing Results in degrees (Figure 11)

5 jammers θ_J = 12°, 14°, 16°, 18°, 20° all J/N = 10^5

Figure 11a

SUM AND DIFFERENCE PATTERNS - FULLY ADAPTIVE ARRAY

10 elements	λ/2 spacing	-6° scan angle
5 jammers	θ_J = 12°	$P_J = 10^5$
	14°	10^5
	16°	10^5
	18°	10^5
	20°	10^5

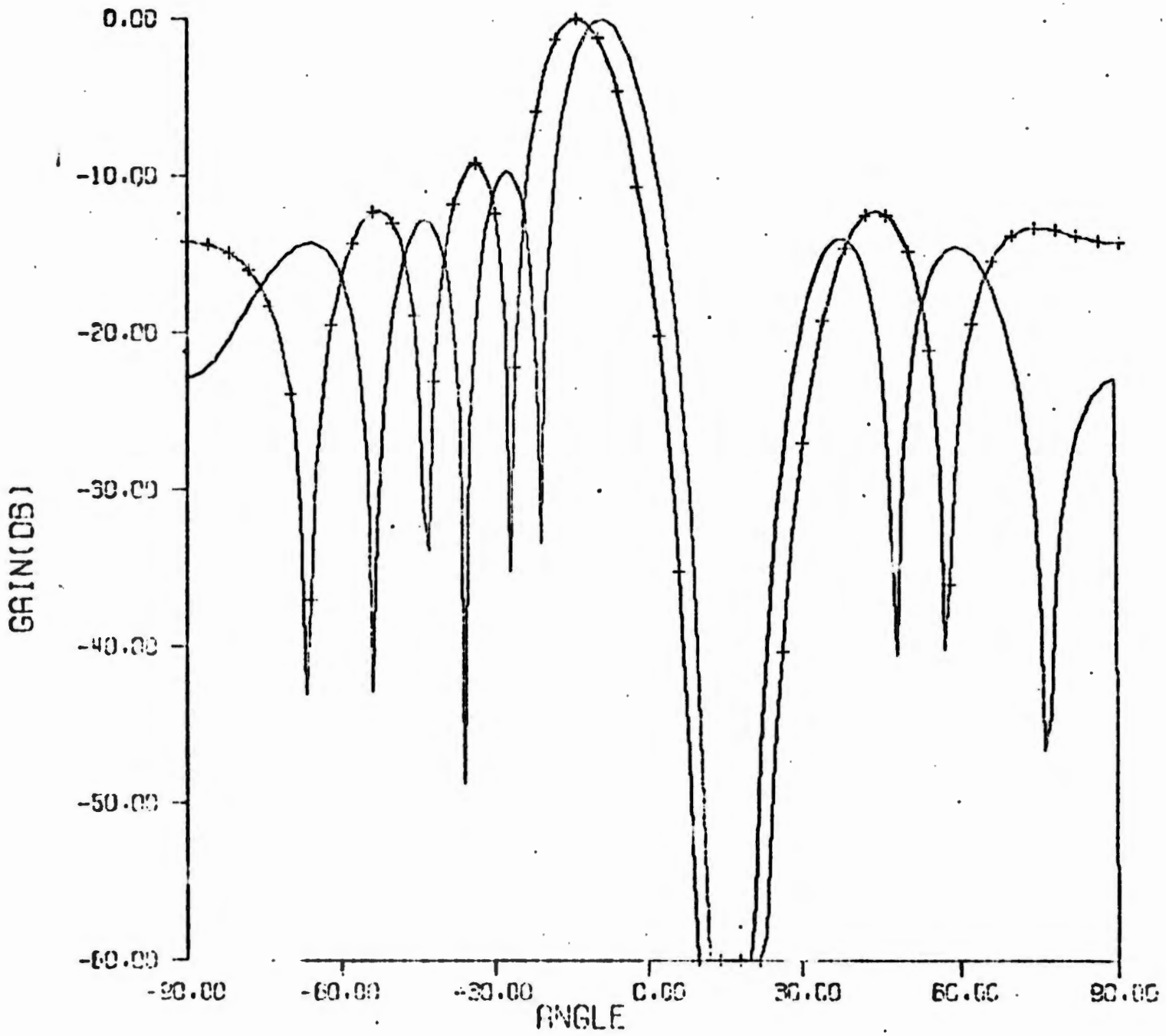

Figure 11b

SUM AND DIFFERENCE PATTERNS - SYMMETRICAL PAIRS

10 elements	/2 spacing	-6° scan angle
5 jammers	J = 12°	P_J = 10^5
	14°	10^5
	16°	10^5
	18°	10^5
	20°	10^5

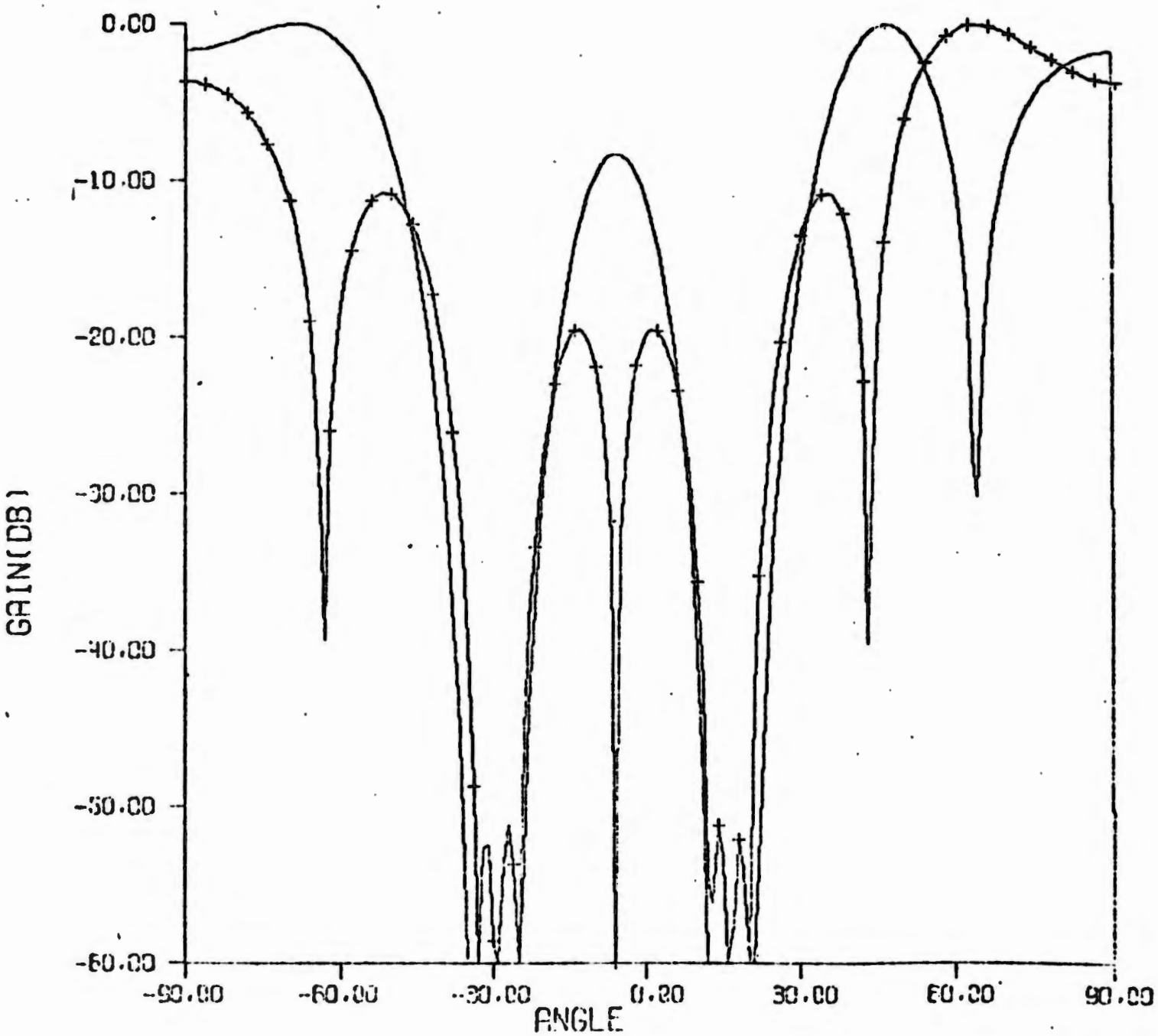

6. ELECTRONIC SCAN

The angle tracking equations and simulation program allow for electronic scan of the boresight angle. One simulation result where the boresight is scanned 6° from the array normal was shown in Figures 11a and 11b. Additional examples are included in this section to show that the various tracking techniques perform well with electronic scan and that the conclusions reached earlier concerning the relative accuracy of the different algorithm apply to all scan angles.

The first example, with patterns shown in Figures 12a and 12b, is for a 10 element linear array with the boresight angle scanned 30° from the array normal. A single jammer is located at 10°. The symmetry around boresight is not as apparent in Figure 12b as in earlier examples without electronic scan. Actually the symmetry occurs in $\xi = \sin\theta$, so it would not be evident on the plot of gain versus θ. Simulation results for this example are shown in Table 7. Again, the best accuracy at low S/N (0dB) was achieved with the new maximum likelihood estimator of Case 6. The symmetrical pairs algorithm of Case 4 performed well since the single jammer is far from boresight and does not require reduction of antenna gain near boresight.

A second example for the same array and jammer environment, with 60° electronic scan, is shown in Figure 13. Again, all antenna patterns have nulls at the 10° jammer angle. Simulation results for this example, shown in Table 8, sustain the same conclusions concerning relative accuracy of the different tracking techniques. In this example, the pattern distortion in

Figure 12a

SUM AND DIFFERENCE PATTERNS - FULLY ADAPTIVE ARRAY

10 elements λ/2 spacing 30° scan angle
1 jammer θ_j = 10° P_j - 10^5

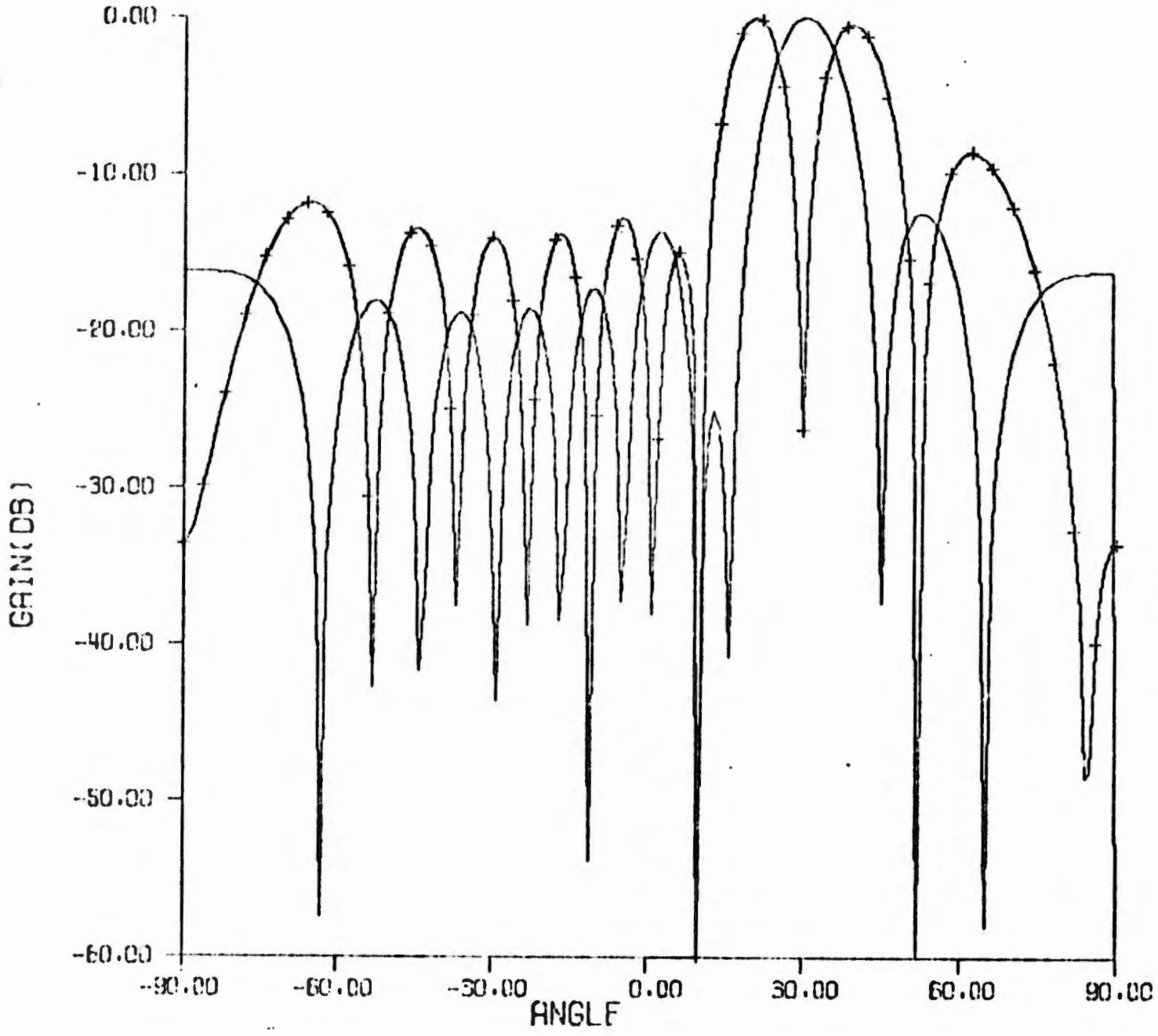

Figure 12b

SUM AND DIFFERENCE PATTERNS - SYMMETRICAL PAIRS

10 elements λ/2 spacing 30° scan angle
1 jammer $\theta_j = 10°$ $P_j = 10^5$

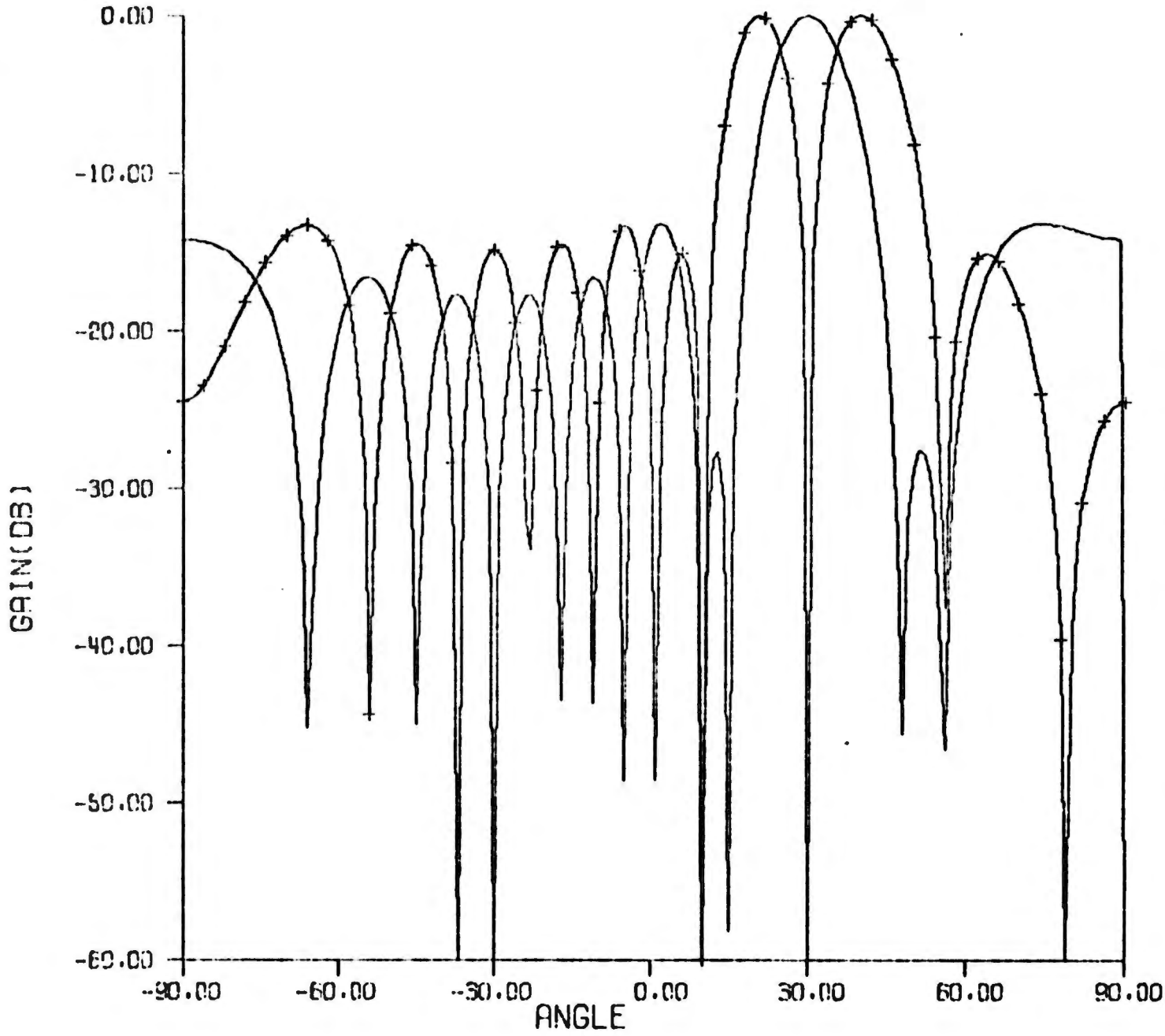

Table 7

Simulation Results for 30^0 Scan Angle

SIGNAL-TO-NOISE RATIO(DB) 0.000

TARGET ANGLE(DEG)=-1.00

CASE 1	BIAS -6.84	ST DEV .318	RMS= 6.846
CASE 2	BIAS .64	ST DEV 1.654	RMS= 1.774
CASE 3	BIAS .32	ST DEV 1.830	RMS= 1.857
CASE 4	BIAS .37	ST DEV 1.685	RMS= 1.726
CASE 5	BIAS .20	ST DEV 2.398	RMS= 2.407
CASE 6	BIAS .35	ST DEV 1.665	RMS= 1.703

TARGET ANGLE(DEG)= -.50

CASE 1	BIAS -7.36	ST DEV .205	RMS= 7.360
CASE 2	BIAS .53	ST DEV 1.953	RMS= 2.023
CASE 3	BIAS .29	ST DEV 2.223	RMS= 2.241
CASE 4	BIAS .25	ST DEV 2.005	RMS= 2.021
CASE 5	BIAS 2.81	ST DEV 24.151	RMS=24.313
CASE 6	BIAS .24	ST DEV 1.967	RMS= 1.982

TARGET ANGLE(DEG)= 0.00

CASE 1	BIAS -7.65	ST DEV .278	RMS= 7.656
CASE 2	BIAS .34	ST DEV 1.633	RMS= 1.664
CASE 3	BIAS .44	ST DEV 3.695	RMS= 3.721
CASE 4	BIAS .06	ST DEV 1.901	RMS= 1.902
CASE 5	BIAS -.41	ST DEV 2.888	RMS= 2.917
CASE 6	BIAS .05	ST DEV 1.846	RMS= 1.847

TARGET ANGLE(DEG)= .50

CASE 1	BIAS -8.39	ST DEV .170	RMS= 8.396
CASE 2	BIAS .30	ST DEV 1.762	RMS= 1.788
CASE 3	BIAS .05	ST DEV 1.825	RMS= 1.825
CASE 4	BIAS .03	ST DEV 1.818	RMS= 1.818
CASE 5	BIAS -3.36	ST DEV 35.664	RMS=35.822
CASE 6	BIAS .02	ST DEV 1.774	RMS= 1.775

TARGET ANGLE(DEG)= 1.00

CASE 1	BIAS -8.89	ST DEV .252	RMS= 8.882
CASE 2	BIAS .01	ST DEV 2.090	RMS= 2.177
CASE 3	BIAS .24	ST DEV 2.274	RMS= 2.287
CASE 4	BIAS .36	ST DEV 2.174	RMS= 2.203
CASE 5	BIAS .32	ST DEV 25.828	RMS=25.830
CASE 6	BIAS .34	ST DEV 2.105	RMS= 2.131

10 elements $\lambda/2$ spacing 1 jammer $\theta_J = 10^0$ $J/N = 10^5$

Table 8

Simulation Results for 60° Scan Angle

SIGNAL-TO-NOISE RATIO(DB) 0,000

TARGET ANGLE(DEG)=-1,00

CASE 1	BIAS 2,46	ST DEV ,309	RMS= 2,479
CASE 2	BIAS ,55	ST DEV 2,848	RMS= 2,900
CASE 3	BIAS ,54	ST DEV 3,099	RMS= 3,145
CASE 4	BIAS ,58	ST DEV 2,813	RMS= 2,872
CASE 5	BIAS ,78	ST DEV 4,032	RMS= 4,107
CASE 6	BIAS ,57	ST DEV 2,812	RMS= 2,870

TARGET ANGLE(DEG)= -,50

CASE 1	BIAS 1,97	ST DEV ,197	RMS= 1,979
CASE 2	BIAS ,39	ST DEV 3,358	RMS= 3,381
CASE 3	BIAS ,57	ST DEV 3,499	RMS= 3,546
CASE 4	BIAS ,41	ST DEV 3,321	RMS= 3,347
CASE 5	BIAS ,66	ST DEV 8,768	RMS= 6,795
CASE 6	BIAS ,41	ST DEV 3,316	RMS= 3,342

TARGET ANGLE(DEG)= 0,00

CASE 1	BIAS 1,51	ST DEV ,237	RMS= 1,526
CASE 2	BIAS ,07	ST DEV 3,150	RMS= 3,151
CASE 3	BIAS ,70	ST DEV 5,674	RMS= 5,716
CASE 4	BIAS ,09	ST DEV 3,121	RMS= 3,123
CASE 5	BIAS -,52	ST DEV 4,722	RMS= 4,751
CASE 6	BIAS ,09	ST DEV 3,111	RMS= 3,112

TARGET ANGLE(DEG)= ,50

CASE 1	BIAS 1,02	ST DEV ,150	RMS= 1,033
CASE 2	BIAS ,01	ST DEV 3,031	RMS= 3,031
CASE 3	BIAS ,06	ST DEV 3,117	RMS= 3,117
CASE 4	BIAS ,03	ST DEV 2,996	RMS= 2,996
CASE 5	BIAS -7,88	ST DEV 81,976	RMS=82,354
CASE 6	BIAS ,03	ST DEV 2,993	RMS= 2,993

TARGET ANGLE(DEG)= 1,00

CASE 1	BIAS ,51	ST DEV ,228	RMS= ,556
CASE 2	BIAS ,57	ST DEV 3,539	RMS= 3,584
CASE 3	BIAS ,50	ST DEV 3,838	RMS= 3,870
CASE 4	BIAS ,57	ST DEV 3,502	RMS= 3,548
CASE 5	BIAS -25,94	ST DEV 4,869	RMS=*6,008
CASE 6	BIAS ,57	ST DEV 3,495	RMS= 3,540

10 elements $\lambda/2$ spacing 1 jammer $\theta_J = 10^\circ$ $J/N = 10^5$

Figure 13a

SUM AND DIFFERENCE PATTERNS - FULLY ADAPTIVE ARRAY

10 elements λ/2 spacing 60° scan angle
1 jammer $\theta_J = 10°$ $P_J = 10^5$

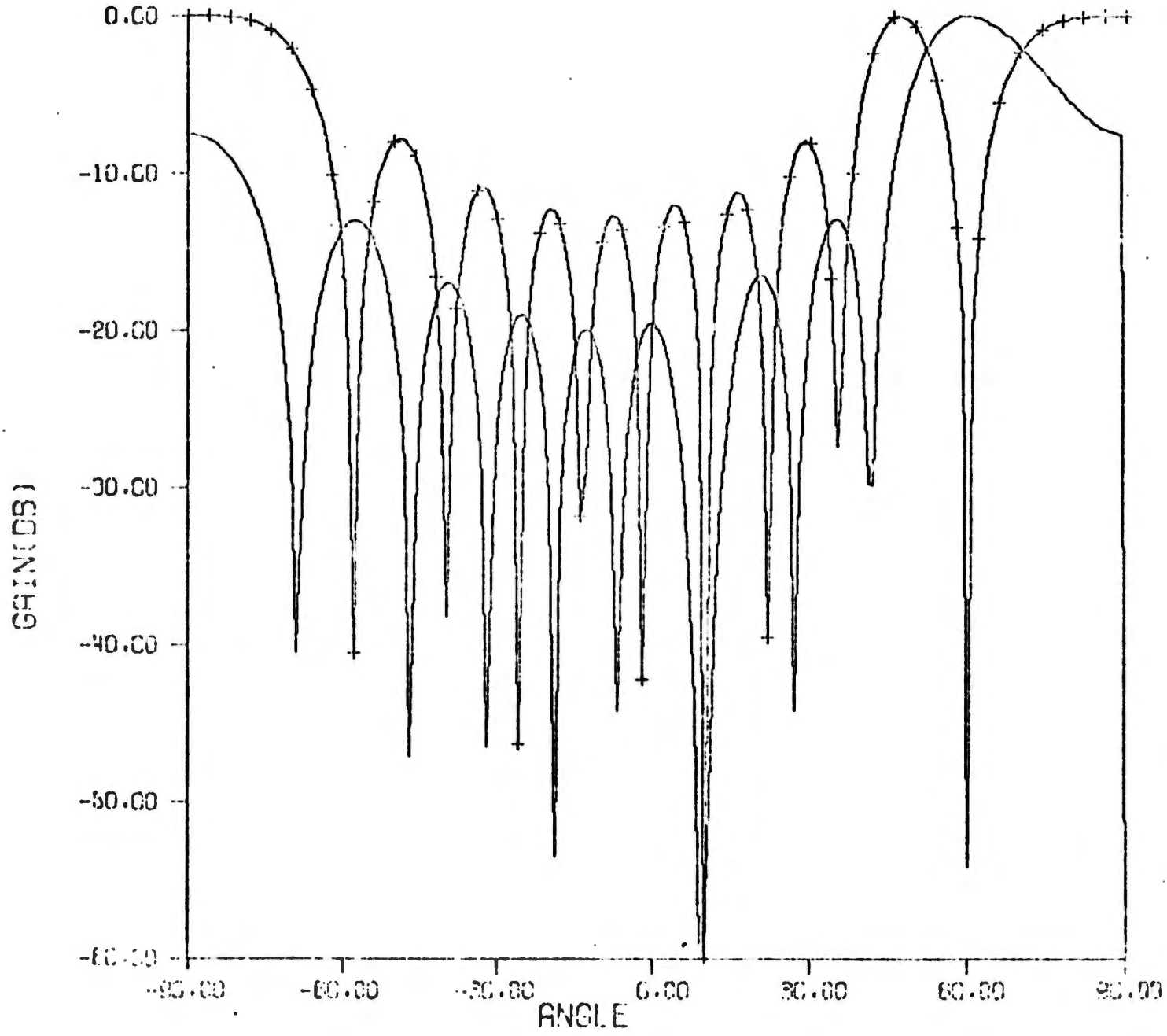

Figure 13b

SUM AND DIFFERENCE PATTERNS - SYMMETRICAL PAIRS

10 elements $\lambda/2$ spacing 60° scan angle
1 jammer $\theta_J = 10°$ $P_J = 10^5$

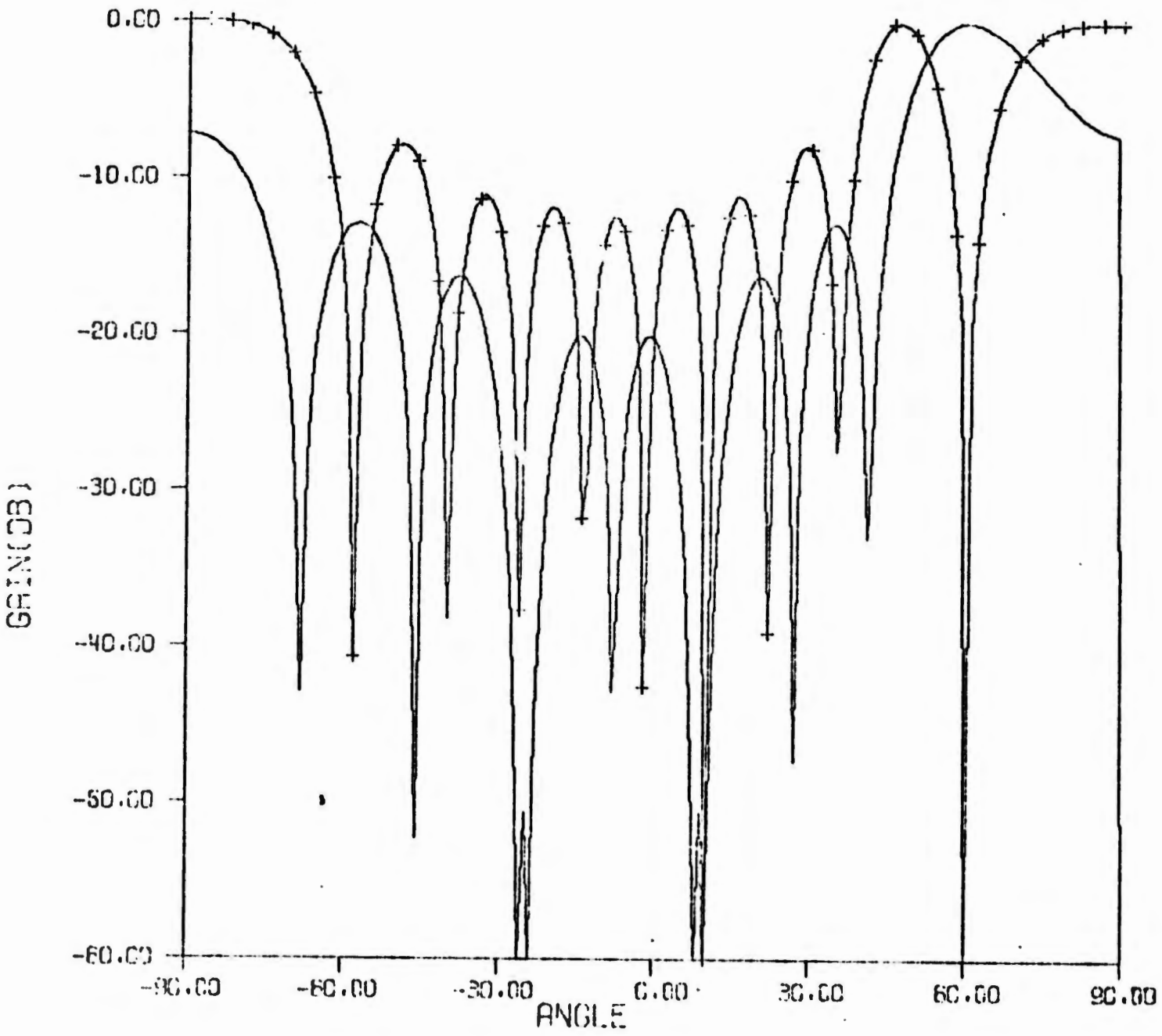

nulling the 10° jammer is small, so the uncorrected algorithm (Case 2) works well. The rms errors are larger at 60° electronic scan angle than at 30°. This would be expected due to the reduced effective aperture of the array.

Patterns for a 10° scan angle and 1 jammer at 0° are shown in Figures 14a and 14b. Simulation results for this example, shown in Table 9, correspond closely to the results for a 0° scan angle and 1 jammer at 10°. This can be verified by cross-reference with Table 1.

The final two examples show some results obtained for a 20 element array. In the first 20-element example of Figure 15, three jammers are present, located at -45°, 30°, and 60°. The scan angle is 20°. Simulation results are shown in Table 10 for a S/N ratio of -10.5 dB per element. The rms errors are large and comparable to the nominal 5° beamwidth in this example. The new estimator (Case 6) is superior to the other two maximum likelihood estimators (Cases 3 and 5), as was generally found to be the case at low S/N ratio. Symmetrical pairs work well in this example, since the 3 jammers are in the far sidelobes and easily nulled without reducing the gain near boresight.

The 20 element array was also simulated with one jammer moved into the main beam region. In the example of Figure 16 and Table 11, the three strong jammers are located at 15°, 30°, and 45°. Again, the scan angle is 20°. Note the distortions of the patterns in this case (Figure 16) relative to the sidelobe jamming example in Figure 15. The simulation results for a -10.5 dB S/N ratio per element are shown in Table 11a. As a result of moving a jammer from the sidelobes (-45°) to the main beam region (15°),

Figure 14a

SUM AND DIFFERENCE PATTERNS - FULLY ADAPTIVE ARRAY

10 elements $\lambda/2$ spacing 10° scan angle
1 jammer $\theta_J = 0°$ $P_J = 10^5$

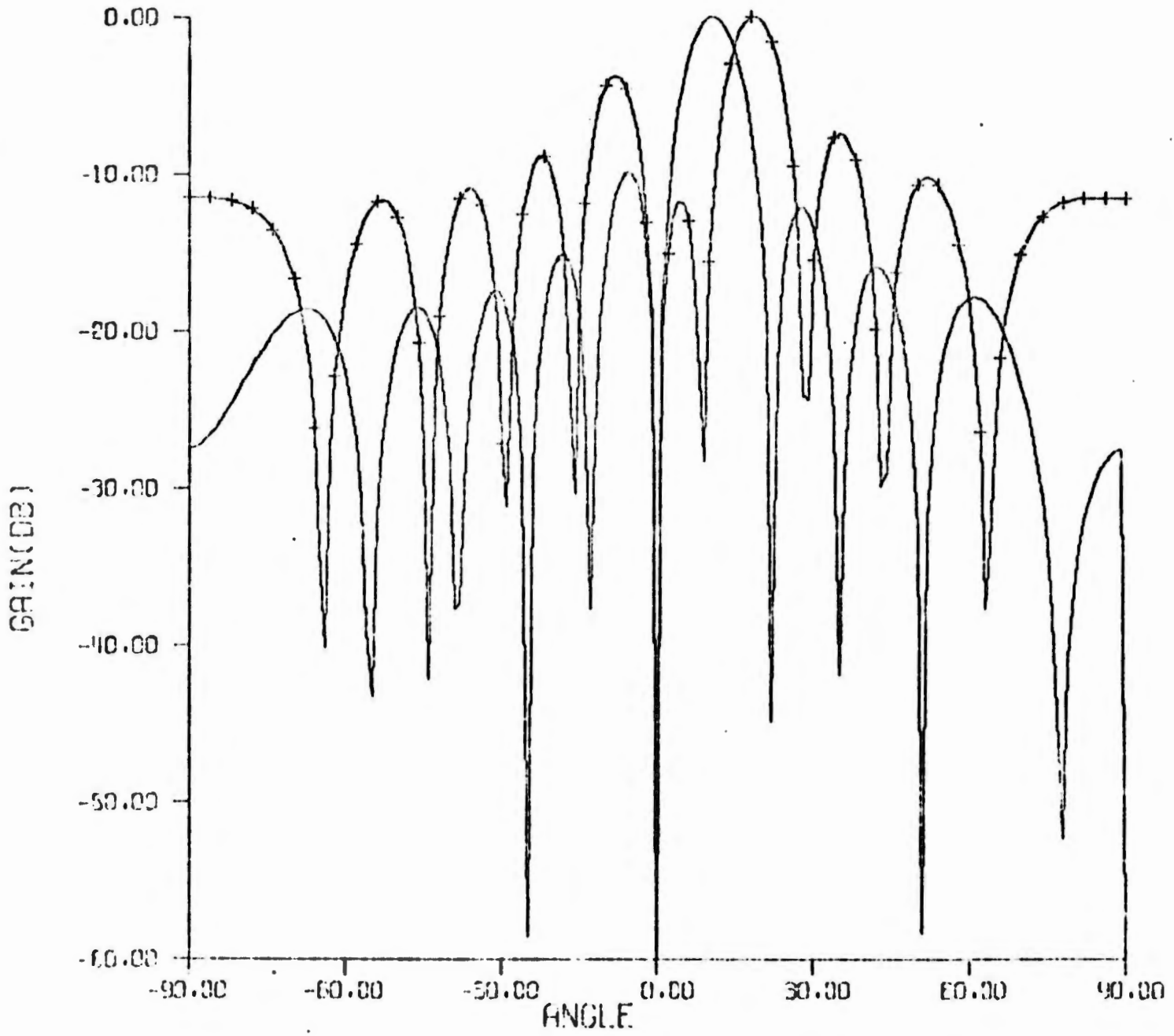

Figure 14b

SUM AND DIFFERENCE PATTERNS - SYMMETRICAL PAIRS

10 elements $\lambda/2$ spacing 10° scan angle
1 jammer $\theta_J = 0°$ $\Gamma_J = 10^5$

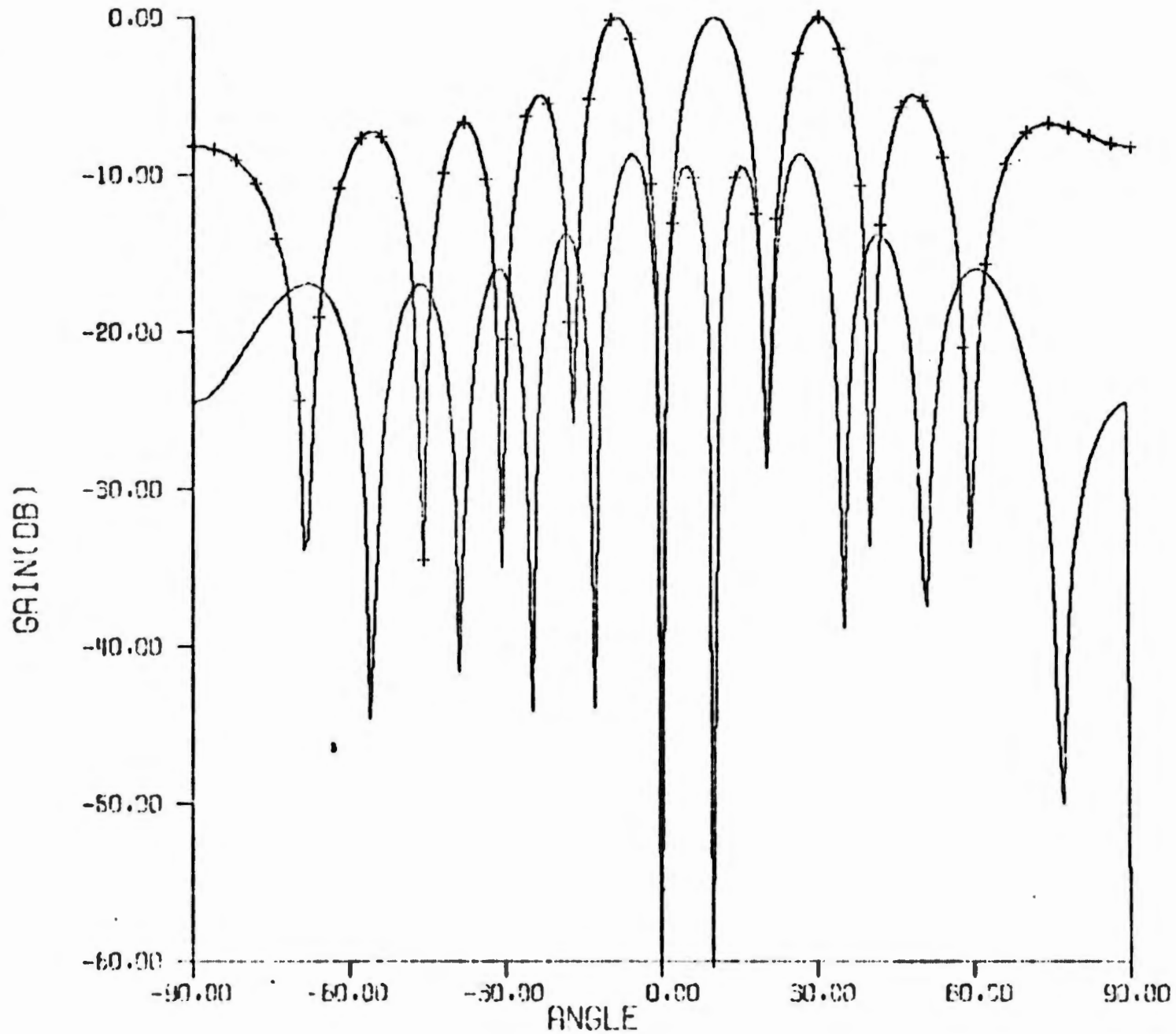

Table 9

Simulation Results for 10° Scan Angle

SIGNAL-TO-NOISE RATIO(DB) 0.000

TARGET ANGLE(DEG)=-1.00			
CASE 1	BIAS -28.81	ST DEV 2.329	RMS=28.902
CASE 2	BIAS 1.40	ST DEV 1.079	RMS= 1.765
CASE 3	BIAS .44	ST DEV 2.254	RMS= 2.297
CASE 4	BIAS .72	ST DEV 3.423	RMS= 3.498
CASE 5	BIAS 4.27	ST DEV 26.318	RMS=26.662
CASE 6	BIAS .48	ST DEV 2.026	RMS= 2.082
TARGET ANGLE(DEG)= -.50			
CASE 1	BIAS -29.16	ST DEV 1.050	RMS=29.183
CASE 2	BIAS 1.07	ST DEV 1.259	RMS= 1.652
CASE 3	BIAS .39	ST DEV 2.598	RMS= 2.626
CASE 4	BIAS .51	ST DEV 4.012	RMS= 4.044
CASE 5	BIAS 1.17	ST DEV 5.072	RMS= 5.205
CASE 6	BIAS .30	ST DEV 2.364	RMS= 2.384
TARGET ANGLE(DEG)= 0.00			
CASE 1	BIAS -29.63	ST DEV 1.158	RMS=29.654
CASE 2	BIAS .71	ST DEV 1.169	RMS= 1.366
CASE 3	BIAS .50	ST DEV 4.095	RMS= 4.125
CASE 4	BIAS .11	ST DEV 3.772	RMS= 3.773
CASE 5	BIAS .47	ST DEV 3.594	RMS= 3.624
CASE 6	BIAS .06	ST DEV 2.195	RMS= 2.195
TARGET ANGLE(DEG)= .50			
CASE 1	BIAS -29.95	ST DEV .739	RMS=29.956
CASE 2	BIAS .46	ST DEV 1.118	RMS= 1.210
CASE 3	BIAS .06	ST DEV 2.166	RMS= 2.167
CASE 4	BIAS .03	ST DEV 3.608	RMS= 3.608
CASE 5	BIAS .52	ST DEV 4.375	RMS= 4.407
CASE 6	BIAS .04	ST DEV 2.100	RMS= 2.100
TARGET ANGLE(DEG)= 1.00			
CASE 1	BIAS -30.50	ST DEV .991	RMS=30.521
CASE 2	BIAS .45	ST DEV 1.316	RMS= 1.389
CASE 3	BIAS .55	ST DEV 2.606	RMS= 2.630
CASE 4	BIAS .71	ST DEV 4.275	RMS= 4.333
CASE 5	BIAS 11.78	ST DEV 42.619	RMS=43.184
CASE 6	BIAS .45	ST DEV 2.470	RMS= 2.511

10 elements $\lambda/2$ spacing 1 jammer $\theta_J = 0^\circ$ $J/N = 10^5$

Figure 15a

SUM AND DIFFERENCE PATTERNS - FULLY ADAPTIVE ARRAY

20 elements λ/2 spacing 20° scan angle
3 jammers θ_J = -45° P_J = 10^5
30° 10^5
60° 10^5

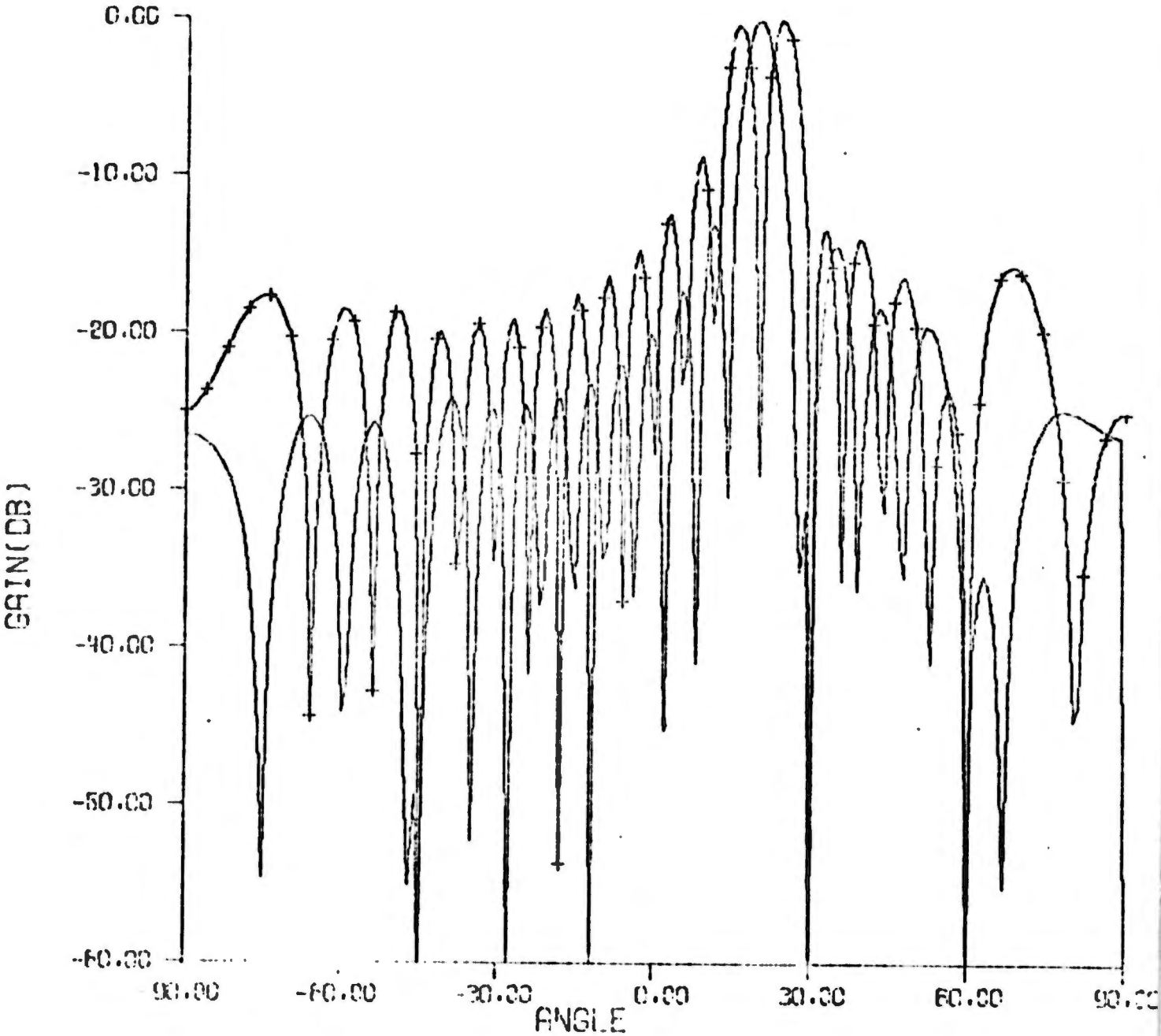

Figure 15b

SUM AND DIFFERENCE PATTERNS - SYMMETRICAL PAIRS

20 elements λ/2 spacing 20° scan angle
3 jammers θ_J = -45° P_J = 10^5
30° 10^5
60° 10^5

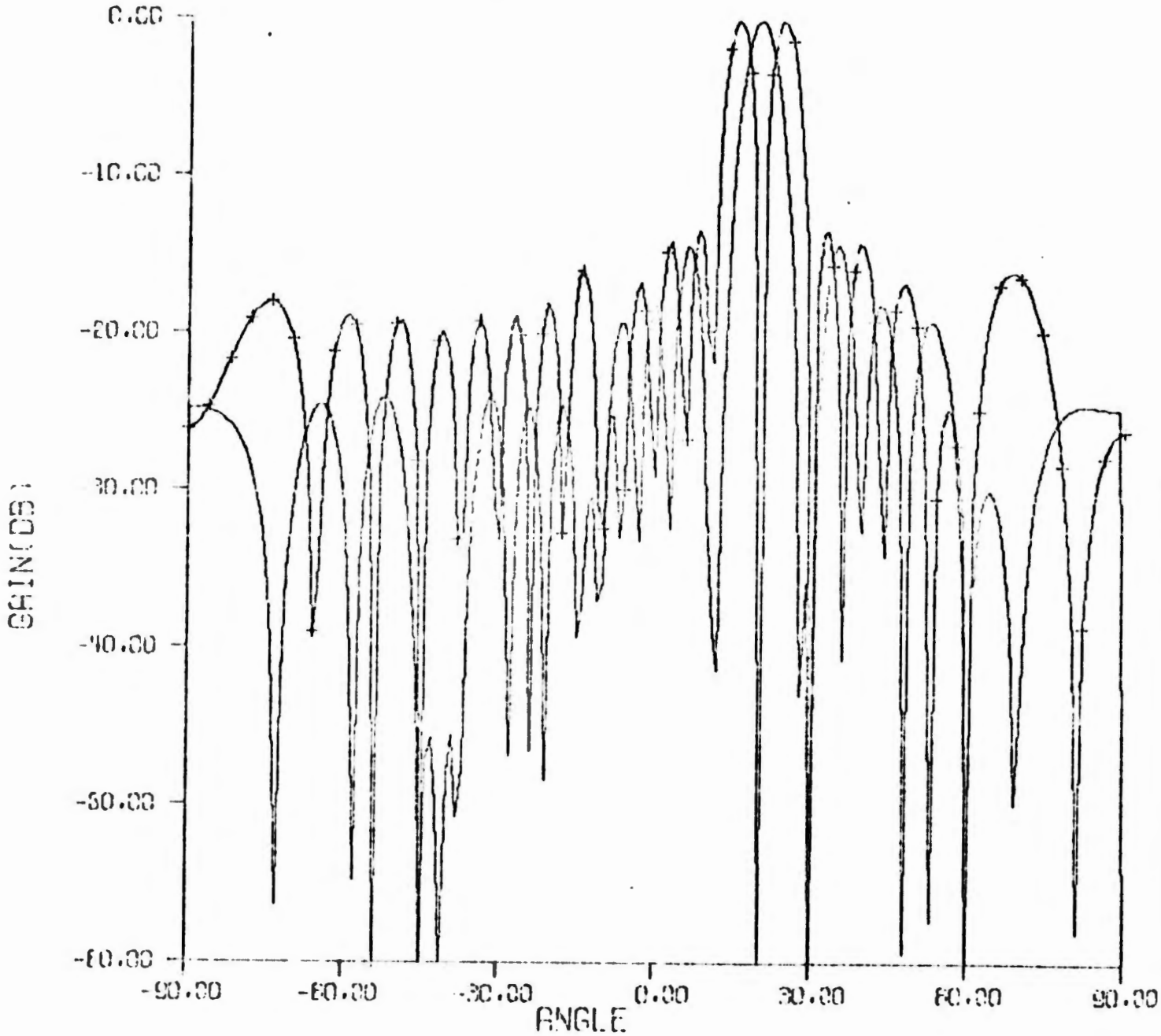

Table 10

Simulation of 20 Element Array with Sidelobe Jamming

SIGNAL-TO-NOISE RATIO(DB) =10,458

TARGET ANGLE(DEG)=-1,00

CASE 1 BIAS	3,11	ST DEV 2,686	RMS= 4,112
CASE 2 BIAS	,66	ST DEV 2,991	RMS= 3,062
CASE 3 BIAS	,82	ST DEV 5,159	RMS= 5,223
CASE 4 BIAS	,73	ST DEV 3,001	RMS= 3,089
CASE 5 BIAS	,53	ST DEV 9,967	RMS= 9,981
CASE 6 BIAS	,76	ST DEV 2,943	RMS= 3,039

TARGET ANGLE(DEG)= -,50

CASE 1 BIAS	2,77	ST DEV 3,299	RMS= 4,307
CASE 2 BIAS	,27	ST DEV 2,139	RMS= 2,156
CASE 3 BIAS	1,40	ST DEV 18,502	RMS=18,555
CASE 4 BIAS	,37	ST DEV 2,144	RMS= 2,176
CASE 5 BIAS	,65	ST DEV 31,058	RMS=31,065
CASE 6 BIAS	,36	ST DEV 2,105	RMS= 2,137

TARGET ANGLE(DEG)= 0,00

CASE 1 BIAS	1,54	ST DEV 2,746	RMS= 3,150
CASE 2 BIAS	-,42	ST DEV 2,301	RMS= 2,338
CASE 3 BIAS	-2,99	ST DEV 14,877	RMS=15,175
CASE 4 BIAS	-,33	ST DEV 2,349	RMS= 2,373
CASE 5 BIAS	-,37	ST DEV 24,449	RMS=24,452
CASE 6 BIAS	-,32	ST DEV 2,264	RMS= 2,286

TARGET ANGLE(DEG)= ,50

CASE 1 BIAS	1,22	ST DEV 3,035	RMS= 3,272
CASE 2 BIAS	,02	ST DEV 2,455	RMS= 2,455
CASE 3 BIAS	-1,15	ST DEV 9,297	RMS= 9,367
CASE 4 BIAS	,10	ST DEV 2,497	RMS= 2,499
CASE 5 BIAS	-,22	ST DEV 7,919	RMS= 7,922
CASE 6 BIAS	,11	ST DEV 2,416	RMS= 2,419

TARGET ANGLE(DEG)= 1,00

CASE 1 BIAS	1,14	ST DEV 3,517	RMS= 3,507
CASE 2 BIAS	-,23	ST DEV 2,330	RMS= 2,341
CASE 3 BIAS	-,72	ST DEV 10,760	RMS=10,785
CASE 4 BIAS	-,16	ST DEV 2,253	RMS= 2,259
CASE 5 BIAS	-,44	ST DEV 25,721	RMS=25,724
CASE 6 BIAS	-,15	ST DEV 2,293	RMS= 2,298

$\lambda/2$ spacing 20° scan angle 3 jammers $\theta_J = -45^\circ, 30^\circ, 60^\circ$

all J/N = 10^5

Figure 16a

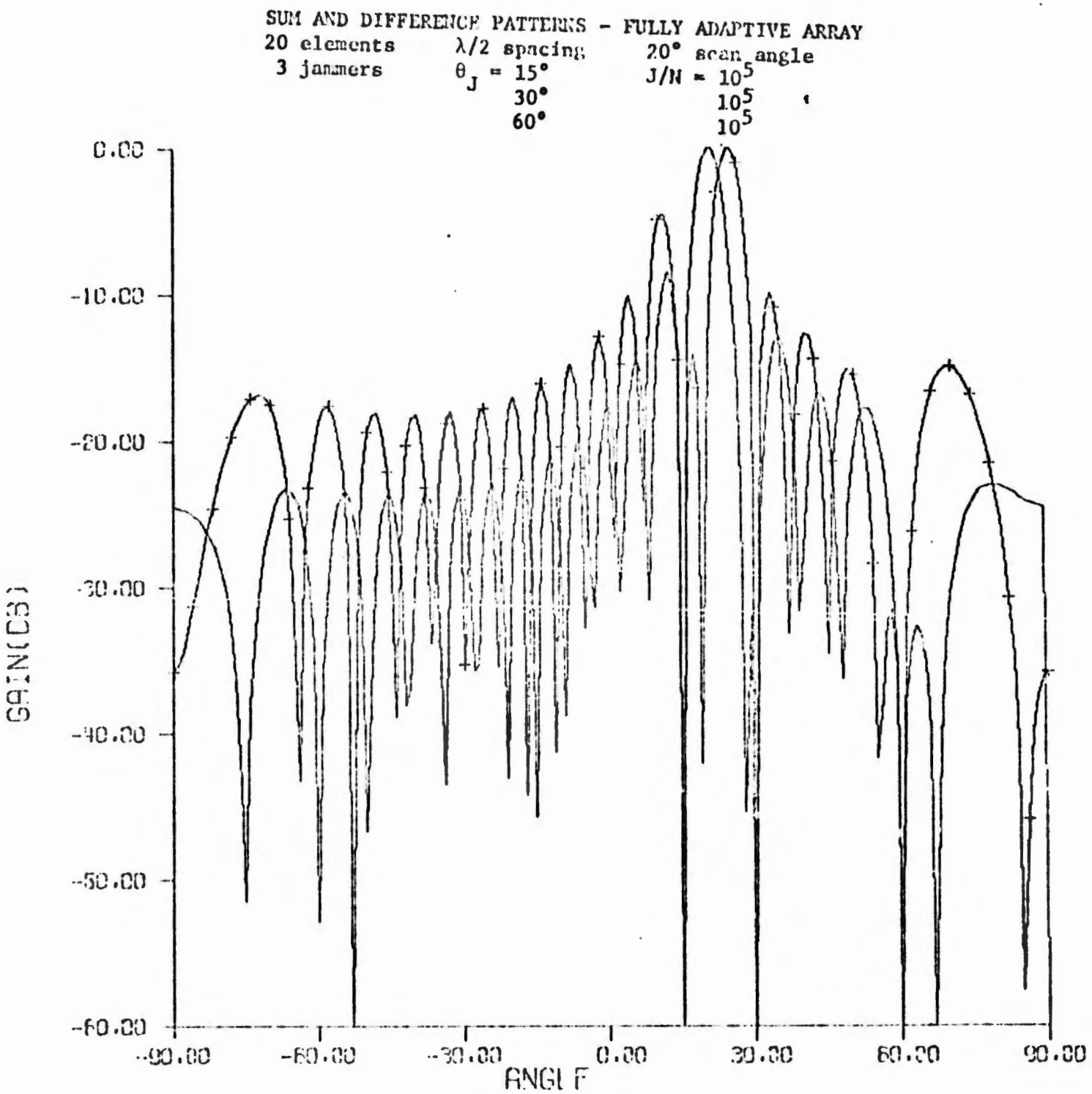
SUM AND DIFFERENCE PATTERNS - FULLY ADAPTIVE ARRAY
20 elements
3 jammers
λ/2 spacing
θJ = 15°
30°
60°
20° scan angle
J/N = 10^5
10^5
10^5
0.00
-10.00
-20.00
-30.00
-40.00
-50.00
-60.00
GAIN(DB)
-90.00
-60.00
-30.00
0.00
30.00
60.00
90.00
ANGLE

Figure 16b

SUM AND DIFFERENCE PATTERNS - FULLY ADAPTIVE ARRAY

20 elements λ/2 spacing 20° scan angle
3 jammers θ_J = 15° J/N = 10^5
30° 10^5
60° 10^5

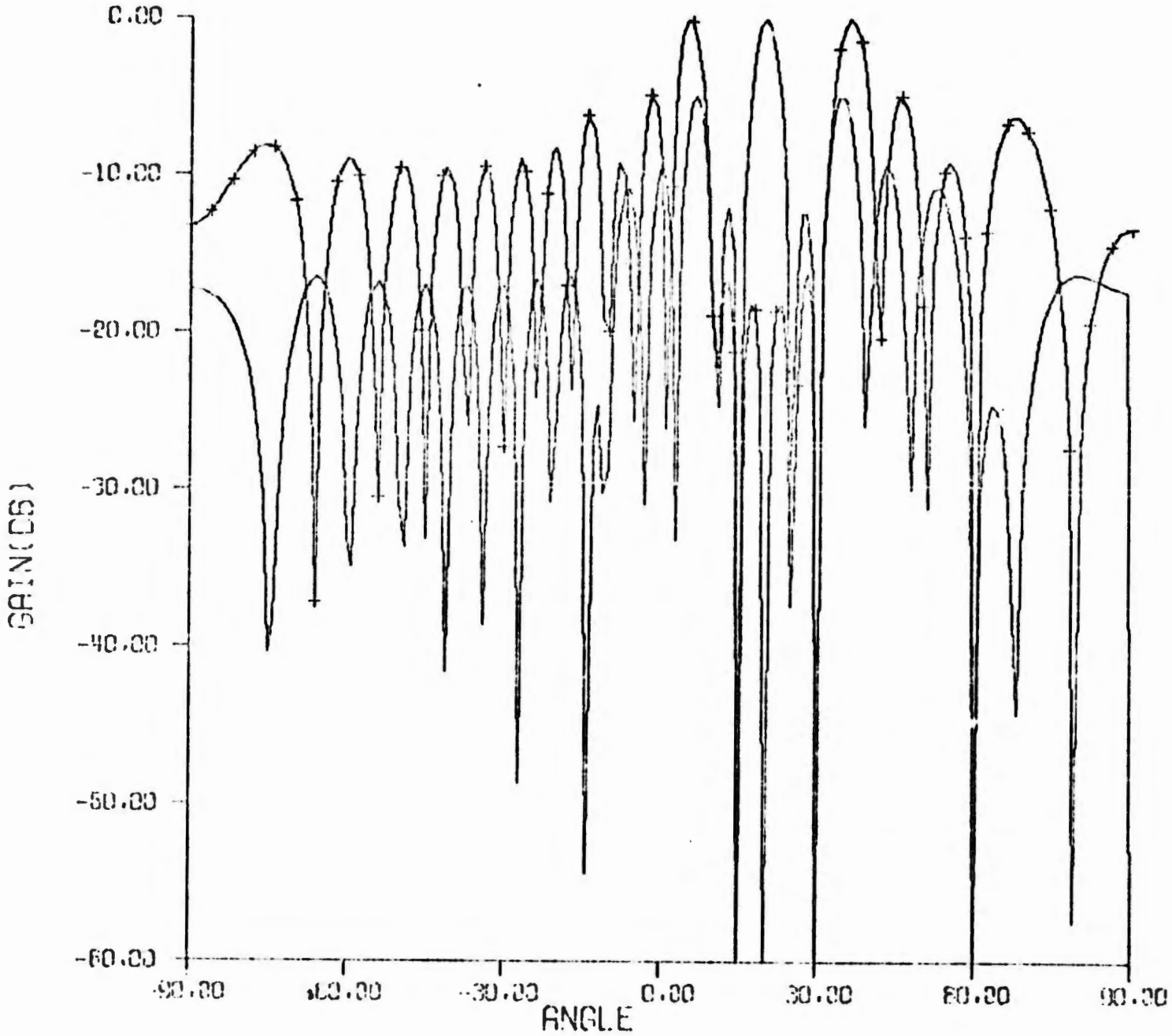

Table 11a

Simulation of 20 Element Array with Main Beam Jamming-Low S/N

SIGNAL-TO-NOISE RATIO(DB) -10,458

TARGET ANGLE(DEG)=-1,00

CASE 1 BIAS	-5,88	ST DEV 24,156	RMS=24,861
CASE 2 BIAS	1,40	ST DEV 2,188	RMS= 2,598
CASE 3 BIAS	-3,18	ST DEV 33,477	RMS=33,627
CASE 4 BIAS	1,29	ST DEV 16,666	RMS=16,715
CASE 5 BIAS	-11,35	ST DEV 96,611	RMS=97,275
CASE 6 BIAS	,87	ST DEV 4,162	RMS= 4,251

TARGET ANGLE(DEG)= -,50

CASE 1 BIAS	-7,76	ST DEV 27,839	RMS=28,899
CASE 2 BIAS	,98	ST DEV 1,555	RMS= 1,841
CASE 3 BIAS	2,52	ST DEV 13,079	RMS=13,321
CASE 4 BIAS	3,31	ST DEV 14,766	RMS=15,132
CASE 5 BIAS	-1,36	ST DEV 21,177	RMS=21,221
CASE 6 BIAS	,52	ST DEV 2,958	RMS= 3,004

TARGET ANGLE(DEG)= 0,00

CASE 1 BIAS	-3,83	ST DEV 12,314	RMS=12,897
CASE 2 BIAS	,22	ST DEV 1,737	RMS= 1,751
CASE 3 BIAS	2,57	ST DEV 49,726	RMS=49,792
CASE 4 BIAS	-2,97	ST DEV 17,973	RMS=18,217
CASE 5 BIAS	-,45	ST DEV 14,086	RMS=14,093
CASE 6 BIAS	-,47	ST DEV 3,304	RMS= 3,337

TARGET ANGLE(DEG)= ,50

CASE 1 BIAS	-4,41	ST DEV 9,196	RMS=10,199
CASE 2 BIAS	,33	ST DEV 1,769	RMS= 1,798
CASE 3 BIAS	,32	ST DEV 11,683	RMS=11,687
CASE 4 BIAS	-,48	ST DEV 28,130	RMS=28,134
CASE 5 BIAS	-21,97	ST DEV *6,034	RMS=*7,100
CASE 6 BIAS	,17	ST DEV 3,364	RMS= 3,368

TARGET ANGLE(DEG)= 1,00

CASE 1 BIAS	-6,26	ST DEV 9,270	RMS=11,183
CASE 2 BIAS	-,04	ST DEV 1,623	RMS= 1,624
CASE 3 BIAS	1,02	ST DEV 8,712	RMS= 8,772
CASE 4 BIAS	,74	ST DEV 16,650	RMS=16,666
CASE 5 BIAS	-1,91	ST DEV 10,544	RMS=10,715
CASE 6 BIAS	-,07	ST DEV 3,087	RMS= 3,088

$\lambda/2$ spacing 20° scan angle 3 jammers $\theta_J = 15^\circ, 30^\circ, 60^\circ$

all J/N = 10^5

Table 11b

Simulation of 20 Element Array with Main Beam Jamming-High S/N

Signal - to - Noise Ratio (DB) = 30

TARGET ANGLE(DEG)=-1.00			
CASE 1 BIAS -4.44	ST DEV 12.952	RMS=13.691	
CASE 2 BIAS .98	ST DEV .014	RMS= .981	
CASE 3 BIAS .10	ST DEV .024	RMS= .105	
CASE 4 BIAS -.00	ST DEV .116	RMS= .116	
CASE 5 BIAS .15	ST DEV .023	RMS= .151	
CASE 6 BIAS .07	ST DEV .027	RMS= .072	
TARGET ANGLE(DEG)= -.50			
CASE 1 BIAS -3.08	ST DEV 11.248	RMS=11.661	
CASE 2 BIAS .72	ST DEV .013	RMS= .718	
CASE 3 BIAS .02	ST DEV .025	RMS= .033	
CASE 4 BIAS -.01	ST DEV .113	RMS= .114	
CASE 5 BIAS .05	ST DEV .023	RMS= .051	
CASE 6 BIAS .02	ST DEV .026	RMS= .031	
TARGET ANGLE(DEG)= 0.00			
CASE 1 BIAS -4.96	ST DEV 11.568	RMS=12.588	
CASE 2 BIAS .47	ST DEV .012	RMS= .472	
CASE 3 BIAS .00	ST DEV .022	RMS= .022	
CASE 4 BIAS .01	ST DEV .099	RMS= .099	
CASE 5 BIAS .00	ST DEV .022	RMS= .022	
CASE 6 BIAS .00	ST DEV .022	RMS= .022	
TARGET ANGLE(DEG)= .50			
CASE 1 BIAS -5.76	ST DEV 11.906	RMS=13.225	
CASE 2 BIAS .24	ST DEV .013	RMS= .245	
CASE 3 BIAS .01	ST DEV .023	RMS= .026	
CASE 4 BIAS -.01	ST DEV .112	RMS= .112	
CASE 5 BIAS .07	ST DEV .030	RMS= .081	
CASE 6 BIAS .02	ST DEV .024	RMS= .030	
TARGET ANGLE(DEG)= 1.00			
CASE 1 BIAS -5.67	ST DEV 9.907	RMS=11.416	
CASE 2 BIAS .05	ST DEV .013	RMS= .048	
CASE 3 BIAS .04	ST DEV .021	RMS= .042	
CASE 4 BIAS .02	ST DEV .112	RMS= .113	
CASE 5 BIAS .44	ST DEV .044	RMS= .446	
CASE 6 BIAS .09	ST DEV .024	RMS= .097	

$\lambda/2$ spacing 20° scan angle 3 jammers θ_J = 15°, 30°, 60°

all J/N = 10^5

Table 11c

Simulation of 20 Element Array with No Jamming

SIGNAL-TO-NOISE RATIO(DB) =10,458

TARGET ANGLE(DEG)=-1,00

CASE 1 BIAS	-,04	ST DEV 2,697	RMS= 2,698
CASE 2 BIAS	-,04	ST DEV 2,697	RMS= 2,698
CASE 3 BIAS	-,72	ST DEV 12,219	RMS=12,241
CASE 4 BIAS	-,04	ST DEV 2,697	RMS= 2,698
CASE 5 BIAS	-7,54	ST DEV 47,720	RMS=48,312
CASE 6 BIAS	-,04	ST DEV 2,697	RMS= 2,698

TARGET ANGLE(DEG)= -,50

CASE 1 BIAS	,07	ST DEV 1,822	RMS= 1,823
CASE 2 BIAS	,07	ST DEV 1,822	RMS= 1,823
CASE 3 BIAS	-,32	ST DEV 9,311	RMS= 9,316
CASE 4 BIAS	,07	ST DEV 1,822	RMS= 1,823
CASE 5 BIAS	4,34	ST DEV 19,142	RMS=19,629
CASE 6 BIAS	,07	ST DEV 1,822	RMS= 1,823

TARGET ANGLE(DEG)= 0,00

CASE 1 BIAS	-,15	ST DEV 2,184	RMS= 2,189
CASE 2 BIAS	-,15	ST DEV 2,184	RMS= 2,189
CASE 3 BIAS	-,62	ST DEV 11,041	RMS=11,059
CASE 4 BIAS	-,15	ST DEV 2,184	RMS= 2,189
CASE 5 BIAS	-1,68	ST DEV 7,278	RMS= 7,469
CASE 6 BIAS	-,15	ST DEV 2,184	RMS= 2,189

TARGET ANGLE(DEG)= ,50

CASE 1 BIAS	-,14	ST DEV 3,143	RMS= 3,146
CASE 2 BIAS	-,14	ST DEV 3,143	RMS= 3,146
CASE 3 BIAS	,21	ST DEV 3,609	RMS= 3,615
CASE 4 BIAS	-,14	ST DEV 3,143	RMS= 3,146
CASE 5 BIAS	-2,93	ST DEV 24,792	RMS=24,964
CASE 6 BIAS	-,14	ST DEV 3,143	RMS= 3,146

TARGET ANGLE(DEG)= 1,00

CASE 1 BIAS	-,03	ST DEV 2,549	RMS= 2,550
CASE 2 BIAS	-,03	ST DEV 2,549	RMS= 2,550
CASE 3 BIAS	-5,89	ST DEV 53,058	RMS=53,384
CASE 4 BIAS	-,03	ST DEV 2,549	RMS= 2,550
CASE 5 BIAS	-2,85	ST DEV 14,360	RMS=14,640
CASE 6 BIAS	-,03	ST DEV 2,549	RMS= 2,550

N_2 spacing 20° scan angle No jammers

the gain of the symmetrical pairs patterns is reduced (compare Figures 15b and 16b). The resulting accuracy of the symmetrical pairs technique is much poorer in the main beam jamming case.

As before, at this low S/N ratio the new (Case 6) maximum likelihood estimator performs better than the other two (Cases 3 and 5). It happened in this particular example that the technique of Case 2, uncorrected adapted beams, performed best. Results of the same simulation with 30 dB S/N ratio per element are shown in Table 11b. The Case 2 technique does not perform as well as the adaptive algorithms at the higher S/N. As expected, it shows large bias errors.

Results for the 20 element array with no jamming are shown in Table 11c. Cases 1, 2, 4, and 6 all provide the same accuracy in this case. The other two maximum likelihood estimators (Cases 3 and 5) show larger errors in the interference-free environment.

7. CONCLUSIONS

A method of angle tracking with an adaptive array antenna has been described and shown by simulation to perform well in a wide variety of different external noise environments. This preferred technique employs adaptive sum and difference beams which automatically place nulls on external noise sources. An angle estimator which compensates for the pattern distortions due to adaptation and provides good angular accuracy in both main beam and sidelobe jamming environments was derived (Eq. 8). Simulation of this and other algorithms shows that it provides the best accuracy at low S/N ratios. At large S/N ratio, the estimator of R. Davis performs equally well. Both of these estimators provide good angular accuracy in noise fields where conventional monopulse tracking fails.

A tracking technique based on symmetrical pairs was also described. While the symmetry constraints of this technique assure unbiased estimates for targets near boresight, and it would be somewhat easier to implement than the fully adaptive maximum likelihood estimators, the symmetrical pairs technique is significantly less accurate in many cases.

REFERENCES

1. I. Reed and L. Brennan, "Adaptive Angle Tracking", Technology Service Corporation, TSC-PD-119-3, 8 November 1974, Third Quarterly Report Contract N00019-74-C-0227.

2. S. P. Applebaum, "Adaptive Arrays", Syracuse University Research Corporation, SPL-769, June 1964.

3. I. Reed, J. Mallett, and L. Brennan, "Rapid Convergence Rate in Adaptive Arrays", IEEE Trans. AES, November 1974, pp. 853-863.

4. L. Brennan, "Adaptive Angle Tracking", Technology Service Corporation, TSC-PD-119-2, 8 August 1974, Second Quarterly Report on Contract N00019-74-C-0227.

APPENDIX I

FORTRAN PROGRAM FOR SIMULATION OF ADAPTIVE ANGLE TRACKING

Many of the variables used in this program are defined in comment statements at the beginning of the listing. Element weights for the sum and difference patterns are computed for both the fully adaptive arrays and symmetrical pairs. The simulation compares the accuracy of the six tracking algorithms defined in Section 4 of the report.

The major part of the computation and simulation is performed in the main program, TRACK. Subroutine GAUSS generates the complex gaussian random variables used in simulation. These gaussian variables are derived from uniformly distributed (0,1) random numbers obtained by calling RANF. Subroutine GCALC computes the antenna patterns which are plotted by calling the subroutine PATPLT. Matrix inversion is performed in MATINV.

Inputs to the program include the number of array elements (NEL), number of jammers (NJ), number of samples per simulation (NSIM), scan angle (SCAN), signal to noise ratio (SN), and jammer powers (PJ(J)) and angles (THJ(J)). Both the signal to noise ratio and the jammer-to-noise ratio (PJ(J)) are specified for a single array element.

```
      PROGRAM TRACK (INPUT,OUTPUT,TAPE5=INPUT,TAPE6=OUTPUT)
*     NEL=NUMBER OF ELEMENTS
*     NJ=NUMBER OF JAMMERS
*     NSIM=NUMBER OF SAMPLES IN SIMULATION RUN
*     SCAN=ELECTRONIC SCAN ANGLE
*     ELSPAC=ELEMENT SPACING/WAVELENGTH
*     PJ(J),THJ(J) ARE JAMMER POWERS AND ANGLES
*     WS(I,J) ARE SUM BEAM WTS FOR I-TH CASE AND J-TH ELEMENT
*     WD(I,J) ARE DIFF BEAM WEIGHTS
*     CM(M,N) IS COVARIANCE MATRIX OR INVERSE
*     CASE 1  =  NO ADAPTATION
*     CASE 2  =  ADAPTIVE SUM AND DIFFERENCE BEAMS - NO CORRECTION
*     CASE 3  =  DAVIS ALGORITHM, USES CASE 2 WEIGHTS
*     CASE 4  =  PAIRS ALGORITHM
*     SS(N),SD(N) ARE STEERING SIGNALS
*     SS(N),SD(N) ARE ALSO USED IN SIMULATION AS SIG AND DEL OUTPUTS
*     A(K),B(K),C(K) ARE NOISE COEFFICIENTS FOR SIMULATION OF K-TH CASE
*     SSIG(K),DSIG(K) ARE SIGNAL COEFFICIENTS FOR K-TH CASE IN SIMULATION
*     CJS(K,J),CJD(K,J) ARE JAMMER COEFF. FOR K-TH CASE AND J-TH JAMMER
*     B11,B12,B21,B22 ARE COEFFICIENTS IN DAVIS ALGORITHM
*     BP11,BP22 ARE COEFFICIENTS IN PAIRS ALGORITHM
      COMPLEX DSIG(4),SSIG(4),BP11,BP22
      DIMENSION GS(183),GD(183),ANGLE(183)
      DIMENSION PJ(10),THJ(10),A(4),C(4),AV(8),VAR(8),TH(8)
      COMPLEX B(4),CM(20,20),BB,B11,B12,B21,B22,CJS(4,10),CJD(4,10)
      COMPLEX SS(20),SD(20),WS(4,20),WD(4,20),CP,GAM,EX,GG(22)
      COMPLEX WDD(4,20),B13,B31,DD,EE,FF,CJDD(10),DDSIG,SDD,EPS,ETA
      NAMELIST /PARAM/ NEL,NJ,NSIM,SCAN,SN,PJ,THJ
      NAMELIST/EXACT/ B13,B31,DD,EE,FF,A,B,C,DDSIG,SDD,EPS,ETA,CJDD,
     1ALFA,BETA,GAM,CJS,CJD,DELT,SS,SD
      READ(5,12)  NEL,NJ,NSIM,SCAN,SN
   12 FORMAT(3I5,2F10.2)
      IF (NJ.EQ.0) GO TO 11
      DO 10 J=1,NJ
   10 READ(5,22) PJ(J),THJ(J)
   22 FORMAT(2F10.2)
   11 CONTINUE
      SN=10.**(SN/20.)
      NCASE=3
*     TRY THREE DIFFERENT JAMMER LEVELS
*
      DO 100 LMN=1,3
      DO 707  JNJ=1,NJ
      IF(LMN.EQ.1) GO TO 707
      PJ(JNJ)=100.*PJ(JNJ)
      IF(LMN.EQ.3) PJ(JNJ)=0.
  707 CONTINUE
      WRITE(6,PARAM)
*     COMPUTE WEIGHTS FOR NON-ADAPTIVE ARRAY
*     COMPUTE STEERING SIGNALS
      PI=4.*ATAN(1.)
      CP=CMPLX(0.,2.*PI)
      AVN=(NEL+1)/2.
      ELSPAC=.5
      ST=SIN(PI/180.*SCAN)
```

```
      DO 20 N=1,NEL
      SS(N)=CEXP(-CP*ELSPAC*(N-AVN)*ST)
      SD(N)=-CP*ELSPAC*(N-AVN)*SS(N)
      WS(1,N)=SS(N)
   20 WD(1,N)=SD(N)
*    FORM COVARIANCE MATRIX
      DO 30 M=1,NEL
      DO 30 N=1,NEL
      CM(M,N)=0.
      IF(M.EQ.N) CM(M,N)=1.
   30 CONTINUE
      DO 40 J=1,NJ
      SJ=SIN(PI/180.*THJ(J))
      DO 40 M=1,NEL
      DO 40 N=1,NEL
   40 CM(M,N)=CM(M,N)+PJ(J)*CEXP(-CP*ELSPAC*(M-N)*SJ)
*    INVERT COVARIANCE MATRIX
      CALL MATINV(CM,NEL)
*    FORM ADAPTIVE ARRAY WEIGHTS
      DO 50 M=1,NEL
      WS(2,M)=WD(2,M)=0.
      WDD(2,M)=0.
      DO 50 N=1,NEL
      WS(2,M)=WS(2,M)+SS(N)*CM(M,N)
      WDD(2,M)=WDD(2,M)-CP*ELSPAC*(N-AVN)*SD(N)*CM(M,N)
   50 WD(2,M)=WD(2,M)+SD(N)*CM(M,N)
      IF(LMN.NE.1) GO TO 321
      NPLOT=2
      CALL  GCALC(WS,WD,GS,GD,ANGLE,NEL,NPLOT,ELSPAC)
  321 CONTINUE
*    COMPUTE BIJ FOR DAVIS ALGORITHM
      SUMN=DIFN=0.
      B11=B22=B21=0.
      B31=0.
      DO 60 N=1,NEL
      DIFN=DIFN+CABS(WD(2,N))**2
      SUMN=SUMN+CABS(WS(2,N))**2
      B11=B11+WS(2,N)*CONJG(SS(N))
      B21=B21+WD(2,N)*CONJG(SS(N))
      B31=B31+WDD(2,N)*CONJG(SS(N))
   60 B22=B22+CP*ELSPAC*(N-AVN)*WD(2,N)*CONJG(SS(N))
      B12=CONJG(B21)
      B13=CONJG(B31)
      WRITE(6,131) B11,B12,B22
  131 FORMAT(*   B11=*,2E12.5,5X,*B12=*,2E12.5,5X,*B22=*,2E12.5)
      WRITE(6,404) SUMN,DIFN
  404 FORMAT(/*    SUM NOISE=*,E12.5,*   DIFF NOISE=*,E12.5)
*    FORM COVARIANCE MATRICES AND WEIGHTS FOR PAIRS
      N2=NEL/2
*    SUM PAIRS MATRIX
      DO 32 M=1,N2
      DO 32 N=1,N2
      CM(M,N)=0.
      IF(M.EQ.N) CM(M,N)=2.
   32 CONTINUE
```

```
      DO 33 J=1,NJ
      SJ=SIN(PI/180.*THJ(J))*ST
      DO 33 M=1,N2
      DO 33 N=1,N2
      XX=COS(2.*PI*ELSPAC*(M-AVN)*SJ)*COS(2.*PI*ELSPAC*(N-AVN)*SJ)
   33 CM(M,N)=CM(M,N)+PJ(J)*4.*XX
*    SUM PAIRS INVERSION
      CALL MATINV(CM,N2)
*    SUM PAIRS WEIGHT CALCULATION
      DO 34 M=1,N2
      WS(3,M)=0.
      DO 97 N=1,N2
      WS(3,M)=WS(3,M)+CM(M,N)*2.
   97 CONTINUE
      MM=NEL+1-M
      WS(3,MM)=WS(3,M)*CEXP(-CP*ELSPAC*ST*(MM-AVN))
   34 WS(3,M)=WS(3,M)*CEXP(-CP*ELSPAC*ST*(M-AVN))
*    DIFFERENCE PAIRS MATRIX
      DO 36 M=1,N2
      DO 36 N=1,N2
      CM(M,N)=0.
      IF(M.EQ.N) CM(M,N)=2.
   36 CONTINUE
      DO 37 J=1,NJ
      SJ=SIN(PI/180.*THJ(J))*ST
      DO 37 M=1,N2
      DO 37 N=1,N2
      XX=SIN(2.*PI*ELSPAC*(M-AVN)*SJ)*SIN(2.*PI*ELSPAC*(N-AVN)*SJ)
   37 CM(M,N)=CM(M,N)+PJ(J)*4.*XX
*    DIFFERENCE PAIRS INVERSION
      CALL MATINV(CM,N2)
*    DIFFERENCE PAIRS WEIGHT CALCULATION
      DO 38 M=1,N2
      WD(3,M)=0.
      DO 99 N=1,N2
   99 WD(3,M)=WD(3,M)+CM(M,N)*CP*2.*ELSPAC*(N-AVN)
      MM=NEL+1-M
      WD(3,MM)=WD(3,M)*CEXP(-CP*ELSPAC*ST*(MM-AVN))
   38 WD(3,M)=-WD(3,M)*CEXP(-CP*ELSPAC*ST*(M-AVN))
      IF(LMN.NE.2) GO TO 666
      NPLOT=2
      CALL GCALC(WS,WD,GS,GD,ANGLE,NEL,NPLOT,ELSPAC)
      CALL PATPLT(GS,GD,ANGLE)
      NPLOT=3
      CALL  GCALC(WS,WD,GS,GD,ANGLE,NEL,NPLOT,ELSPAC)
      CALL PATPLT(GS,GD,ANGLE)
  666 CONTINUE
*    PAIRS NORMALIZATION COEFFICIENTS
      SUMN=DIFN=0.
      BP11=BP22=0.
      DO 230 N=1,NEL
      SUMN=SUMN+CABS(WS(3,N))**2
      DIFN=DIFN+CABS(WD(3,N))**2
      EX=CEXP(CP*(N-AVN)*ELSPAC*ST)
      BP11=BP11+WS(3,N)*EX
```

```
  230 BP22=BP22+WD(3,N)*EX*CP*(N-AVN)*ELSPAC
      WRITE(6,403) BP11,BP22
  403 FORMAT(//*     BP11=*,2E12.5,*     BP22=*,2E12.5//)
      WRITE(6,404) SUMN,DIFN
      DO 132 LX=1,NCASE
      WRITE(6,133) LX
  133 FORMAT(*       WEIGHTS FOR CASE*,I4)
      DO 132 N=1,NEL
  132 WRITE(6,134) WS(LX,N),WD(LX,N),WDD(2,N)
  134 FORMAT(6E18.9)
*   COMPUTE RECEIVER NOISE COEFFICIENTS
      DO 77 NC=1,NCASE
      ALFA=BETA=0.
      GAM=0.
      IF(NC.EQ.2) DELT=EPS=ETA=0.
      DO 78 N=1,NEL
      ALFA=ALFA+CABS(WS(NC,N))**2
      BETA=BETA+CABS(WD(NC,N))**2
      IF(NC.NE.2) GO TO 78
      DELT=DELT+CABS(WDD(2,N))**2
      EPS=EPS+WS(NC,N)*CONJG(WDD(2,N))
      ETA=ETA+WD(NC,N)*CONJG(WDD(2,N))
   78 GAM=GAM+WS(NC,N)*CONJG(WD(NC,N))
      A(NC)=SQRT(ALFA/2.)
      B(NC)=CONJG(GAM)/SQRT(2.*ALFA)
      IF(NC.NE.2) GO TO 77
      DD=CONJG(EPS)/SQRT(2.*ALFA)
      EE=CONJG(ETA)/2.-CONJG(EPS)*GAM/2./ALFA
      EE=EE/SQRT(BETA/2.-CABS(GAM)**2/2./ALFA)
      FF=SQRT(DELT/2.-CABS(DD)**2-CABS(EE)**2)
   77 C(NC)=SQRT(BETA/2.-CABS(GAM)**2/2./ALFA)
*   COMPUTE JAMMER COEFFICIENTS
      DO 87 NC=1,NCASE
      DO 88 J=1,NJ
      CJS(NC,J)=CJD(NC,J)=0.
      IF(NC.EQ.2) CJDD(J)=0.
      SJ=SIN(PI*THJ(J)/180.)
      DO 89 N=1,NEL
      EX=CEXP(CP*ELSPAC*(N-AVN)*SJ)
      CJS(NC,J)=CJS(NC,J)+WS(NC,N)*EX
      IF(NC.EQ.2) CJDD(J)=CJDD(J)+WDD(2,N)*EX
   89 CJD(NC,J)=CJD(NC,J)+WD(NC,N)*EX
      CJS(NC,J)=SQRT(PJ(J)/2.)*CJS(NC,J)
      IF(NC.EQ.2) CJDD(J)=SQRT(PJ(J)/2.)*CJDD(J)
   88 CJD(NC,J)=SQRT(PJ(J)/2.)*CJD(NC,J)
   87 CONTINUE
*    SIMULATION FOR FIVE TARGET ANGLES
      FR=12.*NEL/(NEL**3-NEL)
*   TRY FOUR DIFFERENT S/N RATIOS
      DO 100 NSN=1,4
      SN=SQRT(10.**(NSN-1))
      SNDB=20.*ALOG10(SN)
      WRITE(6,505) SNDB
  505 FORMAT(///*   SIGNAL-TO-NOISE RATIO(DB)  *,F10.3)
*   TRY DIFFERENT TARGET LOCATIONS
```

```
      DO 100 NA=1,5
      SEP=.5
      ATARG=SEP*(NA-3)
      WRITE(6,121) ATARG
  121 FORMAT(/4X*TARGET ANGLE(DEG)=*,F5.2/)
      ATARG=PI/180.*SEP*(NA-3)
      THT=PI/180.*SCAN+ATARG
      FRR=FR/4./PI**2/ELSPAC**2/COS(PI/180.*SCAN)
*   COMPUTE TARGET ANGLE GAINS
      AV(4)=VAR(4)=0.
      AV(5)=VAR(5)=0.
      AV(6)=VAR(6)=0.
      DO 110 NC=1,NCASE
      AV(NC)=VAR(NC)=0.
      SSIG(NC)=0.
      IF(NC.EQ.2) DDSIG=0.
      DSIG(NC)=0.
      DO 110 N=1,NEL
      EX=CEXP(CP*ELSPAC*(N-AVN)*SIN(THT))
      SSIG(NC)=SSIG(NC)+SN*WS(NC,N)*EX
      IF(NC.EQ.2) DDSIG=DDSIG+SN*WDD(2,N)*EX
  110 DSIG(NC)=DSIG(NC)+SN*WD(NC,N)*EX
      NJ1=NJ+1
      NJ2=NJ+2
      NJ3=NJ+3
*   SIMULATION ROUTINE
      DO 200 NS=1,NSIM
*   GENERATE RANDOM NUMBERS
      CALL GAUSS(NJ3,GG,XR,CP)
      DO 210 NC=1,NCASE
      SS(NC)=A(NC)*GG(NJ1)+SSIG(NC)
      SD(NC)=B(NC)*GG(NJ1)+C(NC)*GG(NJ2)+DSIG(NC)
      IF(NC.EQ.2) SDD=DDSIG+DD*GG(NJ1)+EE*GG(NJ2)+FF*GG(NJ3)
      DO 210 J=1,NJ
      SS(NC)=SS(NC)+GG(J)*CJS(NC,J)
      IF(NC.EQ.2) SDD=SDD+GG(J)*CJDD(J)
  210 SD(NC)=SD(NC)+GG(J)*CJD(NC,J)
      TH(1)=REAL(SD(1)/SS(1))*FRR
      TH(2)=REAL(SD(2)/SS(2))*FRR
      EX=-B11*(CONJG(SS(2))*SD(2)+CONJG(SD(2))*SS(2))
      EX=EX+(B12+B21)*SS(2)*CONJG(SS(2))
      BB=B22*SS(2)*CONJG(SS(2))-B21*SS(2)*CONJG(SD(2))
      BB=BB-B12*CONJG(SS(2))*SD(2)+B11*SD(2)*CONJG(SD(2))
      BB=BB-2.*(B11*B22-B21*B12)
      TH(3)=-REAL(EX/2./BB)/COS(SCAN*PI/180.)
      TH(4)=REAL(SD(3)/SS(3)*BP11/BP22/COS(PI/180.*SCAN))
      BB=B22*SS(2)*CONJG(SS(2))-B11*SD(2)*CONJG(SD(2))
      BB=2.*BB-2.*(B12+B21)/B11*EX
      BB=BB-B11*(SS(2)*CONJG(SDD)+SDD*CONJG(SS(2)))
      BB=BB+SS(2)*CONJG(SS(2))*(B31+B13)
      TH(5)=-REAL(EX/BB)/COS(SCAN*PI/180)
      BB=2.*SS(2)*CONJG(SS(2))*(B22-B21*B12/B11)
      TH(6)=-REAL(EX/BB)/COS(SCAN*PI/180)
      DO 200 KK=1,6
      AV(KK)=AV(KK)+TH(KK)-ATARG
```

```
      VAR(KK)=VAR(KK)+(TH(KK)-ATARG)**2
  200 CONTINUE
      NCASE1=NCASE+1
      NCASE2=NCASE+2
      NCASE3=NCASE+3
*   NORMALIZE BIAS AND VARIANCE ESTIMATES
      DO 215 N=1,NCASE3
      AV(N)=AV(N)/NSIM*180./PI
      VAR(N)=VAR(N)/NSIM*(180./PI)**2
      RMSE=SQRT(VAR(N))
      VAR(N)=VAR(N)-AV(N)**2
      STD=SQRT(VAR(N))
  215 WRITE(6,216) N,AV(N),STD,RMSE
  216 FORMAT(7H  CASE ,I2,7H BIAS  ,F6.2,5X,7HST DEV ,F6.3,5X,4HRMS=,F6.
     13)
  100 CONTINUE
      WRITE(6,EXACT)
      END
```

```
      SUBROUTINE GCALC(WS,WD,GS,GD,ANGLE,NEL,NCASE,ELSPAC)
      COMPLEX WS(4,20),WD(4,20),CP,ES,ED,XX
      DIMENSION GS(183),GD(183),ANGLE(183)
      PI=4.*ATAN(1.)
      CP=CMPLX(0.,2.*PI)
      DMX=SMX=-10000000000.
      DO 10 J=1,181
      PSID=J-91
      ANGLE(J)=PSID
      PSI=PSID*PI/180.
      ES=ED=0.
      DO 20 N=1,NEL
      XX=CEXP(CP*ELSPAC*N*SIN(PSI))
      ES=ES+WS(NCASE,N)*XX
   20 ED=ED+WD(NCASE,N)*XX
      ESS=AMAX1(CABS(ES),.000001)
      EDD=AMAX1(CABS(ED),.000001)
      GS(J)=20.*ALOG10(ESS)
      GD(J)=20.*ALOG10(EDD)
      SMX=AMAX1(SMX,GS(J))
      DMX=AMAX1(DMX,GD(J))
   10 CONTINUE
      DO 30 J=1,181
      GS(J)=AMAX1((GS(J)-SMX),-60.)
   30 GD(J)=AMAX1((GD(J)-DMX),-60.)
      RETURN
      END


      SUBROUTINE PATPLT(GS,GD,ANGLE)
      DIMENSION GS(183),GD(183),ANGLE(183)
      GS(181)=-60.
      CALL PLOTS(SHLEB,3)
      CALL SCALE(ANGLE,6.,181,1)
      CALL SCALE(GS,6.,181,1)
      CALL SCALE(GD,6.,181,1)
      CALL AXIS(0.,0.,5HANGLE,-5,6.,0.,ANGLE(182),ANGLE(183),0.)
      CALL AXIS(0.,0.,8HGAIN(DB),8,6.,90.,GS(182),GS(183),-1)
      CALL LINE(ANGLE,GS,181,1,0,0)
      CALL LINE(ANGLE,GD,181,1,4,3)
      CALL PLOT(10.,0.,-3)
      RETURN
      END
```

```
      SUBROUTINE MATINV(A,N)
      COMPLEX A(20,20)
      DO 11 N1=1,N
      DO 12 J=1,N
      IF(J.EQ.N1) GO TO 12
      A(N1,J)=A(N1,J)/A(N1,N1)
   12 CONTINUE
      DO 15 I=1,N
      IF(I.EQ.N1) GO TO 15
      DO 16 J=1,N
      IF(J.EQ.N1) GO TO 16
      A(I,J)=A(I,J)-A(I,N1)*A(N1,J)
   16 CONTINUE
      A(I,N1)=-A(I,N1)/A(N1,N1)
   15 CONTINUE
      A(N1,N1)=1./A(N1,N1)
   11 CONTINUE
      RETURN
      END


      SUBROUTINE GAUSS(N,GG,XR,CP)
      COMPLEX CP,GG(22)
      DO 10 M=1,N
      AMP=RANF(0.)
      XR=RANF(0.)
   10 GG(M)=SQRT(-2.*ALOG(AMP))*CEXP(CP*XR)
      RETURN
      END
```

APPENDIX II

SIMULATION OF RECEIVER NOISE

In simulating the angle estimator of Eq. 5 (i.e., Case 5), three beam outputs are required, Σ, Δ, and Δ_ε. Since each of these beams is generated by weighting and summing the same array element outputs, the receiver noise components in these outputs would be correlated. The assumed model is one in which each element is followed by an amplifier and the amplifier outputs are weighted and added. Receiver noise is equal and independent in each channel. Rather than generate a separate complex Gaussian number to represent the receiver noise in each element, it is more efficient during the simulation to generate three correlated noise components. The correlations between the three outputs, Σ, Δ, and Δ_ε, are computed at the beginning of a simulation run and used in generating the appropriately correlated noise components.

The statistics of these three noise components are described completely by their second moments. Let W_S denote the array element weights in the sum channel, W_D in the difference (Δ) channel, and W_{D2} in the Δ_ε channel. The required second moments are:

$$E\,|\Sigma|^2 = \Sigma\,|W_S|^2 = \alpha$$

$$E\,|\Delta|^2 = \Sigma\,|W_D|^2 = \beta$$

$$E\,|\Delta_\varepsilon|^2 = \Sigma\,|W_{D2}|^2 = \delta$$

$$E\,\Sigma\bar{\Delta} = \Sigma\,W_S\,\bar{W}_D = \gamma$$

$$E\,\Sigma\bar{\Delta}_\varepsilon = \Sigma\, W_S\, \bar{W}_{D2} = \varepsilon \qquad \text{(II-1)}$$

$$E\,\Delta\bar{\Delta}_\varepsilon = \Sigma\, W_D\, \bar{W}_{D2} = \eta$$

where E denotes average and bar denotes complex conjugate.

To simulate the three properly correlated receiver noise components, three independent complex Gaussian numbers are generated, say r_1, r_2, and r_3. Each has unit variance in each quadrature component, so

$$E\,|r_j|^2 = 2$$
$$E\,r_j\,\bar{r}_k = 0 \qquad j \neq k \qquad \text{(II-2)}$$

The three noise components are

$$N_\Sigma = ar_1$$
$$N_\Delta = br_1 + cr_2 \qquad \text{(II-3)}$$
$$N_{\Delta\varepsilon} = dr_1 + er_2 + fr_3$$

It can easily be shown that these components have the second moments of Eq (II-1) when

$$a = \sqrt{\alpha/2}$$
$$b = \bar{\gamma}/\sqrt{2\alpha}$$
$$c = \sqrt{\beta/2 - |\gamma|^2/2\alpha} \qquad \text{(II-4)}$$
$$d = \bar{\varepsilon}/\sqrt{2\alpha}$$
$$e = \frac{\bar{\eta}}{2} - \frac{\bar{\varepsilon}\gamma}{2\alpha\sqrt{\beta/2 - |\gamma|^2/2\alpha}}$$

$$f = \sqrt{\frac{\delta}{2} - |d|^2 - |e|^2}$$

For example:

$$\begin{aligned} E\, N_\Sigma\, \overline{N}_{\Delta\epsilon} &= E\,(ar_1)(\overline{dr}_1 + \overline{er}_2 + \overline{fr}_3) \\ &= 2a\overline{d} \qquad\qquad (II\text{-}5) \\ &= \epsilon \end{aligned}$$

Similar expansion of the other second moments, noting the independence of the r_j, will verify the other equations in (II-1).